DOE/NE-0076

SYD BALL

Report of the U.S. Department of Energy's Team Analyses of the Chernobyl-4 Atomic Energy Station Accident Sequence

November 1986

U.S. Department of Energy
Assistant Secretary for Nuclear Energy

This report has been reproduced directly from the best available copy.

Available from the National Technical Information Service, U. S. Department of Commerce, Springfield, Virginia 22161.

Price: Printed Copy A10
Microfiche A01

Codes are used for pricing all publications. The code is determined by the number of pages in the publication. Information pertaining to the pricing codes can be found in the current issues of the following publications, which are generally available in most libraries: *Energy Research Abstracts, (ERA); Government Reports Announcements* and Index (*GRA* and I); *Scientific and Technical Abstract Reports (STAR);* and publication, NTIS-PR-360 available from (NTIS) at the above address.

DOE/NE-0076

Report of the U.S. Department of Energy's Team Analyses of the Chernobyl-4 Atomic Energy Station Accident Sequence

November 1986

U.S. Department of Energy
Assistant Secretary for Nuclear Energy
Washington, D.C. 20585

NTIS DE87003614

TABLE OF CONTENTS

EXECUTIVE SUMMARY i

SECTION 1. Introduction 1-1

SECTION 2. History of the U.S. Team's Activities 2-1

SECTION 3. Description of the Chernobyl-4 Accident 3-1

SECTION 4. Analyses of Initial Power Increase 4-1

SECTION 5. Rapid Power Excursion Analysis 5-1
(1:23:40 to 1:23:43)

SECTION 6. Energetic Event Analyses (After 1:23:43).....6-1

Appendices

Appendix A - Analyses Performed Prior to the Vienna Chernobyl-4 Post Accident Review Meeting in August 1986

Appendix B - The Chernobyl-4 Accident Analyses Workshop Held on September 16, 1986

Appendix C - Summary Paper on the Possiility of Chernobyl-4 Type Transient Overpower Accidents in U.S. Reactors

Appendix D - Assessment of Actions Identified by the Soviets to Improve the Safety of RBMK Reactors

Appendix E - Background Information on Chernobyl-4, RBMK Type Reactors, and the Soviet Nuclear Power Program

Appendix F - Chernobyl-4 Void Coefficients and Neutron Kinetics Parameters

Appendix G - RBMK Control Rod System Description

Appendix H - Three-Dimensional Transient Calculations

EXECUTIVE SUMMARY

In an effort to better understand the Chernobyl-4 accident of April 26, 1986, the U.S. Department of Energy (DOE) formed a team of experts from the National Laboratories including Argonne National Laboratory, Brookhaven National Laboratory, Oak Ridge National Laboratory, and Pacific Northwest Laboratory. The DOE Team provided the analytical support to the U.S. delegation for the August meeting of the International Atomic Energy Agency (IAEA), and to subsequent international meetings.

The DOE Team has analyzed the accident in detail, assessed the plausibility and completeness of the information provided by the Soviets, and performed studies relevant to understanding the accident. The results of these studies are presented in this report.

The accident at Chernobyl-4 occurred during the running of a test to determine a turbogenerator's ability to provide in-house emergency power after shutting off it's steam supply. The accident was the result of a large, destructive power excursion. The major design-related factor in the accident was the large positive void coefficient of reactivity. This feature, not present in U.S. reactors, means that an increase in power is likely to lead to an increase in reactivity which will further increase power. Any increase in the amount of void, that is steam, in the reactor core, decreases the neutron absorption by the water, leading to greater neutron flux and hence greater reactivity. The major operational factors were a long series of procedural and operator errors. These errors put the Chernobyl-4 reactor into a very unstable operating condition.

With the plant in this very unstable condition, the closing of the steam valve starting at 1:23:04 on April 26, 1986, to begin the test, began the final accident sequence. The first phase of the accident was a gradual power increase over a period of about 36 seconds. This power increase was caused by the coastdown of the four main coolant pumps that resulted in increased void formation and a positive reactivity addition. This was caused by the large void coefficient and cannot occur in U.S. reactors. The second phase, starting at about 1:23:40, was the rapid power excursion when the void formation began to accelerate. This effect was possibly accelerated by a positive reactivity insertion introduced during the initial portion of the scram that took place when the operator scrammed the control rods to stop the power rise. This feature is unique to the RBMK reactor and is not present in any U.S. plants. When an RBMK control rod is inserted from the fully withdrawn position, in the condition the Chernobyl-4 reactor was in at 1:23:40 for the first meter of travel, the extension on the bottom of the rod displaces water, a neutron poison in this reactor, from the bottom of the core, thus

adding reactivity. The third phase, that began at about 1:23:43, was the energetic phase during which fuel coolant interactions, fission product vapor expansion, and destruction of the reactor occurred.

The entire accident occurred in a period of only about 40 seconds. At the beginning (1:23:04) any pertubation in the system which increased void formation even slightly could have led to a major power excursion accident. At any time during the slow power buildup, up until the power began to rise rapidly, system changes which reduced void formation, such as reducing steam flow, could have prevented the accident. Once the power began to rise rapidly, there was nothing that could have been done to stop it. From the time the reactor was out of control until it was completely destroyed was a matter of 1 to 2 seconds.

Accident Analyses and Results

The DOE Team's analyses of the first two phases of the accident initially used relatively simple point kinetic computer models. Subsequently, three-dimensional analyses were performed using both static and dynamic models. The third phase was modeled using accident analysis codes modified to depict the Chernobyl-4 system and conditions.

As a result of these analyses, a number of important conclusions were reached. These are summarized below:

- The reactor was placed in such an unstable condition that any event that resulted in significantly increased void fraction would have resulted in a damaging power excursion.

- The DOE Team's analyses have confirmed the plausibility of the Soviet's claim that the reactivity excursion was caused primarily by increased void formation due to reduced coolant flow. The severity of the power excursion may have been exacerbated by a positive reactivity addition from the scram insertion of the control rods.

- The power excursion may have peaked significantly above 350,000 MWt.

- When the fuel failed, due to power excursion, a fraction of the fuel was forcibly ejected into the coolant causing rapid formation of steam from interaction of the fuel and coolant. This lead to the destruction of the Chernobyl-4 reactor.

- The expansion of the fission product vapor, and the steam resulting from the fuel coolant interaction, ejected water from portions of the core, adding more reactivity and further increasing power.

- There were probably not two distinct power peaks (such as the Soviet analysis results, figure 4 show), but rather the continuous progression of the initial event into a larger explosion.

- The release of energy from the core to the reactor building may have been enhanced by the failure from severe water hammer of the zirconium-to-stainless transition weld at the top of the pressure tubes.

- The accident was not the result of a steam explosion, but rather an energetic fuel coolant interaction event.

- Similarly, the accident did not result from zirconium water reaction or graphite burning. While zirconium water reactions may well have occurred as a result of the power excursion, it is not apparent that a hydrogen explosion occurred or was a significant contributor damaging to the reactor. If in fact there were any hydrogen explosions, these would have occurred away from the core and after the destruction of the reactor.

- The U.S. experimental bases and analytical capabilities provide a good understanding of the processes involved in the progression of the accident. No areas have been identified which require additional testing or research and development.

Assessment of Soviet Fixes

In addition to analyzing the accident, the DOE Team assessed the actions identified by the Soviets to improve the safety of RBMK reactors. In general, the stated fixes will improve RBMK safety for the type of accident that occurred at Chernobyl-4. However, while many questions remain unanswered, our assessment indicates that these fixes may reduce plant safety margins under other conditions. In addition, the method of implementing many of the changes is not clear, raising concerns that some of the fixes could be easily defeated by operators.

Significance with Respect to U.S. Reactors

Based on the detailed understanding of the accident that came from the Team's analyses, the potential for a Chernobyl-4 type accident in U.S. reactors was evaluated. The Team found that U.S. reactors are designed such that a large overpower excursion

due to core instability from a positive void reactivity coefficient is not possible.

DOE/NE-0076
(11/86)

SECTION 1. INTRODUCTION

The purpose of this report is to provide the results of the efforts of the team of experts formed by the U.S. Department of Energy (DOE) to analyze and understand the Chernobyl-4 accident.

The analyses in this report were based on information obtained from the Soviet report to the IAEA Vienna meeting and from discussions with the Soviets at Vienna, as well as from various other literature references. This has been a major effort, completed in a short time with little opportunity to perform an extensive quality assurance of the data. It is possible that new information could alter some of the conclusions to date.

Key participants in the Team are:

Department of Energy:	Edward E. Purvis, III (Team Leader)
Argonne National Laboratory:	John Marchaterre Bruce W. Spencer
Brookhaven National Laboratory:	John F. Carew James G. Guppy Gregory J. Van Tuyle
Oak Ridge National Laboratory:	S. J. Ball R. M. Harrington L. C. Oakes (Coordinator)
Pacific Northwest Laboratory:	Laurin R. Dodd James P. McNeece

This report consists of the following sections:

Section 1: Introduction, provides the purposes and scope of the report and identifies key participants in the Department of Energy's analytic team.

Section 2: History of the U.S. Team's Activities.

Section 3: Description of the Chernobyl-4 Accident, provides a chronology of the accident, describes the events leading to the accident, and the Chernobyl-4 accident sequence.

Section 4: Analyses of Initial Power Increase, covers the time period from 1:23:04 to about 1:23:40.

Section 5: Rapid Power Excursion Analysis, covers the time period from about 1:23:40 to approximately 1:23:43.

Section 6: Energetic Event Analyses, covers the time period after 1:23:43 during which failure of the fuel and destruction of the reactor occurred.

The report also contains eight appendices.

APPENDIX A: ANALYSES PERFORMED PRIOR TO THE VIENNA CHERNOBYL-4 POST ACCIDENT REVIEW MEETING IN AUGUST 1986

APPENDIX B: THE CHERNOBYL-4 ACCIDENT ANALYSES WORKSHOP HELD ON SEPTEMBER 16, 1986

APPENDIX C: SUMMARY PAPER ON THE POSSIBILITY OF CHERNOBYL-4 TYPE TRANSIENT OVERPOWER ACCIDENTS IN U.S. REACTORS

APPENDIX D: ASSESSMENT OF ACTIONS IDENTIFIED BY THE SOVIETS TO IMPROVE THE SAFETY OF RBMK REACTORS

APPENDIX E: BACKGROUND INFORMATION ON CHERNOBYL-4, RBMK TYPE REACTORS, AND THE SOVIET NUCLEAR POWER PROGRAM

APPENDIX F: CHERNOBYL-4 VOID COEFFICIENTS AND NEUTRON KINETICS PARAMETERS

APPENDIX G: RBMK CONTROL ROD SYSTEM DESCRIPTION

APPENDIX H: THREE-DIMENSIONAL TRANSIENT CALCULATIONS

The efforts of the U.S. Department of Energy's Team to analyze the Chernobyl-4 Atomic Energy Station Accident sequence was part of a larger effort including preparation of briefing material to support the U.S. Delegation to the Chernobyl-4 Post-Accident Review Meeting held in Vienna, Austria on August 25-29, 1986 and providing support to the preparation of the U.S. factual report on the Chernobyl-4 accident (to be published).

SECTION 2. HISTORY OF THE U.S. TEAM'S ACTIVITIES

On April 26, 1986, an accident occurred at the Chernobyl-4 Nuclear Power Plant in the Soviet Union. A post accident meeting was held in Vienna during the week of August 25, 1986. In the months between the accident and the post accident review meeting, there was a scarcity of information available about the accident that led to considerable speculation as to the causes and sequence of events.

In mid-July 1986, the Department of Energy formed a Team to analyze the accident. In late July, this Team began preparations to analyze information to be provided by the Soviets at the Vienna meeting. The goal was to assess the information's plausibility, provide analytic support to the U.S. Delegation during the post-accident review meeting, and obtain a technical understanding of the accident. The initial tasks of this Team were (1) to assemble data concerning Chernobyl-4 that would allow modeling and analysis of the Chernobyl-4 accident; (2) to prepare and have operational codes and the associated analytic capability to both analyze the accident based on any information that might be provided by the Soviet Union and to evaluate the plausibility of such information; (3) to have an "online" capability to provide any technical support that might be required to support the U.S. Delegation at the August 25-29, 1986 Post-Accident Review meeting; and (4) to analyze the accident based on available information sufficient to provide a technical understanding of the accident sequence and it's causes. Subsequent to the post-accident review meeting, this activity was expanded to include an analysis of the "fixes" identified by the Soviets.

Argonne National Laboratory (ANL) focused primarily on establishing a capability to assess various core energetic events and analyzing core sequence of energetic related aspects of the accident together with the associated accident sequence and damage. Brookhaven National Laboratory (BNL) began work using MINET, a generalized systems code used for LMR, HTGR, and LWR transient analysis. An extensive representation of the Chernobyl-4 system was specified through input data. Work was initiated to modify a RAMONA-3B to model the Chernobyl-4 system and provide a multi-dimensional dynamic capability for modeling RBMK. Oak Ridge National Laboratory (ORNL) began their analysis using a specially assembled code named CRAS-1 (Chernobyl-4 Reactor Accident Simulator, Version 1) and specially written subroutines for components unique to the RBMK reactor concept. These were implemented using CSMP simulation language. Pacific Northwest Laboratory (PNL) performed a wide variety of analytic activities including determining detailed information required for the analysis being performed by others and performing a variety of physics and systems analyses.

Calculation of the Chernobyl-4 power excursion began after a July 31, 1986 meeting of the Team. Discussion at this meeting centered on the speculation that the accident involved a power excursion. The most likely enabling mechanism for the power excursion was felt to be the void coefficient that was positive at the time of the accident. Since other reports indicated that the Chernobyl-4 operators had been performing some kind of testing on the turbines, the Team assumed that the excursion was brought on by spurious opening of the turbine inlet or bypass valves, or by some sort of steam line break. Either of these initiators, a break or a sudden steam valve opening, could rapidly reduce reactor pressure and cause additional voiding within the core; the positive void coefficient would then result in positive excess reactivity accompanied by a rapid power increase. It was resolved at the July 31 meeting that calculations should be performed to estimate the magnitude of power excursions that might follow a steam line break or a spurious turbine valve opening.

Within approximately 2 weeks, the initial model was completed and was applied to the study of steam line break events. An intermediate break size,with flow area equal to the inlet flow area of one of the two Chernobyl-4 turbines, was selected for analysis. After consultation with PNL analysts, it was determined that a range of void coefficient curves should be examined. The best information at that time indicated that the void coefficient versus void fraction function varied in a straight line, with the greatest (or most positive) coefficient occurring at the zero-voiding point, and the least positive (or, depending on time in core life, most negative) coefficient occurring for maximum voiding. The results of the steam line break calculations indicated that the positive void feedback effect would, as expected, lead to a power increase. At this time, it was concluded that a similar power excursion could occur after any upset that leads to increased voiding of the coolant in the reactor core. This conclusion was subsequently confirmed.

On August 14, 1986, the International Atomic Energy Agency received a working draft of the Soviet's report on the accident at Chernobyl-4. The Department of Energy received this report, in Russian, on August 16, 1986. A translation was provided to the Team for analysis on August 18, 1986. As MINET and CRAS-1 representations of the Chernobyl-4 system were in place, BNL and ORNL were able to provide preliminary analyses in time for the August 25th meeting. In these calculations, both the MINET and CRAS-1 analyses gave similar results, thus lending confidence that the models were reasonable. The BNL analysis, based on a full systems representation, indicated that a major power excursion was likely to come in the correct time frame, given that some steam was released during the transient. The ORNL analysis represented less system details, which facilitated sensitivity and parameter analysis that indicated a power

excursion could be expected at various times, depending on various factors, such as core inlet subcooling. These initial analytic results were provided to the U.S. Delegation and to the technical community in the U.S. Appendix A provides this information.

On August 25, 1986, the Soviets provided "figure 4", a graphical presentation of the results of the Soviet analysis of the accident. This figure was not included in the Soviet's report. The Team's analyses, as it existed when figure 4 was received, confirmed the plausibility of the information provided by the Soviet Union.

The analysis continued after this meeting using the information provided by the Soviets at the post-accident review meeting. Appendix B is a report of the workshop held September 16, 1986 concerning the Team's analyses.

Efforts of the Team after the Vienna meeting have been focused in two areas: (1) fully understanding the Soviet's analysis presented in figure 4, and (2) analyzing the accident using the best available computer models. This effort is detailed in sections 4 through 6.

An evaluation was performed to assess the potential for a Chernobyl-4 type accident to occur in a U.S. power reactor. The results of this evaluation are contained in Appendix C, Summary Paper on the Chernobyl Transient Overpower Accident and Its Implications for U.S. Power Reactors. An initial version of this paper was provided to the U.S. Delegation for the Chernobyl-4 post-accident review meeting.

There is only limited information available on the actions to improve RBMK safety. Appendix D provides the result of a qualitative evaluation of actions to improve the safety of RBMK type reactors. Many questions remain. While the actions identified by the Soviets may improve the safety of RBMK type reactors in the event of a Chernobyl-4 accident, it appears that these fixes may reduce plant safety margins under operating conditions. The method and time scale for implementing many of the changes is not clear, leaving questions as to the possibility that the "fixes" could be easily bypassed and that, if no "fixes" are effective, what is the effect on RBMK safety of the delay in their implementation.

For the convenience of the reader, Appendix E contains summary information on Chernobyl-4, RBMK-type reactors, and the Soviet nuclear program.

SECTION 3. DESCRIPTION OF THE CHERNOBYL-4 ACCIDENT

The RBMK reactors are graphite moderated, water cooled, tube type reactors. It is a uniquely Soviet design which is not utilized anywhere else in the world. Appendix E provides background information on Chernobyl-4, the RBMK type reactors, and the Soviet Union's Nuclear Power Program.

The accident at Chernobyl occurred during the running of a test to determine a turbogenerator's ability to provide in-house power after shutting off its steam supply for the short time needed for the emergency diesels to start and come online. This test had been run on a previous occasion at Chernobyl; however, it was found that the voltage output decreased faster than desired. The purpose of the test was to verify proper operation of a new voltage regulator design for the generator. The test was to demonstrate that the inertia of the large turbine generator, following closure of the turbine steam emergency shutoff valve, could provide sufficient energy to power a subsystem of the emergency core cooling system (ECCS) long enough for the emergency diesel generators to get up to speed, nominally 40 to 50 seconds.

Table 1 provides the chronology of the accident.

The accident was a direct result of fundamental design and administrative deficiencies. Strong management emphasis had been given to the importance of running this test before Chernobyl-4 was shutdown for scheduled maintenance. Management and operator actions placed the reactor in progressively more unsafe configurations. The test procedure itself called for turning off the emergency core cooling system. Operator actions included disconnecting the signal that automatically shuts down the reactor when two turbogenerators are disconnected, operating the main coolant pumps in a regime where cavitation might occur, turning off various protection system signals, and operating with less than the minimum required number of inserted control rods.

Power reduction to the test power level of 700-1000 MWt began early on April 26. At 1600, MWt power reduction was halted while the operators disconnected (removed from service) one of the two turbogenerators (TG #7) from the reactor. Four main cooling pumps, and two feedwater pumps were connected to the turbogenerator to be run down (TG #8). The operators also disabled the signal for automatic reactor shutdown when both turbogenerators are disconnected. This would permit rerunning the test if needed. The test procedure did not call for disabling this emergency system. In addition, the operators disabled the emergency core cooling system. The Soviets report that this was required by the test procedure.

Before power reduction could continue, the power dispatcher requested they hold power and not continue with the test. Continuous operation at power with the emergency core cooling system disabled was a violation of normal plant operating procedures.

After 9 hours, the power dispatcher gave permission to continue the test. Up until the point when the power dispatcher requested a hold at 1600 MWt, the operators had been reducing power slowly to allow the xenon poisoning to equilibrate with the lowering power levels. Following the delay, however, a rapid unplanned power reduction occurred when the operator switched control to the backup automatic power controller. When he disengaged the local automatic power regulation (LAR) system, he failed to set the backup automatic controller to its proper "hold power" setpoint. As a result, the reactor power rapidly fell to as low as 30 MWt before he was able to stabilize power at about 200 MWt. This unplanned power reduction allowed the xenon poison level to increase such that the loss of core reactivity had to be compensated by withdrawal of control rods. Attempts to increase power to the required level of 700-1000 MWt were unsuccessful due to low core reactivity and insufficient rod worth remaining in the mostly withdrawn control rods. The operator had pulled many of the control rods out of the core to compensate for the buildup of neutron absorbing fission products (xenon-135) and reactivity loss due to the cooling of the reactor core caused by the rapid power reduction to 30 MWt.

With the reactor at 200 MWt, the decision was made to proceed with the test. Two additional main coolant pumps (MCP) were started so that there were a total of eight pumps running. This was done so that four MCPs were powered by offsite power and would remain running after the four MCPs connected to TG #8 were rundown. When they added the fourth MCP in each of the two primary loops, the pumps put out greater flow than normal since, at the lower power, the reduced two phase flow in the core offered less flow resistance. The excess flow was such that pump cavitation limits were exceeded, but, the operators proceeded with the test. The higher flows resulted in lower coolant void fractions, thus further reducing the core reactivity.

In trying to control the steam drum levels in the face of the high primary flow and low steaming rate, the operators had difficulties due to the coarseness of control when small makeup flows are needed. Feedwater flow increases that were needed to raise the drum levels just preceding the test resulted in lowering the core inlet temperature and reducing coolant voiding even more. As a result, the remaining inserted rod worth was the equivalent of 6 to 8 rods as compared to a minimum allowable of 16. This was also a serious violation of procedures. The requirement to have at least a certain minimum number of control rods inserted during operation is apparently to ensure proper

spatial power control, scram effectiveness, and limit the positive void coefficient.

At 01:23:04 hours on April 26, the operator began the coastdown test by closing the steam valve to TG #8. Normally there is an automatic reactor scram on loss of the second TG, but this interlock had been overridden by the operators in order to allow for a repeat of the test if this first one had failed. The reactor did not need to remain critical after the steam flow valve was closed; in fact, it is understood that previous similar tests had been done with the reactor shutdown during the rundown. During the TG coastdown and the subsequent primary flow reduction, void formation in the core increased, leading to higher powers and further voiding. The shift foreman ordered actuation of the manual scram at 01:23:40.

After the operator activated the manual scram, he felt a number of "shocks" and noticed that the rods stopped before reaching their lower limits. He than cut off power to the servos to allow the rods to fall under their own weight. (Their movement after cutting off the servo power is not reported.) The fact that most of the control rods were withdrawn completely out of the core made them ineffective in producing a rapid shutdown of the reactor. The power level rose extremely fast and resulted in fuel fragmentation, fission product vapor expansion, rapid steam generation, and severe damage to the core and reactor.

Observers outside the plant heard two explosions reportedly two or three seconds apart and saw hot fragments and sparks shoot into the sky above the reactor. A number of fires were started as these hot fragments (burning fuel, zirconium, and hot graphite moderator blocks) fell onto the turbine hall and reactor building roofs.

Figure 1.a. Closeup View of Core Debris on Roof

Figure 1.b. Closeup View of Core Debris on Roof

TABLE 1

Chronology of the Accident*

Time	Power	Event
April 25		
0100	3200 MWt	Begin power descent to 700-1000 MWt as required for test.
1305	1600 MWt	Turbogenerator #7 disconnected. Power for auxiliaries (4 main cooling pumps, 2 feedwater pumps, etc.) was transferred to turbogenerator #8 (TG 8).
1400	1600 MWt	Emergency core cooling system disengaged as required by test procedure.
		Continued power reduction was delayed for 9 hours due to request from dispatch center to maintain full output of TG #8 to the grid. Operation with emergency core cooling system out of service was a violation of regulations.
2310	1600 to 30 MWt	Tests were resumed and the operator began reducing power.
		During the process, the operator disengaged the automatic control rod system (LAR) and failed to properly set "hold power" setpoint on backup power controller. As a result reactor power rapidly fell to 30 MWt before he could regain control.
April 26		
0100	200 MWt	Power stabilized at this level. Attempts to increase power to the desired 700-1000 MWt was difficult

*From the description provided in the Soviet Accident Report.

Time	Power	Event
		(never accomplished) due to the low amount of operating reactivity reserve. Operating reactivity reserve was below that requiring reactor shutdown. Operating reactivity reserve is given in terms of equivalent number of inserted rods. The normal value is 30. The absolute minimum is 16.
0103-0107	200 MWt	Two additional main cooling pumps were placed into service for a total of 8 pumps as the test program directed. Since the reactor power was far below the planned test power of 700-1000 MWt, the total flow increased above that allowed in the operating regulations. This resulted in a decrease in steam pressure and water level in steam separators and the inlet coolant temperature approaching saturation. (Pumps were operating in a regime where cavitation was possible.)
0119	200 MWt	Operator began manual replenishment of water to steam separator. As this colder water reached the reactor core, there was a sharp drop in the steam fraction of the coolant, and a corresponding power decrease. The AR (automatic power regulating) rods moved upward to compensate. Operator also moved manual rods out to "help" the automatic regulating rods. In order to keep steam pressure and water level from causing reactor shutdown, the operators blocked the emergency protection signals related to these parameters. Control rod positions were recorded at this time.
0122	200 MWt	Operator reduced feedwater flow rate. This allowed increase of inlet temperature and compounded the events 1 minute later.

Time	Power	Event
0122:30	200 MWt	Operator noted reactivity to reserve was about 6-8 rods as opposed to the to the normal of 30 rods. Far below the value where reactor shutdown is required. No action taken. A printout of the actual core flux monitor outputs and the position of all the regulating rods was obtained at this time ("Skala" system). The axial flux double peaked with the higher peak in the top section of the core.
0123:04	200 MWt	Steam flow valve to TG #8 was closed to begin test. The signal for reactor shutdown on closure of both turbogenerator steam valves had been disengaged in order to allow repeating the test if needed. This was in violation of the test program and normal operating procedures. Flow rate began to fall as the 4 main cooling pumps powered by TG #8 began to run down. Steam pressures also began to increase due to removal of TG steam load and the reduction (by operator action) of the feedwater rate about 1 minute before. All these factors lead to an increase in the coolant void fraction (positive reactivity insertion) and a resulting power increase. Due to the reactor conditions at the time of the test, the void fraction increased many times more sharply than at normal power. (Also the void reactivity coefficient was at a higher value than at normal operating conditions.)
	530 MWt and	Power began to increase. After 3 seconds it was 530 MWt and the increasing "runaway period came to be much less than 20 seconds." The positive void coefficient "promoted deterioration of the situation." Only the Doppler effect partially compensated for the void reactivity increase. Water flow continued to decrease (due to run

Time	Power	Event
		down of 4 main cooling pumps) and the power continued to increase. This led to a "crisis of convective heat transfer"; i.e. heating up of the fuel, its disintegration, rapid voiding of the coolant, sharp increase in pressure in the operating channels, rupture of the channels and a "thermal explosion." The steam formation and sharp temperature increase created conditions for steam zirconium and other exothermic reactions. A fuel failure specific energy release was greater than 300 cal/gm.
		Recorded data shows the check valves between the coolant pumps on the fuel channel inlets closed. this was due to the rapid rise in the fuel channel pressure.
0123:40	Unknown	Shift director gave order to press scram button. Operator saw rods were stopping before they reached bottom. He "felt shocks" (other translations are loud reports, banging). He released servo mechanism to allow rods to fall into core, but their actual movements are uncertain.
0124 (Estimate)		Two explosions were heard - "hot fragments and sparks flew up above the fourth plant, some of which fell on the roof of the turbogenerator room and started a fire".

SECTION 4. ANALYSES OF INITIAL POWER INCREASE (From 1:23 to about 1:23:40)

At 1:23 a.m., the Chernobyl-4 reactor was in a highly unstable condition. The high flow, low power, low void fraction condition was precarious because the void coefficient was very positive and because of the unstable condition that resulted from the sequence of events discussed in section 3 of this report. Appendix F of this report provides a detailed discussion of the RBMK reactivity effects including the void coefficient.

To understand this phase of the accident, the void coefficient versus void fraction curve (figure 2) was constructed by the Team. The basic shape of the curve comes from the Soviet report and Soviet responses to questions at the Vienna meeting. Three points on the curve come from Soviet comments: $0.03\,\Delta K/K/\Delta\alpha$ at the start of the Chernobyl-4 accident sequence, $0.02\,\Delta K/K/\Delta\alpha$ at full power, and $0.01\,\Delta K/K/\Delta\alpha$ at full power for the RBMK-1500. The corresponding void fraction values were calculated using a simple reactor model that used a homogeneous equilibrium model (no subcooled boiling) and a flat power profile. (Should a model be used with subcooled boiling, different power profiles, or other changes, the curve could change significantly.)

The effective void coefficient varies with fuel burnup, rod positions, power distribution, and other effects. Because of the importance of this parameter to the outcome of accident predictions, sensitivity studies (discussed later) were performed.

Although the Team's initial analysis used the variable value of void coefficients shown in figure 2 it was subsequently decided from examination of figure 4 and other associated information that the Soviets used a constant value of $0.03\,\Delta K/K/\Delta\alpha$ for the void coefficient and that this value was appropriate. Hence, the final calculations, both point kinetic and three dimensional, were performed using this value.

Many control and safety systems were inoperative or less effective than normal. Appendix G, RBMK Control Rod System Description, provides a description of the Control Rod System. All but the equivalent of six to eight control rods had been withdrawn from the core (the Soviets say that the plant was not to be operated with less than 16 rods available, hence the plant should have been shut down). Under these conditions, inherent system feedbacks became dominant in controlling the reactor power production, (figure 3). Because of the large positive void coefficient, the reactor power level could potentially drop sharply or go into an excursion, if left on its own.

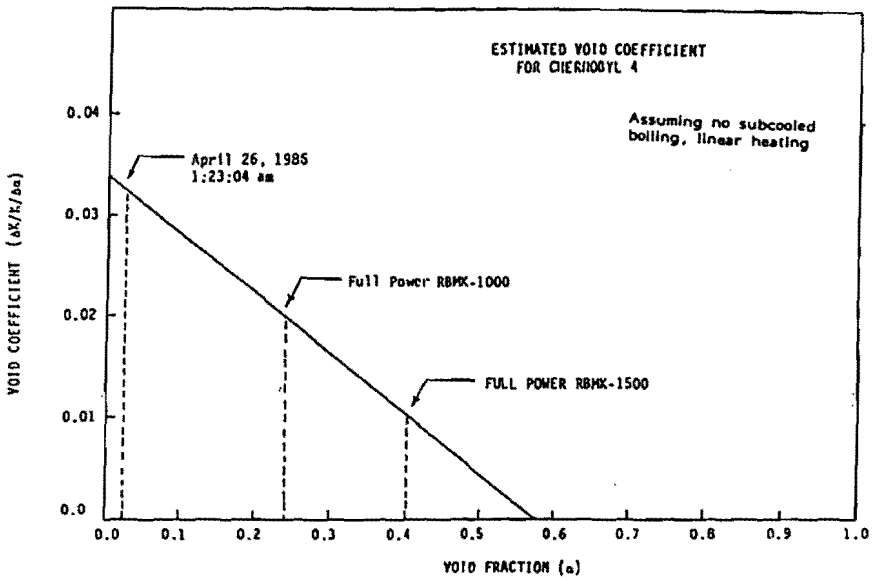

Figure 2. Void Coefficient as a Function of Void Fraction in Chernobyl-4 Core, as constructed from Soviet Comments

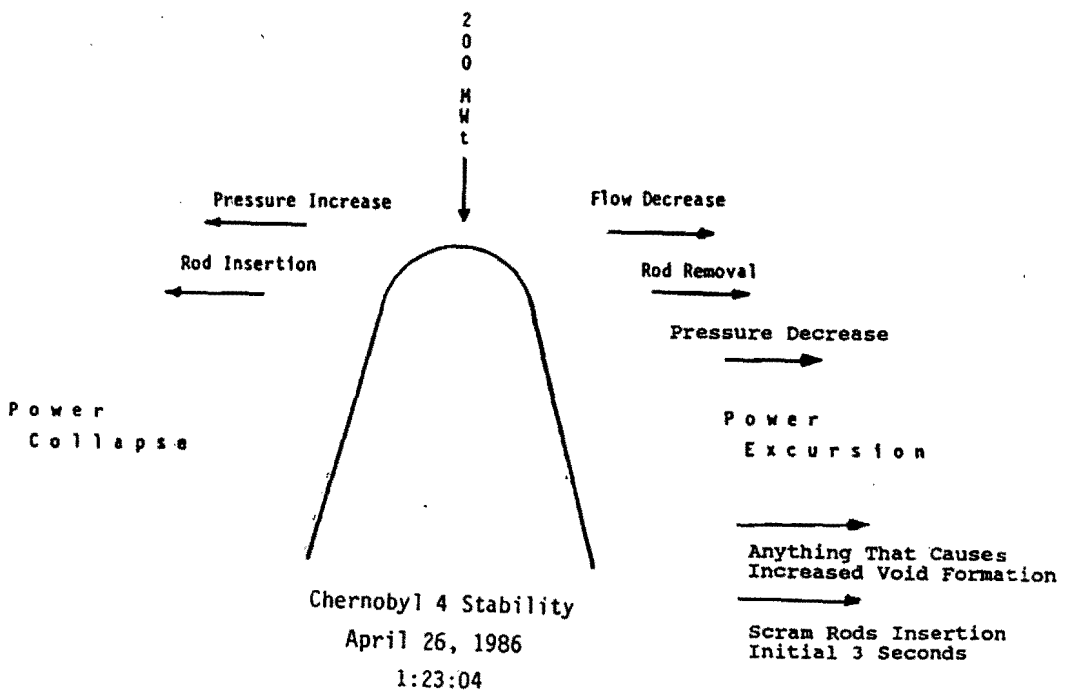

Figure 3.

Figure 4 of this report is the same as the figure 4 provided by the Soviets on August 25, 1986. Figure 4 shows some data (circled) and the results of Soviet analyses of the accident. Figure 5 provides the legend for Figure 4.

Figure 4 Description

Since the Soviets released figure 4 in Vienna, the Team has made a considerable effort trying to decipher all the information contained therein. This figure was released with minimal description, and with a key (legend) having gaps and apparent errors.

At 1:19 a.m., the Chernobyl system was in relative equilibrium, so the Soviets began their analysis at that time. Shortly after 1:19, the operator increased the feedwater in order to restore level in the separators. This set off a small transient that was nearly completed by 1:23 a.m. Because there is a lot of control rod motion during this transient, it is difficult to replicate this analysis without knowing the various control rod worths. However, the system is nearly at equilibrium at 1:23 a.m.

At 1:23:04, the operator reportedly initiated the test by closing off steam flow to turbine generator #8. Data on figure 4 shows the flow coastdown (K) (as pumps coast down), as well as the pressure (C) and water level (L) in the separator. Almost everything else in figure 4 after 1:23 a.m. is from Soviet calculations. However, because most of this analysis has now been replicated, one can attach some credibility to most of the traces on figure 4.

There are two areas where one must be particularly careful. First, the control rod motion is hypothetical, although it is apparent that control rods were being inserted in the 1:23:30 + period. Second, there is a major problem with the steam flow rate. The Team analysis has consistently shown that the pressure build-up in a closed system suppresses a power excursion. Thus, curve M cannot represent the total steam leaving the system. The Soviets have stated informally that steam was being released. The four pressure data circles (C) between 1:23:04 and 1:23:30 indicate that the pressure was indeed being relieved. Examination of figure 4 to determine the total steam flow rate leads to curve (scale 0 to 600 Kg/s), which the Soviets labeled as steam mass quality. However, at 1:23:22 a.m., the 0 and P (void fraction) curves cross, which contradicts the definition of 0 as (steam mass quality). Curve 0 appears to represent the total flow out the turbine bypass valve plus that to turbine generator #8. If this is correct, the bypass valve was re-opened at 1:22:10. Early MINET calculations used curve 0 as the steam flow rate boundary conditions. Current analysis uses the

pressure data as the transient boundary condition and calculates a steam flow rate that looks somewhat like curve O.

At 1:23:40, there is a subtle change in the figure 4 traces, particularly curve B (total reactivity) and curve P (void fraction). The void fraction flattens out, for no apparent reason, yet the reactivity climbs linearly. It is possible the Soviets changed computer codes at this state, or there was an error in the plotting of curve P. There is no apparent reason for the voiding to level out at this stage of the transient.

Between 1:23:40 and 1:23:45, a positive void coefficient driven power excursion is shown. After 1:23:44, the Soviets show their analysis of the reactor disassembly process, complete with fuel coolant interactions and recriticality. At the initial power excursion, reaching about 350,000 MWt, would result in severe fuel damage and rapid changes in the core geometry, this part of the Soviet analysis is speculative.

As part of the U.S. analysis effort, this phase of the accident was initially simulated using relatively simple computer models, e.g., point kinetics, single channel, homogeneous equilibrium modeling, and no subcooled boiling. These point kinetic analyses clearly showed trends similar to that indicated in the Soviet analysis. Subsequently three-dimensional analyses were performed using both static and dynamic models. The three-dimensional analyses are consistent with the point kinetic results. Details are provided and discussed later in this section 4 and in appendix G.

Key to the Curves on Figure 4

SYM		MIN	MAX
A	Neutron power (%)	0	120
B	Reactivity, sum. (%)	-1	+5
C	Pressure, steam drum (bar)	54	90
D	Neutron power (fraction of nom. power)	0	480
E	Rod group AR-1 (fraction inserted)	0	1.2
G	Rod group AR-2 (fraction inserted)	0	1.2
H	Rod group AR-3 (fraction inserted)	0	1.2
K	Flow, MCP (m^3/s) (per loop - 2 loops)	2	8
L	Flow, Feedwater (kg/s)	0	600
M	Flow, steam (kg/s)	0	600
N	Fuel temp (C)	200	2000
O	Steam mass quality (Exit of core, %) (??)	0	6
P	Steam vol. quality (Core average, void fraction)	0	1.2
S	Level (steam drum, mm)	-1200	0

Time Interval changes from 10 seconds to 1 second at 1:23:30

Figure -5.

KEY TO THE CURVES ON FIG. 1

SYM		MIN	MAX	SYM		MIN	MAX
▬	A Neutron power (%)	0	120	—	K Flow, MCP (m^3/s)	2	8
—	B Reactivity, sum. (%)	-1	+5	---	L Flow, Feedwater (kg/s)	0	600
—	C Pressure, steam drum (bar)	54	90	---	M Flow, steam (kg/s)	0	600
---	D Neutron power (%)	0	48000	---	N Fuel temp. (°C)	200	2000
—	E Rod group AR-1 (fraction inserted)	0	1.2	---	O Steam mass quality (Exit of core, %)	0	6
—	G Rod group AR-2 (fraction inserted)	0	1.2	---	P Steam vol. quality (Core average, void fraction)	0	1.2
—	H Rod group AR-3 (fraction inserted)	0	1.2	---	S Level (steam drum, mm)	-1200	0

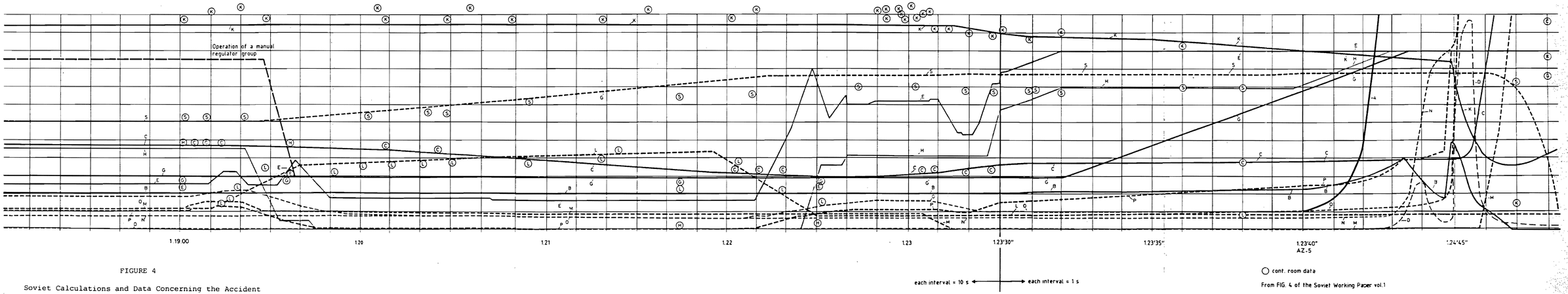

FIGURE 4

Soviet Calculations and Data Concerning the Accident

FIG. 1. The time variation of reactor parameters in the simulation of the Chernobyl accident. Source: Fig. 4 of the Soviet Working Documents, Part I.

MINET Analysis

The MINET Code [NUCL. Eng. Des. 91, p.17] is a highly modular system code used for simulating various LMR, HTGR, and LWR thermal hydraulic systems. The reactor module is relatively simple, using a single coolant channel and point kinetics. The kinetics calculation uses six delayed neutron groups, the prompt jump approximation for a below 50 cents positive reactivity insertion, and an exact solution for larger reactivity insertions. Reactivity feedbacks due to fuel temperature are calculated and utilized. Standard MINET modules were used for the separators, the pumps, and the pipes. The homogeneous equilibrium model option was utilized for the high flow, low void fraction (initially) in the Chernobyl system at the time of the accident.

The MINET representation utilized is shown schematically in figure 6. Key input parameters are shown in table 2. At this stage, the Chernobyl-4 system design details, as well as the information shown in the table, are known fairly well (although not precisely).

MINET has a full steady state capability, with almost no user specified parameters. Form loss factors, representing core inlet orificing were adjusted iteratively to achieve the correct core flow rate. Otherwise, MINET uses mass, energy, and momentum balances to correctly initialize conditions.

In performing transient analysis, there are only a few boundary conditions: the pump coastdown rate, the feedwater flow rate, and the steam pressure which were obtained from data on figure 4. The only inferred boundary condition is the reactivity insertion at the time of scram, which will be discussed later. In the analysis shown here, a small insertion (+0.00048 ^ K) was input at the start of scram (negative reactivity was to come later).

Results of the MINET (M) analysis, starting at 1:23 a.m., are shown in figures 7 through 11, and in many cases with corresponding Soviet (S) calculations. The MINET calculated core flow rates shown figure 7 are actually in better agreement with the data (K circled) than the Soviet curve is. Note that the flow conditioned at 42 seconds is the result of the power excursion, which causes a rapid evacuation of the coolant inventory from the core in both directions. Pressures and water levels in the separators (steam drums) are shown in figure 8. The MINET (M) pressure curve passes through the pressure data (C circled) on Soviet figure 4. Core average fuel temperatures and void fractions are shown in figure 9. The MINET calculated core outlet void fraction agrees closer with the Soviet value, so that value is also plotted. As void fraction and fuel temperature are the dominant reactivity feedback mechanisms, it is the change in these parameters that are important.

MINET Representation of Chernobyl-4 System

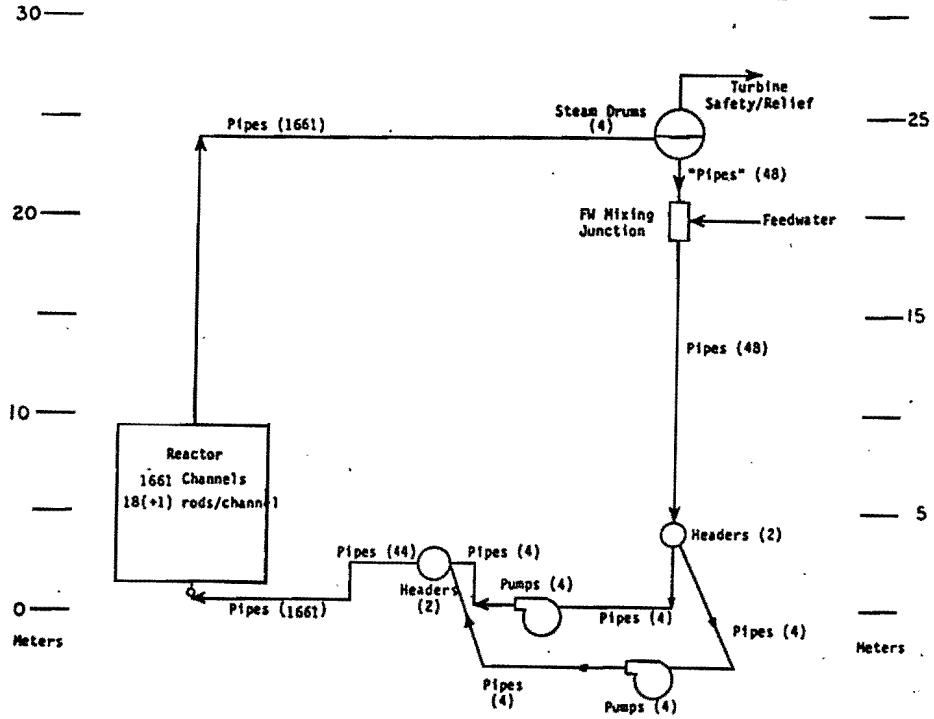

Figure 6.

TABLE 2 Key Parameters and Boundary Conditions in MINET Simulation

Kinetics Parameters

Prompt Neutron Lifetime	0.77 sec
Delayed Neutron Fraction (Total)	0.0048
Void Coefficient ($\Delta K/K\Delta$) (Note 1)	0.03 (constant)
Doppler Coefficient	-1.0×10^{-5} $\Delta K/K/\Delta C$

Initials Conditions

Feed and Steam Flow	100.0 Kg/sec
Power (Thermal)	200.0 MWt
Water Level in Separators	.71 Relative
Pressure in Separators	6.27 MPa
Feedwater Temperature	432.0 K
Pump Heat Input	1.2 MWt/Pump

Transient Boundary Conditions

Feedwater Reset to 80.0
Steam Pressure Controlled Using Data on Figure 4
Pumps Coasted Down to Match Data on Figure 4
10 Cent Reactivity Inserted Right After "Scram" Starts

Note 1: Even though the Soviet comments consistently support a void coefficient curve as shown in our Figure 1, it has become apparent that they've used a constant value of 0.03 in their analysis. This may be due to the fact that almost all the control rods were out of the core, which makes the water even more of a poison (relative) and thus shifts the void coefficient curve upward.

Note that the void fractions are increasing throughout the transient, but that there is little fuel temperature change until the very end. This is because there is excellent cooling core due to high velocity water flow. The fuel is well-cooled until the void fraction grows significantly. The various reactivity parameters are shown in figure 10, along with the Soviet (S) calculated total reactivity (curve B) (the scale on Soviet figure 4 is too coarse to interpret curve B very accurately before 1:23:30). The total reactivity is dominated by the void contribution until the last moments. The peak reactivity in the MINET calculation is about $1.50. The calculated powers are shown in figure 11. The two calculated power peaks are in good agreement (around 300,000 MWt), and both are large enough to cause severe core damage. The MINET thermal hydraulics calculations failed just before 1:23:43 due to the rapid ejection of water from the core and the distortions that resulted.

The agreement between the MINET calculations and the Soviet analysis is striking, despite the small difference in timing. (The timing difference could be due to the control rod movement, which was left out of the MINET analysis.) This MINET analysis clearly established the type of transient displayed in Soviet figure 4, i.e., a power excursion driven by the large positive void coefficient.

It should be noted that the steam flow rate calculated by MINET was indeed non-zero. During the period of 0 seconds to 18 seconds it was determined to be at least 100 Kg/s. Between 18 seconds and 28 seconds it was calculated to be somewhat less, perhaps 60 Kg/s. Between 28 and 38 seconds the calculated steam flow rate dropped off to 10-20 Kg/s on average. Once the excursion begins, the calculated steam flow rate grows substantially. Because the steam flow rate is quite sensitive to the power level, and vice versa, the error in the steam flow rate calculated can be quite large. However, it is quite clear that <u>steam had to be leaving the Chernobyl-4 reactor system during the transient for the pressure data to be correct (and for the power excursion to take place)</u>.

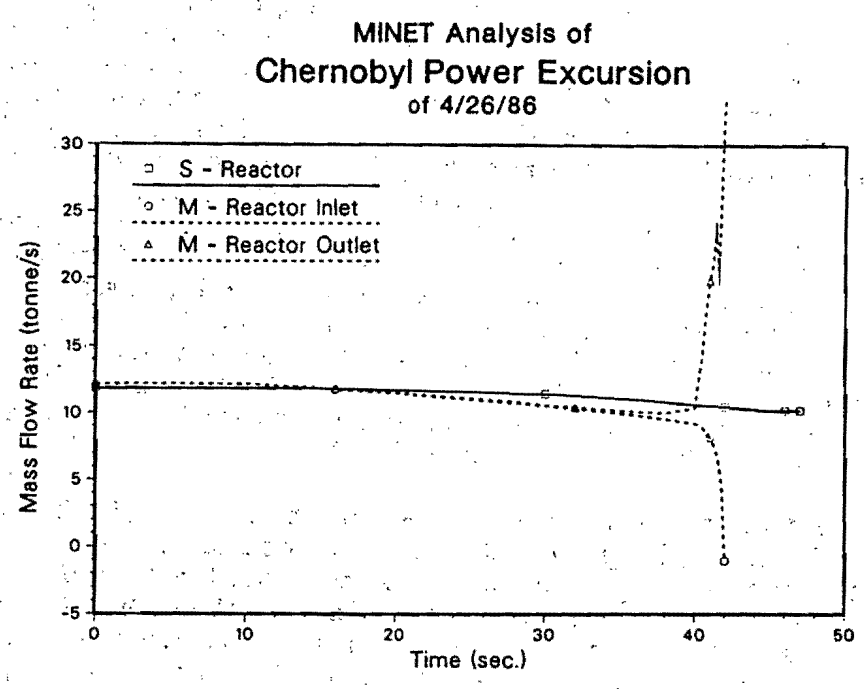

Figure 7. Soviet (S) and MINET (M) Reactor Flow Rates

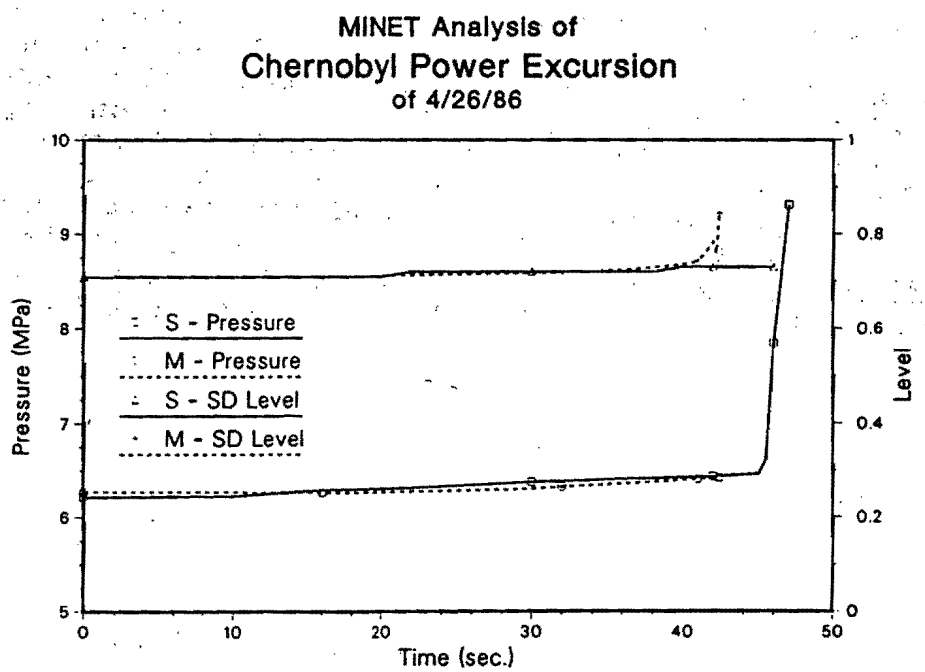

Figure 8. Soviet (S) and MINET (M) Separator Pressures and Water Levels

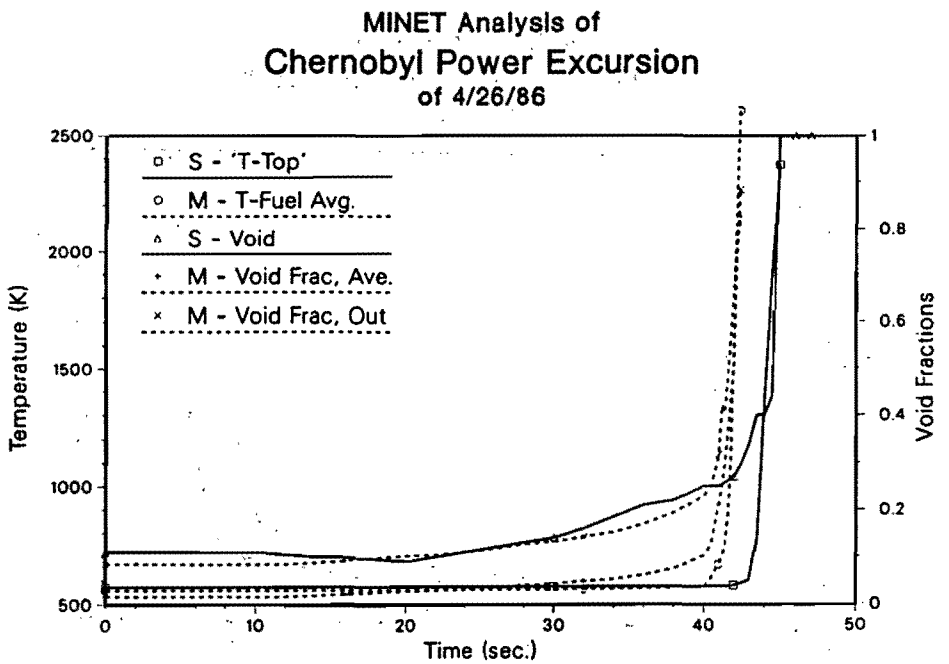

Figure 9. Soviet (S) and MINET (M) Void Fractions and Fuel Temperatures

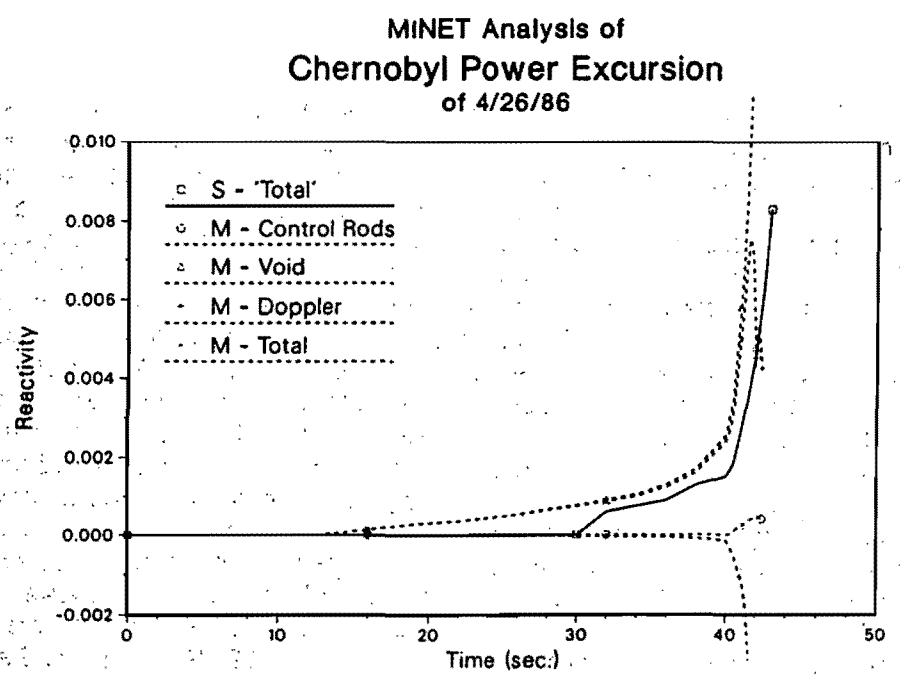

Figure 10. Soviet (S) Reactivity Curve B and MINET (M) Calculated Reactivity, K

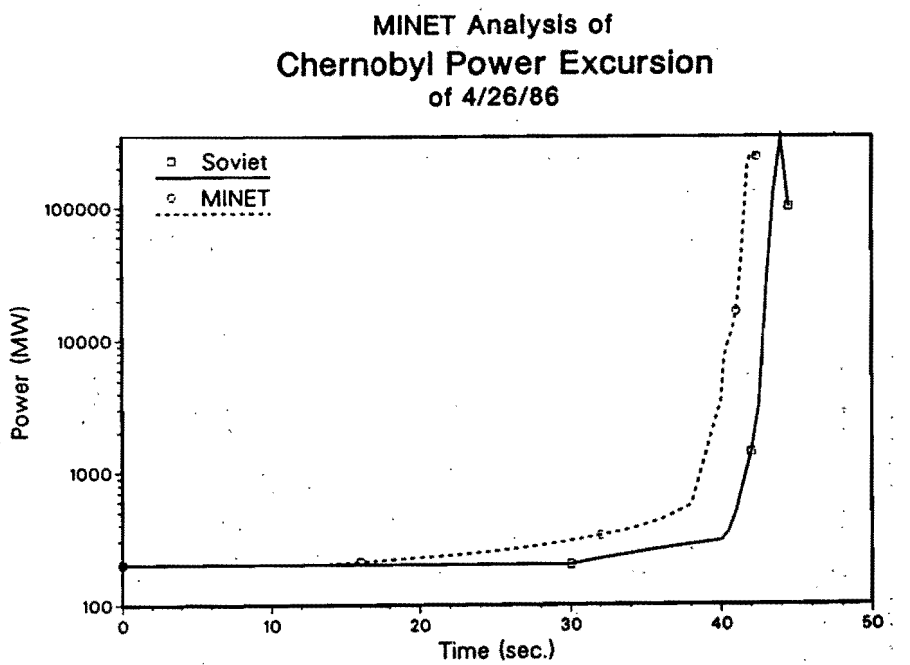

Figure 11. Calculated Power Excursions

CRAS Analysis

Analyses performed by ORNL using the CRAS-1 (Chernobyl Reactor Accident Simulator, Version 1) code show similar power excursions for similar assumptions and boundary conditions. The CRAS-1 includes mathematical models for the calculation of reactor core power generation and heat storage, the mass and energy transported within the coolant system, including the steam drums, and steam flow from the steam drums to the steam lines. Steam property routines and a routine for calculating the density of boiling cooling in an average channel were taken from the BWR-LTAS code, developed at ORNL for severe accident analysis of boiling water reactors. The power generation is described by a six-delayed neutron group point kinetics representation with provision for reactivity feedback due to changes in fuel temperature and coolant void, and for user-input reactivity changes due to control rod movement. Thermal coupling between the graphic moderator and either the coolant or the fuel was neglected because such interaction would take place on a much slower time scale than of interest for the present calculations. The CRAS-1 models are implemented in the IBM CSMP simulation language, using a time step size of 0.01 seconds.

Figure 12 shows CRAS-1 calculations of the April 26, 1986 power excursion at Chernobyl-4. These calculations used the current best estimate of void coefficient (0.03 Δ K/K/ $\Delta \alpha$,constant with void fractions), an average neutron lifetime of 0.0078 seconds, and a total delayed neutron fraction of 0.0048. The CRAS-1 results compare reasonably well with results of the Soviet calculations. The Soviet power curve shown (solid line) is a composite of the Curve A narrow range and Curve D wide range reactor power plotted on figure 4.

CRAS-1 results (figure 12.a and 12.b) were obtained both with (dotted line), and without (dashed line) the initial positive scram reactivity insertion phenomenon as hypothesized by PNL analysts. The code input to describe this phenomenon includes a large (approximately $1.00) positive ramp reactivity insertion of 0.0045 Δ k/k $\Delta\alpha$ over the first 3 seconds of the scram. The higher power peak of the case with initial positive scram reactivity is closer to the Soviet analysis results, lending credence as it includes the 1.5 millik/second positive reactivity ramp observed in figure 4, curve B. Recall, however, that the Team analysis currently indicated a smaller reactivity persions insertion 0.16 is more accurate.

The ORNL CRAS-1 code has a single-node fuel representation, point kinetics for the neutronics, and rudimentary models for the balance of the primary system. This was used for scoping and sensitivity analyses, but it could not give extremely close quantitative predictions of some of the main features of the accident, such as the timing of the pulse(s) and the total energy release.

The Chernobyl-4 core was very large, and the reactivity excursion was very fast, so that a <u>very</u> fine-structure distributed model (both neutronic and thermohydraulic) would be needed for accurate predictions. Detailed input data that is not currently available, would also be needed to set up such a model. Simple models such as CRAS-1 and MINET were used to obtain estimates of the accident's initiating events. Results are generally non-conservative because in the distributed core, local excursions could (and probably did) occur before, and more severely than, the "global" ones.

The CRAS-1 sensitivity studies investigated the uncertainties in both the modeling assumptions and the plant operating parameters that could have been accident initiators. The major, most important model uncertainty was the global void coefficient of reactivity. Originally, the void coefficient function (versus void fraction) shown in figure 2 was used. Later estimates of constant values (0.03 to 0.02 Δ K/K/ $\Delta\alpha$) were determined to be representative of global values. Analysis showed that very large (global) power excursions would not occur for void coefficients

below 0.02, although local ones were not precluded. Variations in assumed total delayed neutron fraction (Beta) between 0.004 and 0.005 had relatively small effects on timing or pulse peak heights. The "effective" core thermal hydraulic response time was varied from 1 to 5 seconds, with the shorter times giving more severe responses (by a factor of about 3). Several other model parameter variations were run which had only minor effects.

Major effects of plant operating parameter variations were seen for primary recirculation flow reductions due to pump rundown or cavitation, increased steam flow from the system (e.g., through an increase in turbine bypass valve flow, opening of pressure relief valves or rupture discs, failure of a transition joint, etc. and core inlet enthalpy increase e.g., through reductions in feedwater flow, increases in feedwater temperature, etc). These analyses showed that any of these three effects could act as an initiator to a serious reactivity accident or exacerbate the excursion with the reactor in the low power-to-flow ratio mode due to the high, positive void coefficient.

CRAS-1 ANALYSIS OF THE CHERNOBYL POWER EXCURSION
OF APRIL 26, 1986

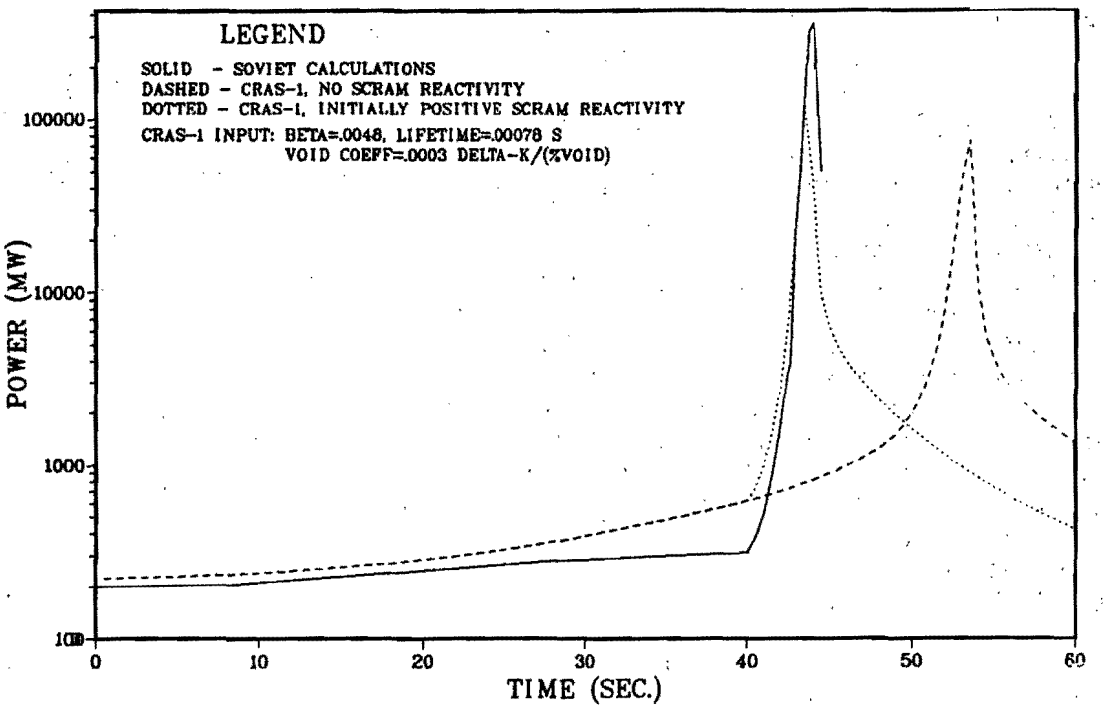

Figure 12.a

CRAS-1 ANALYSIS OF THE CHERNOBYL POWER EXCURSION
OF APRIL 26,1986

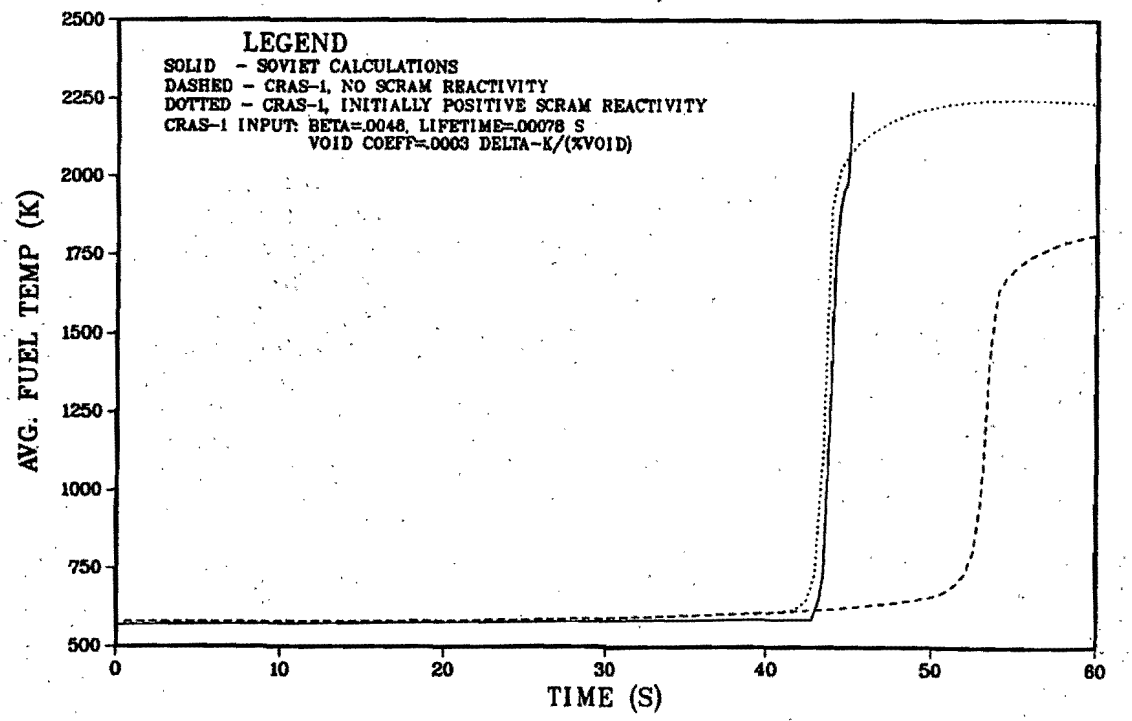

Figure 12.b

SECTION 5. Rapid Power Excursion Analysis (From about 1:23:40 to approximately 1:23:43)

The second phase began at 1:23:40 a.m. This is the time when the operator pushed the scram button. This action initiated the insertion of scram rods. This is believed to have resulted in a positive reactivity insertion during the first 3 seconds, which appears to be present in curve B of figure 4. Both the MINET and CRAS-1 analyses showed that, due to the unstable condition of the reactor, the initial excursion could have occurred without this mechanism for reactivity insertion. It is quite possible that the overpower transient excursion (shown by figure 4 and figures 7 through 12) that lead to the destruction of the plant could have occurred without any additional mechanism to insert reactivity. It is also obvious that the reactor was close to being prompt critical at 1:23:40, and any mechanism that added reactivity to the core would have caused or exacerbated a reactivity insertion and power excursion. The following mechanisms have been identified that could have resulted in such a reactivity insertion.

- A failure of the pressure tube transition joints (see appendix D)
- Opening of the pressure relief valves or rupture discs in the coolant system
- Any failure of the coolant system pressure boundary of other action that increased steam flow from the system
- Main coolant pump cavitation
- Initial Positive Reactivity Insertion or Scram

A sketch of the scram rods is shown in figure 13. Appendix G provides a more detailed description of the Control Rod System. The ends of the scram rods are made of graphite. When the scram rods are reintroduced into the core, some water in the bottom of the core is replaced by graphite. Soviet figure 4 and the Team's neutronics analyses indicate that positive reactivity was inserted over the first 3 seconds after scram. While there is some negative insertion during this period near the top of the core the positive insertion at the bottom is believed to be dominant. Other effects, including flux redistribution, also contributed to this positive reactivity.

Analysis of figure 4 (section 4 of this report) shows that the Soviets believe the scram resulted in the insertion of 1.5 millik/second for a period of 3 seconds starting at 1:23:40.25. However, as the Team's neutronic analyses indicate that actual reactivity effect of the scram may have totaled only about 0.5 millik (see appendix F).

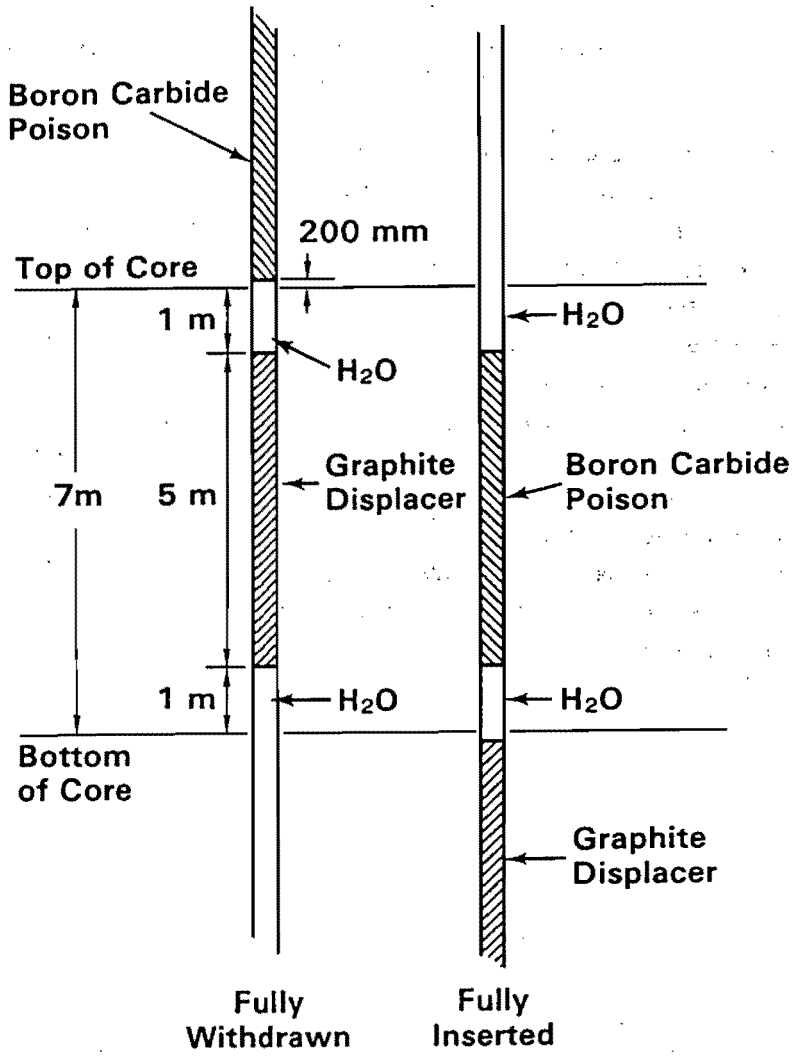

Figure 13. Control Rod/Graphite Locations

Figure 14 provides a quote from the Soviet report that describes a "fix" of inserting the control rods 1.2 meters. Comparison with figure 13 shows that insertion of the rods by 1.2 meters should eliminate this effect.

PRIORITY MEASURES FOR IMPROVING THE SAFETY OF NUCLEAR POWER PLANTS WITH RBMK REACTORS

It has been decided, for the existing nuclear power plants with RBMK reactors, to alter the limit stop switches of the control rods in such a way that, in the extreme position, all the rods are inserted in the core to a depth of 1.2 m This measure will increase the speed of effective protection and eliminate the possibility of a continuing increase in the multiplying characteristics of the core in its lower part as the rods move down from the upper stops. At the same time, the number of absorber-type control rods constantly present in the core will be increased to 70-80, thereby reducing the void coefficient to a permissible value. This is a temporary measure which will be replaced later on by a conversion of RBMK reactors to fuel with an initial enrichment of 2.4% and by the insertion of additional absorbers in the core to ensure that a positive overshoot of reactivity does not exceed 1 Beta for any change in coolant density.

Figure 14.

QUESTIONS ANSWERED BY SOVIETS:

1) How long did it take to shut the reactor down (neutronically)?

Four seconds.

2) What mechanisms caused this shutdown?

The major power increase occurred in the lower center 30 percent of the core. As a result, this lower portion homogenized and shutdown, the upper portion of the moderator blew out from the top and some fuel blew out from the bottom.

Figure 15.

Figure 15 provides information from the Soviets stating that the power increase occurred in the lower 30 percent of the core.

(There are other potential plausible mechanisms for initiating an excursion in the bottom of the core, for example, a failure of lower transition joints, pump cavitation, opening of pressure relief valves on rupture discs, or injection of a saturated coolant.)

Point kinetics calculations of the reactor power assuming the total reactivity function (curve B) of figure 4 were performed. These calculations required values of the delayed neutron fraction (Beta) and prompt neutron lifetime (Lambda) to be input. The best available estimates for Beta and Lambda for the Chernobyl-4 core at 10.3 GWD/MTU burnup are 0.0048 and 0.77×10^{-3} s, respectively. However, to reproduce the Soviet results, it was necessary to use Beta=0.0063 and Lambda=1.0×10^{-3} s (figure 16). With Beta=0.0045, a value of Lambda=2.0×10^{-3} s is needed to reproduce the power trace of figure 4. In other words, for the total reactivity and reactor power on figure 4 to be consistent, either a value of Beta much larger than the best estimate value or a value of Lambda much larger than the best estimate value, or a combination of both needs to be used.

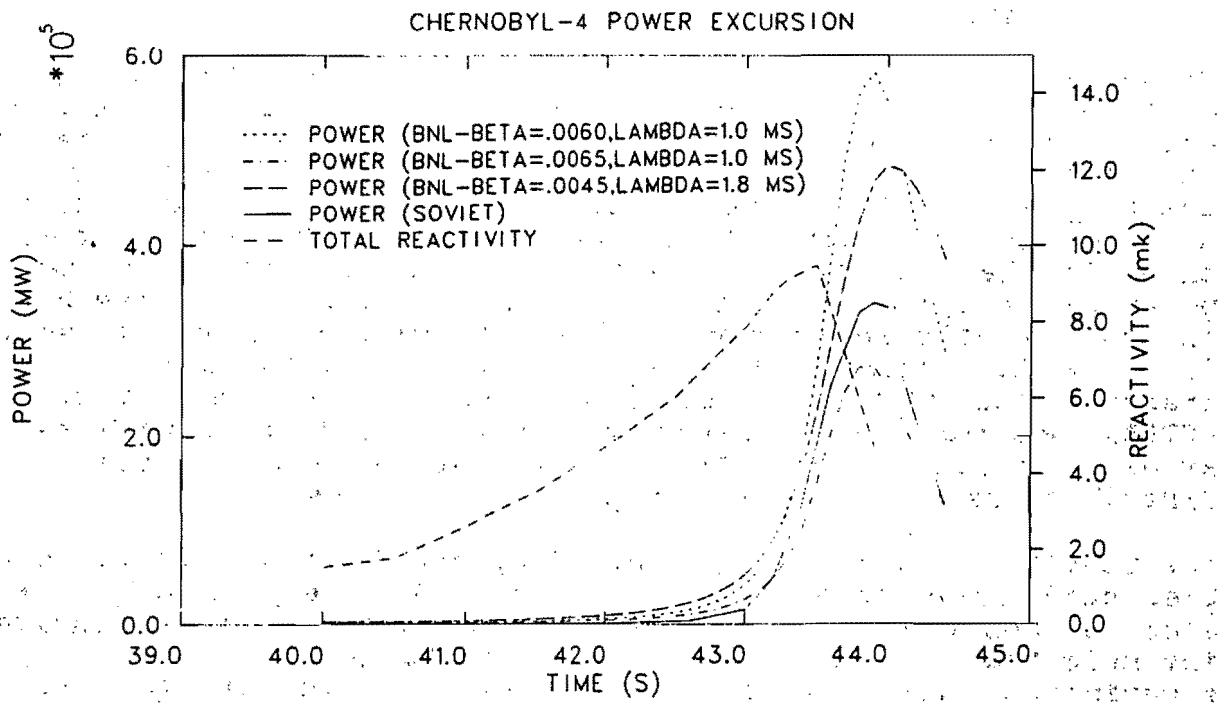

Figure 16. Power Traces Calculated From Soviet Reactivity Curve B Using Point Kinetics With One Delayed Neutron Group

SECTION 6. ENERGETIC EVENT ANALYSES (AFTER 1:23:43)

6.1 Introduction

The energetic events associated with the fuel failures and fuel-coolant thermal interactions (FCIs) were evaluated for the Chernobyl-4 transient overpower (TOP) event using accident analysis codes developed at ANL. The codes had originally been developed to perform safety analyses pertaining to liquid metal fast breeder reactors (LMFBRs). Specifically, the codes were developed to mechanistically describe the phenomena occurring during a severe TOP accident such as rapid energy release and heatup of the fuel, fuel melting, internal fuel pin pressurization, cladding failures, ejection of fuel into the coolant channels, fuel-coolant thermal interactions that cause rapid steam generation in the channels, channel pressurization, coolant slug expulsion, and the response of the piping system to the transient pressurization and coolant dynamics. The codes used in the present analysis of these phenomena included:

FPIN-2	(fuel element mechanics)
EPIC	(fuel-coolant thermal interaction)
ALICE-2	(fluid-structure interaction)

These codes were modified to depict the Chernobyl-4 reactor configuration and the particulars of the fuel and cladding materials and the water coolant. The model used for the code calculations depicts a single representative channel of the Chernobyl-4 1,661 channel core configuration. The channel modeled in the calculations is considered to be an average channel; that is, the values used for coolant flow and reactor power are the core-wide average values. It was not possible in the time available to perform the extensive revisions necessary in FPIN to include all the necessary cladding-to-water heat transfer and flow regimes; hence the approach was to perform RETRAN calculations to determine channel conditions such as the axial cladding temperature distribution and coolant void distributions as far into the transient as possible.

The results of the RETRAN/FPIN, EPIC, and ALICE calculations are presented in sections 6.2, 6.3, and 6.4 respectively. Fuel element behavior and FCI energetics have been extensively investigated in the U.S., and the results of pertinent in-pile experiments are additionally summarized in section 6.1.2. Section 6.5 provides a best estimate evaluation of the initial damaging events of the accident including the effects of noncoherent fuel element failures. Following the initiating events, the uncertainties in the course of the accident become dominant, and although one can speculate about subsequent events, it was judged unwarranted to attempt additional mechanistic calculations with the present state of knowledge.

6.1.1 Interpretation of the Russian Fuel Failure Analysis

Simple calculations were performed to understand the Soviet approach in calculating fuel element failures which resulted from the transient overpower event. Figure 17 is a reproduction of key parameters calculated by the Soviets and presented in their figure 4 from the report on the accident.[1] The figure shows reactivity, reactor power, core average coolant void fraction, and flow from the main coolant pumps during the time interval of the destructive events. The time scale is the same as used by the Soviets; the scram (AZ-5) button had been pressed at 1:23:40. On an expanded scale the reactor power would be seen to increase rapidly starting at 40 seconds; in figure 17 the power axis is in units of multiples of full power (x 3200 MWt), and so the scale is exceedingly compressed. The peak of the first power transient occurred at 43.9 seconds and was about 109 times full power in amplitude (350,000 MWt). The power burst was the result of increasing (uncompensated) channel void reactivity plus the reactivity insertion due to the "positive" scram. These positive reactivity effects were reduced during the TOP only by the fuel Doppler coefficient. In the Soviet model the fuel failed coherently at 44.7 seconds. The results of the fuel failures and ensuing FCI's are apparent in their analysis, namely (1) the remaining coolant was expelled from the channels causing the core average void fraction to increase from 41 percent to 100 percent by 44.9 seconds; (2) the abrupt coolant expulsion caused a step increase in reactivity amounting to .016/.0048 = $3.3; (3) the reactivity step caused a distinct second power burst in the Soviet model where the peak power was 470 times full power (1,500,000 MWt) and the energy release was about four times that of the first calculated burst; and (4) the upstream propagation of the FCI pressure wave caused an abrupt decrease in the flow of the main coolant circulating pumps.

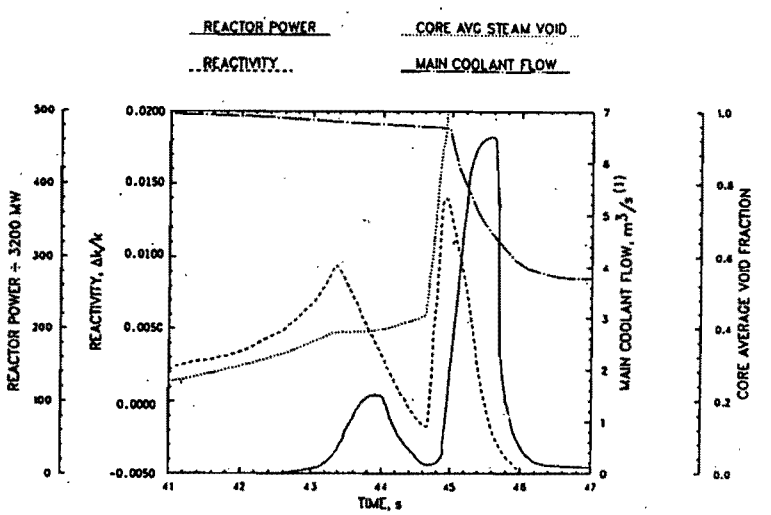

Figure 17. Soviet Calcualtions of Reactor Parameters at Time of Chernobyl-4 Accident Events

The condition of the fuel at the time of failure was estimated using the Soviet analysis results shown in figure 4. Figure 18 shows the first power burst on an expanded scale and also shows the cumulative energy release in the fuel during the transient. The energy release is presented in J/gUO_2, where the total fuel mass is reported to be 215 x 10^3 kg UO_2. The values presented are core wide averages without application of peaking factors for the present. At the Soviet calculated fuel failure time of 44.7 seconds, the energy release in the power excursion was 1360 J/gUO_2 (326 cal/g). The fuel enthalpy was estimated by adding the energy deposition during the transient to the initial enthalpy at the low power operation and subtracting for estimated heat loss to the coolant during the transient. The result is shown in table 3, where enthalpy is referenced to zero at 300K.

The heat loss estimate is based on a representative value of heat flux in the post-CHF domain in a forced convection cooled rod bundle, about 1 x 10^6 BTU/hr ft^2 (3 MW/m^2). The resulting estimated fuel enthalpy is 1242 J/g UO_2. This magnitude of enthalpy is associated with UO_2 fuel that is melting;

Table 3.

		Enthalpy, J/g (cal/g)	
a.	Enthalpy at initial low power operation	67	(16)
b.	Estimated energy release in power burst to time of fuel element failures	1360	(326)
c.	Estimate of energy transferred to coolant during power burst	-185	(-44)
d.	Estimated enthalpy at time of fuel element failures	1242	(298)

Estimate of Fuel Enthalpy at Time of Fuel Element Failures in Russian Model

the value suggests a core-wide average melt fraction of about 35 percent at the time of fuel failures. There appears to have been no attempt by the Soviets to calculate a time sequence of fuel failures based on variation in power-to-flow among the 1,659 channels or upon power peaking within the channels. Fuel failure conditions calculated using FPIN and EPIC are described in

sections 6.2, 6.3, and 6.5 and are compared with the Soviet's results.

It is of interest to apply the estimated fuel failure conditions to arrive at an order of magnitude estimate of the fuel-coolant thermal interaction (FCI) energetics in the coolant channels. Using the average fuel enthalpy of 1.24 MJ/kg UO_2 and a fuel mass of 130 kg UO_2 per operating channel, the total fuel enthalpy is about 160 MJ. Typical efficiencies for the conversion of thermal to mechanical energy by an FCI amount to 0.5 percent or less based on the entire fuel mass. Hence, a reasonable estimate of the mechanical energy release is about 1 MJ, which is sufficient to cause appreciable damage to a piping system such as the Chernobyl-4 operating channels. Mechanical response of the piping system was calculated using the ALICE code, and results are presented in section 6.4.

6.1.2 Data Base for Fuel Behavior During Power Excursions

Beginning in the early 1950s, there were extensive investigations in the U.S. of the phenomena and consequences of power excursions for various core designs and fuel types. These included the early BORAX and SPERT tests that demonstrated that a power excursion would be self-limited by the negative Doppler effect. Other effects also contributed to the self-termination of power transients, notably coolant void formation when the excursion was sufficiently severe to cause boiling. This is because in U.S. reactor designs the coolant is the neutron moderator and so loss of moderator by steam generation causes immediate neutronic shutdown. This is in contrast to the behavior of the Chernobyl-4 design in which increasing steam generation causes reactor power to increase due to the positive coolant void coefficient and fixed graphite (over) moderator. (See appendix C for a discussion of the relevant differences between the RBMK and U.S. reactor designs which preclude a Chernobyl-4-type accident from occurring here.)

Following whole-core transient testing in the BORAX and SPERT programs, transient test reactors such as TREAT, SPERT IV (Capsule Driver Core), and PBF were utilized to test fuel element failure thresholds, fuel-coolant interactions, and metal-water reactions for various fuel element designs and burnups. The severity of the power excursion imposed on the test fuel was typically progressively increased to determine the energy depositions corresponding to cladding failures, fuel element breakup into large fragments, and catastrophic failures involving fine-scale fragmentation and FCI's. Extensive studies of these phenomena were performed to characterize the fuel behavior despite the fact that with the evolution of U.S. reactor designs incorporating inherently stable neutronic approaches, there was no mechanism to produce such severe power excursions. For

example, the common example cited, of a possible power excursion in a U.S. reactor, involves a BWR main steam isolation valve closure ATWS sequence with simultaneous failure to trip the recirculation pump.[3] In this sequence, the transient pressure increases from about 7 to 9 MPa which causes collapse of steam in the core (a positive reactivity effect). According to RAMONA code calculations, the peak of the power excursion is only about 2.2 times full power. This is exceedingly small in relation to the Chernobyl-4 overpower event and is far too small to cause either fuel melting or failures. While power excursion events have been extensively studied in the U.S., there is no identifiable initiator of events of sufficient severity to cause damage to the fuel in U.S. reactor designs.

TREAT LWR Tests[4]

Transient overpower (TOP) testing of sample LWR fuel was conducted in the Transient Reactor Test (TREAT) facility during the 1960s. The fuel element designs tested were of a wide variety including unclad UO_2 rods, unclad Zr-U alloy plates, stainless steel clad UO_2 pins, and Zircaloy clad UO_2 pins. The latter included tests of single fuel elements, four-element clusters, and nine-element clusters. The pins were submerged in water in an autoclave which was placed in the test slot in the center of TREAT. The test fuel of 11.2 percent enrichment was subjected to a power burst from the TREAT driver core. In general, the shorter the reactor period the greater the energy release in the test fuel although this could be varied somewhat. (Shaping of power bursts was introduced later.) The fission energy in the test fuel was determined via calibrations with activation wires. After the transient the residue was removed from the autoclave, characterized, and particle size distributions were determined for those cases where fragmentation was extensive. The extent of metal-water reaction was determined by measuring the mass of hydrogen generated. Test results were interpreted to indicate that fuel failure and extensive fragmentation began at an energy input equivalent to complete melting of the fuel (340 cal/g) although the actual fuel enthalpy would have been less than this owing to heat loss during the transient. The fuel and cladding cracked into large chunks at smaller energy input, thought to be attributable to coolant re-entry effects. The mean partial diameter of fragmented debris decreased sharply at energy inputs above the failure threshold and reached a nearly constant value of about 0.5 millimeters diameter at high energy inputs.

SPERT IV CDC Tests[5]

These capsule tests were similar to the TREAT tests except that the reactor periods available in the SPERT Capsule Driver Core (CDC) facility were significantly shorter than in TREAT. Hence,

the energy deposition was more adiabatic than in TREAT; since all tests were started from room temperature, the energy deposition was probably close to the peak fuel enthalpy. Test results showed that the fuel elements remained intact below about 260 cal/g, fractured into large chunks between about 260 and 300 cal/g, and fragmented into small particles at higher energy depositions. The mean particle diameters were somewhat smaller than those found in the TREAT tests, ~0.15 millimeters for greater than 600 cal/g energy input.

TREAT LMFBR TOP Tests[6]

Numerous in-pile tests of LMFBR fuel behavior were performed at the TREAT reactor in support of FFTF and CRBR licensing issues. Among the tests performed were the H and E-series tests which were performed under severe transient overpower (TOP) accident conditions. The E-series tests were performed under particularly severe conditions analogous to the severity of the Chernobyl-4 power excursion. Test E8,[7] for example, contained a bundle of seven mixed oxide fuel pins which had been irradiated at low power to 5 atm percent burnup. Hence, the fuel was nominally unrestructured and had retained most of the fission gas in the fuel matrix, as was also the case for the Chernobyl-4 fuel. The test fuel was preheated at nominal full power conditions and was then subjected to a $3/second transient (0.16 second initial period), peak power of 33 times nominal power, and pulse width of ~0.8 seconds. The fuel elements began failing when the energy deposition had caused about 50 percent areal melt fraction at the axial peak. Fuel from the central molten cavity plus the unmelted annulus was ejected into the flowing coolant (sodium), driven from the pins by fission gas pressure. The channel subsequently voided in the upward direction, and about 2 percent of the fuel mass was dispersed to above the top of the active fuel where fuel and cladding material froze forming a substantial channel blockage. The channel voiding dynamics were attributed to a mild fuel-coolant thermal interaction which expelled a mixture of fuel, coolant, and fission gas. Subsequent to the upper channel blockage, molten fuel and cladding contacted the flow tube wall and precipitated failure of the channel boundary.

PBF RIA Tests[8]

A series of tests were performed in the Power Burst Facility (PBF) during the late 1970s in which single and multiple-rod bundles of LWR fuel were subjected to severe power excursions, representative of reactivity initiated accidents (RIA). The test fuel was contained in a water loop, and coolant thermal hydraulic conditions were representative of hot-startup conditions in a boiling water reactor (BWR). Although the best estimate of peak fuel enthalpy during a BWR rod drop accident is said to amount to less than 110 cal/g UO_2, the test program examined enthalpies in

the range of 185 to 350 cal/g. Not surprisingly, fuel failures occurred in many of these tests. With one exception, the rod failures occurred for energy releases equivalent to a peak enthalpy of 250 cal/g or greater. Of particular interest was the result of a single-pin, fresh fuel scoping test, designated RIA-ST-4.[9] The fuel element was subjected to a 76 milliseconds power burst; the rod failed 32 milliseconds after initiation of the power burst when the fuel enthalpy radially averaged at the axial flux peak location was 350 cal/g (100 percent local melt fraction). A peak pressure of 35 MPa was reported in the coolant channel (normal pressure = 6.45 MPa), and a peak coolant temperature in excess of 940K was measured above the rod after fuel rod failure. From analysis it was concluded that the transient pressurization event was caused by a fuel-coolant thermal interaction. About 20 percent of the total fuel and cladding mass were fragmented during the test, and of this, about 58 percent (90 g) had been fragmented into small particles less than 2.0 millimeters effective diameter. The median particle size was 1.3 millimeters. The coolant kinetic energy estimated from the interaction amounted to about 3.4 kJ; the overall thermal-to-mechanical energy conversion efficiency was about 0.3 percent.

6.2 Fuel Failure Analysis

This subsection describes the results of RETRAN thermal-hydraulics calculations and FPIN2 fuel failure predictions. Three important input specifications were required for the average channel calculations: (1) the shape of the power transient, (2) the coolant flowrate, and (3) the axial power distribution. The power excursion was selected to be the Soviet calculated transient from figure 4 of the Soviet report on the accident. This power shape was selected as the reference case to enable comparisons with the Soviet calculations (section 6.1.1). This is also consistent with U.S. code calculations of the power transient in that they used the Soviet calculated transient as the basis for comparison. If, in fact, the actual initiating power excursion differed significantly from the Soviet calculation, the timing and details of events will differ accordingly from the results presented here. Timing and details of the calculations aside, channel conditions and fuel behavior under severe overpower heating conditions, which obviously led to fuel failures in this accident, are described. These calculations cease with loss of intact geometry; subsequent events are described in following sections.

The coolant flowrate during the transient was taken from the Soviet calculations (figure 17). The flow given in this figure is per loop, and there are two loops in this reactor design.

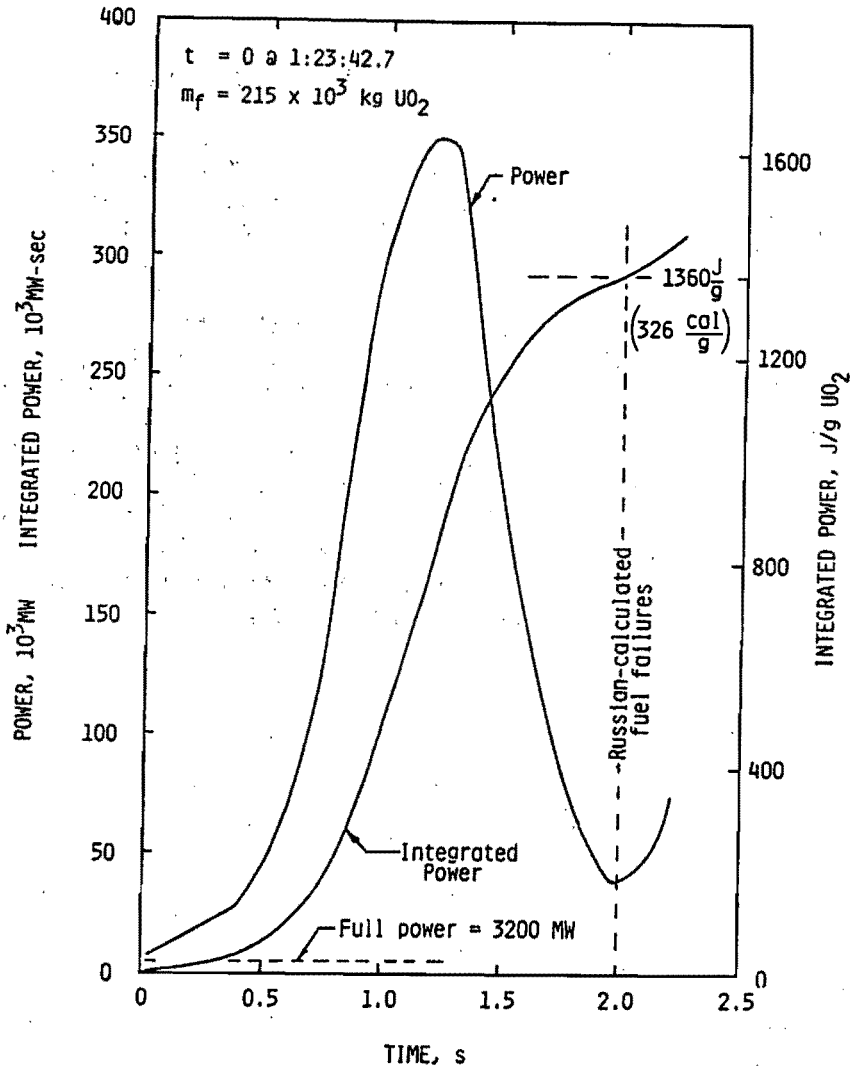

Figure 18. Soviet-Calculated Power and Fuel Energy Deposit for Chernobyl-4 Transient Overpower Accident

One of the objectives of the U.S. analysis of the reactor power behavior was to attempt to quantify the axial power distribution, not only at the beginning of the test when the Soviets reported it to be axially double-humped, but particularly during the power excursion itself when the power distribution was affected by control rod motions and channel void distribution. Without specific knowledge of the distribution during the excursion, the approach was to perform reference calculations using a uniform axial distribution and to revise this with U.S. estimates of the actual distribution as they became available. However, power shape calculations were not available for use in the fuel failure calculations, and so the reference case is the only case presented. The uniform axial distribution is consistent with the Soviet whole-core average approach; the effects of local power peaking will be addressed in later sections.

6.2.1 RETRAN Calculations of the Power Excursion Thermal Hydraulics

The RETRAN02-Mod3 computer code[10] was used to model the thermal hydraulic events during the power excursion that occurred in the Chernobyl-4 RBMK-1000 reactor. A core model was developed which represented a single, average process channel divided axially into 12 equal length fuel sections. Light water coolant is supplied from an inlet plenum at constant enthalpy and at flow rate taken from Soviet data. A very large exit plenum is modeled which provides constant exit pressure during the transient.

To ensure proper modeling of the RBMK-1000, benchmark calculations were first made for full power, steady-state operation. The ensuing RETRAN results were remarkably close to the published plant parameters. Some of these results are shown in figure 19. The agreement achieved gave confidence in the use of the model for the accident conditions.

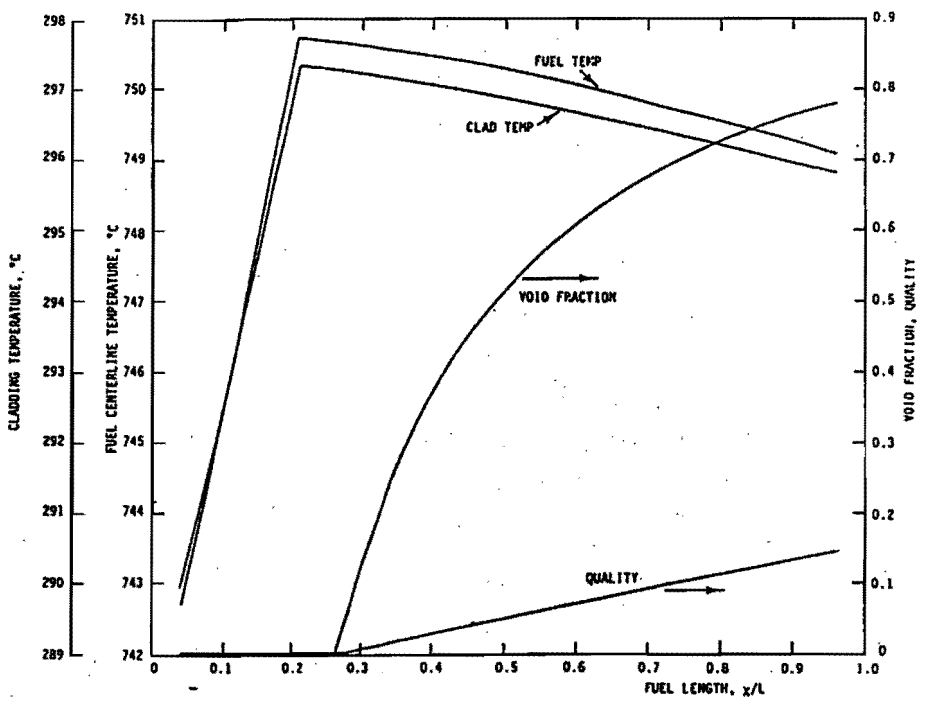

Figure 19. Fuel and Channel Conditions Calculated by RETRAN for Chernobyl-4 Full Power Operation

Proceeding with the accident calculation, certain assumptions were made. The homogeneous equilibrium option was used for the slip model. The axial power profile was assumed uniform, as discussed previously. Thermo-physical properties of the UO_2 fuel, zirconium alloy cladding, and the fuel-to-clad gap conductances were taken from tabulated data for a typical U.S. BWR. The initial reactor power, the subsequent power burst, and the coolant mass flow rate were all taken from the Soviet calculations. The coolant inlet temperature was assumed constant at 270 C.

At the initial power level of 200 Mw (6.3 percent of full power) and full flow, no steam voids were produced in the RETRAN calculation. During the power excursion the fuel centerline axial temperature profile remained flat; this was due to the assumed flat power shape and also to the thermal time constant of the fuel being long compared to transient changes at the surface. The centerline temperature reached melting (2850 C) at 44.15 seconds in these calculations. The development of the axial cladding temperature distributions and channel void distributions are shown in figures 20 and 21, respectively.

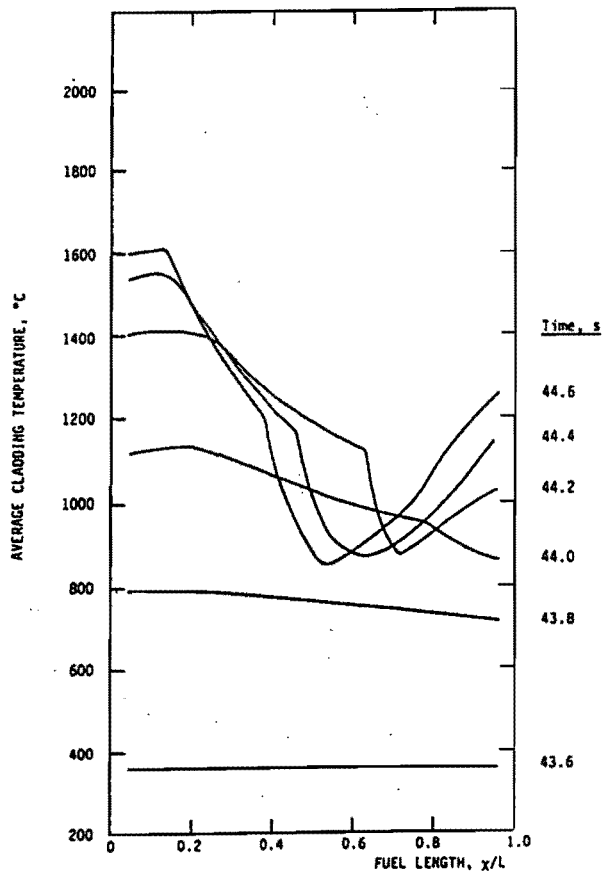

Figure 20. RETRAN Calculations of Development of Cladding Temperature Profiles During Soviet Calculated Power Excursion; Uniform Axial Power Distribution

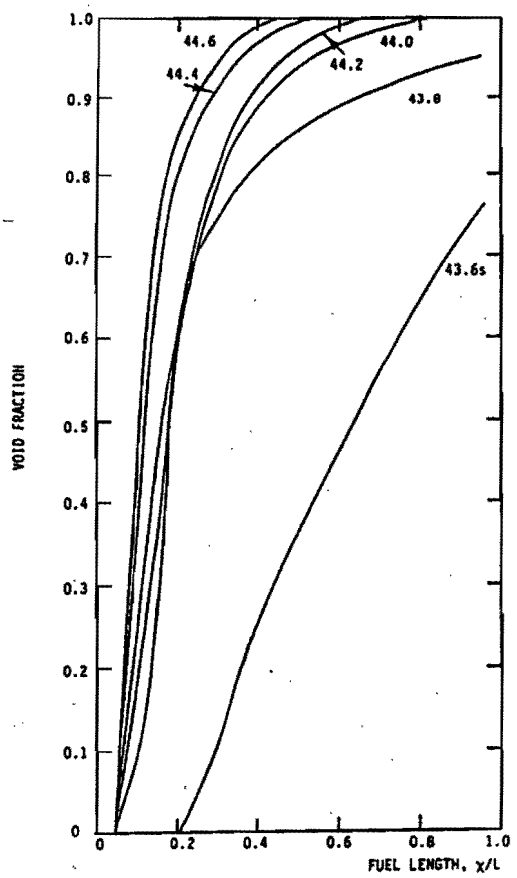

Figure 21. RETRAN Calculations of Development of Channel Void Distributions During Soviet Calculated Power Excursion; Uniform Axial Power Distribution

Initially, the cladding temperature is nominally uniform axially. By 43.8 seconds the entire channel is in film boiling, and the amount of vapor production increases rapidly. Two-phase velocities become large in the upper channel region, and the high velocity flow causes better cooling of the cladding in these calculations than does stable film boiling with a liquid core characteristic of the bottom region. As the void fraction in the upper region becomes unity, RETRAN switches from the Groenveld heat transfer correlation for stable film boiling to the Dittus-Boelter correlation for single phase steam. At 44.2 seconds, for example, this occurs at x/L about 0.62. When the switch in correlation occurs, a large (about 4 times) increase in heat transfer coefficient results, thereby actually causing the cladding temperature to decrease in part of the upper zone, as shown in figure 20. The calculation could not be carried beyond 44.6 seconds with RETRAN, at which time RETRAN predicted a large fuel melt fraction (although fuel melting is not specifically tracked by RETRAN). This is about 0.2 seconds before the fuel failure time calculated by the Soviets.

The RETRAN results show two important features. First, the cladding peak temperature becomes very high although it does not reach melting. The substantial heatup of the cladding suggests an important effect of cladding weakening needed to be modeled by FPIN. Additionally, the cladding temperature is calculated to be hottest in the lowest part of the core, indicating that cladding failures may occur first in the lower core region. If as suspected the axial power shape peaked in the bottom of the core during the power excursion, this would have further biased the fuel failures toward the bottom. Secondly, the channel void fraction is very high. By the end of the excursion, the coolant is largely being converted to steam in the bottom quarter of the core. The upper half of the channel contains single-phase superheated steam. The numerical value of the average void fraction at 44.6 seconds calculated by RETRAN is 72 percent which is significantly larger than the Soviet calculated value of 40 percent. In either case, fuel failures at the cladding hotspot in the bottom zone of the core would lead to forced intermixing of hot fuel and cladding material with liquid water, giving rise to a likely fuel-coolant thermal interaction.

6.2.2 FPIN2 Fuel Failure Analysis

The response and failure of RBMK-1000 fuel pins during the Chernobyl-4 accident event were analyzed using the FPIN2[11] fuel pin behavior code developed at Argonne National Laboratory. The following sections give a brief description of the code and the models that were used for the calculations and present the results of analysis of pin behavior prior to fuel disruption.

6.2.2.1 The FPIN2 Code

The FPIN2 code calculates the transient thermal and mechanical response of a fuel pin which is divided into a number of axial segments (as many as 20 in the current version). In general, each segment can have regions containing molten fuel, solid fuel, cracked fuel, and solid cladding. When the heat transfer option to calculate the coolant temperature is invoked, the fuel pin is surrounded by a circular coolant channel and outer wall. Each axial segment of fuel and cladding is further divided radially into a number of finite element rings (20 in the fuel and 10 in the cladding). Figure 22 shows a schematic of the fuel pin geometry. Axial symmetry of temperatures and external loads is assumed and gradients of temperature and loads in the axial direction are assumed small.

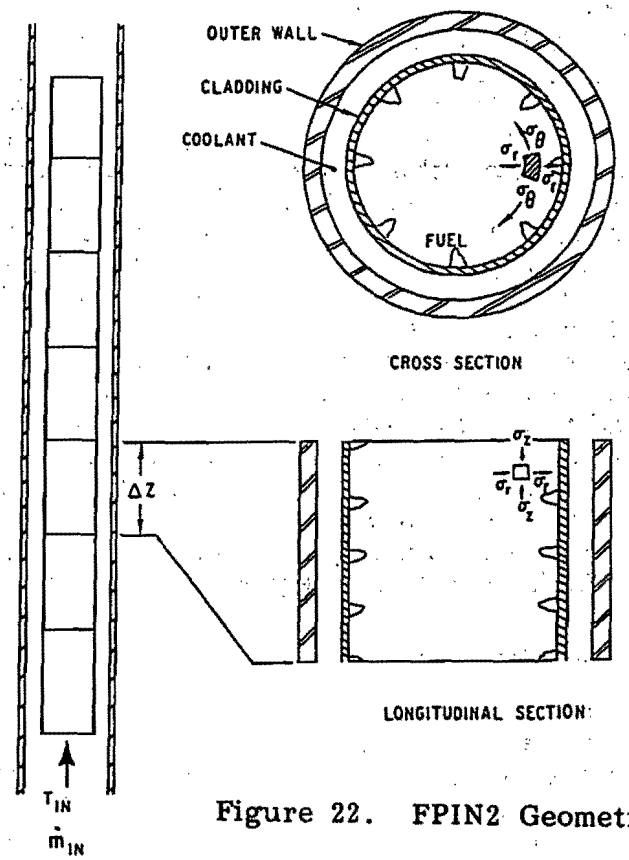

Figure 22. FPIN2 Geometry

Although the primary emphasis in the FPIN code is on the mechanical analysis of fuel and cladding, a complete heat transfer analysis is also included. The basic assumption is that heat is conducted only radially in the fuel and cladding and convected axially by the coolant. Two overall options for the temperature calculation are available. In the first, temperatures are calculated for a symmetric system consisting of a single fuel pin surrounded by an annular coolant flow channel with an outer boundary formed by a cylindrical outer wall. In this case, coolant inlet temperature and flow rate must be provided as a function of time. For the second option, the cladding outer surface temperature is provided and the fuel and cladding temperatures are calculated. The one-dimensional heat conduction problem for the fuel, cladding, and outer wall is then solved using the Crank-Nicholson implicit finite difference method. Since the thermal conductivity and heat capacity are temperature-dependent, the resulting finite difference equations are nonlinear. These equations are solved by a simple iteration in which the material properties are evaluated using the most recently calculated temperatures so that the finite difference equations become linear. Convergence of this direct iteration is very fast for the time steps generally used in FPIN2.

Because axisymmetry and generalized plane strain are assumed, the mechanical analysis is one-dimensional. The FPIN2 code uses a finite-element method that allows flexibility in handling various constitutive equations and cracking models. Simple linear elements are used that provide the framework needed to handle the complications due to complex material behavior and moving boundaries due to fuel cracking and melting. The finite-element equations are derived from the equations of virtual work and linear, one-dimensional shape functions. For each axial segment, the fuel and cladding elements are combined into a single set of equilibrium equations for the radial and axial displacements. In this way, the fuel-cladding contact pressure comes out of the analysis without separate iteration. Since a variety of separate (generally nonlinear) constitutive equations are allowed, the equilibrium equations are nonlinear and are solved using an algorithm based upon residual error balancing. A major aspect of the procedure is the determination of the nonthermal-elastic strains. The basic calculation of the finite-element analysis is the repeated solution of a set of linear equations approximating the equilibrium equations. This yields a set of nodal displacements that are used to calculate total strains. Then a separate iterative calculation is required to split the total strains into elastic, thermal, plastic, creep, swelling, and cracking strain components such that all material constitutive equations are satisfied.

The fuel cracking model used in FPIN2 allows cracks in the radial (R = constant) and/or transverse (z = constant) planes. To account for the four possible crack patterns, four types of elements have been defined as follows:

Type I: Uncracked fuel,
Type II: Only radial cracks are present,
Type III: Only transverse cracks are present,
Type IV: Both radial and transverse cracks are present.

The type of a particular element is determined by a fracture and crack closure rule. The derivation of the element stiffness equations is based on a perturbation of the equations for a three-dimensional fuel pin analysis. The resulting formulation can be shown to converge to the three-dimensional formulation as the numbers of cracks becomes large.

When a reactor transient is severe enough to melt fuel, pressure can build up in the central molten cavity and have considerable influence on the eventual failure of the pin. This pressurization is caused by the release of fission gas and the 10-20 percent expansion of the fuel when it melts. The volume available to the gas comes from the porosity and crack volume released when the fuel melts, and displacement of the solid fuel boundary. This volume is found by calculating the total volume

within the displaced cavity boundaries and subtracting the volume of the incompressible fuel. An iterative procedure is then used to find the cavity pressure that is consistent with this cavity model and volume available due to the displacement of the solid fuel boundary.

6.2.2.2 RBMK-1000 Fuel Characterization

The RBMK-1000 core has upper and lower fuel rods containing stacks of UO_2 pellets with a zirconium-1.0 w/o niobium cladding[12]. Fabricated fuel dimensions and power and burnup conditions that were used for the FPIN2 calculations are given in table 4. Also shown for comparison purposes are characteristics of a similar LWR fuel rod[13] that was used to estimate other parameters needed for the calculations such as fission gas retention, restructuring, and fuel cracking. The fuel is operated at such low power that there is no restructuring, no central void, and essentially 100 percent fission gas retention; i.e., the fuel is very "gassy."

Table 4.

Comparison of Fuel types

	RBMK-1000	U.S. LWR Fuel
Fuel Type	UO2	UO2
Pellet Density, Percent TD	94	92
Enrichment, Percent	2	2.55
Pellet dia., mm	11.5	9.32
Cladding Type	Zr-1 w/o Nb	Zircaloy-2
Cladding OD, mm	13.5	10.7 Cladding
Thickness, mm	0.9	0.61
Peak/Ave Power	1.4	1.3
Average Linear Power, Kw/m	15.3	20
Peak Specific Power, W/g	15	29
Fast Fluence, n/cm^2	[a]1.75×10^{21}	4.2×10^{21}
Average Burnup, a/o	1	2.4
Percent Fission Gas Retention	a100	100

[a]Estimated from burnup and LWR data [13]

Thermal and mechanical properties of UO_2 are contained in FPIN2 as one of the fuel options that can be selected by a single input parameter. However, because the code was initially developed to analyze the response of fast reactor fuel pins, no subroutines were immediately available for properties of zirconium alloy cladding materials. The present calculations were performed by

simply substituting zircaloy cladding properties in the routines. It was considered that the most important changes in these properties for the analysis of fuel disruption were the cladding melting point and the cladding plastic flow behavior. The cladding solidus of 2123K was determined from the zirconium-niobium phase diagram. The mechanical properties of zirconium-niobium alloys, however, were not readily available. The behavior of this material at the steam saturation temperature of 573K was estimated by using the high strain-rate response of irradiated Zircaloy-2 LWR cladding at 600K with a yield strength of 500 MPa, zero work hardening rate and a failure strain of 5 percent.[14]

Fuel cracking plays an important role in governing cladding loading during transient overpower events. The lack of restructuring and crack healing in LWR fuel[13] operated under similar conditions of RBMK-1000 fuel suggests that most of volume inside the cladding that is not occupied by the fuel would consist of cracks and pellet dishes. This geometry was simlulated in FPIN2 by assuming that the fuel was completely cracked into sectors which, in order to have a non-singular stiffness matrix in the mechanics analysis, were in contact with the cladding prior to the transient. If this crack volume was not modeled, unrealistically large cladding stresses from differential thermal expansion would have been calculated along with large cavity pressures once fuel started to melt.

6.2.2.3 Transient Fuel Response Prior to Failure

The power history for the FPIN2 calculations was determined from the graphical presentation of the Soviet's analysis. Only a single axial segment of an average fuel pin was modeled. For preliminary calculations the pin cooling was bracketed by two extreme cases; Case 1 where the cladding outer surface remained at the steam saturation temperature of 573K and Case 2 where the pin was heated adiabatically. Figure 23 shows the fuel and classing temperatures for these two cases at times where the fuel areal melt fractions are 50 percent, which is near the calculated cladding failure times. Also shown on the figure are the phase transition temperatures for zirconium-1 w/o Nb. In the FPIN2 calculations for Case 1 where there was maximum heat transfer to saturated steam at 573K, the average cladding temperatures remained near 600K. However, in Case 2 the cladding provided a substantial heat sink during the transient so that cladding temperatures soon exceeded temperatures where phase transformations might be exptected to yield a weaker more ductile material.

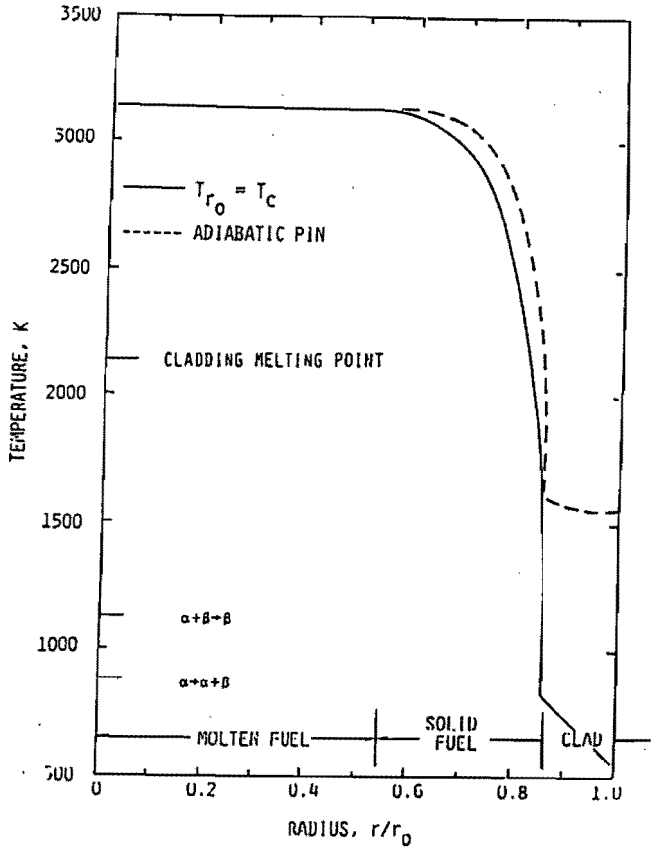

Figure 23. FPIN2-Calculated Fuel and Cladding Temperatures at 50% Fuel Area Melt Fraction

FPIN2 temperature calculations for the above two cases were compared with the subsequent RETRAN calculations of coolant boiling which were discussed in section 6.2.1. The RETRAN results show that once voiding begins, the cladding is the hottest, and therefore most likely to fail, near the bottom of the core. Futhermore, the RETRAN fuel and cladding temperature histories at this elevation are nearly identical to the FPIN results for Case 2, indicating that the heating is approximately adiabatic during the power transient. For this reason the Case 2 heat transfer results are considered the best estimate for the analysis of the fuel pin mechanical response at the failure site.

Calculations of areal melt fraction, cavity pressure and cladding plastic strain for Case 2 are shown in figure 24. The zero of the expanded time scale shown in this figure is referenced to the Soviet time of 1:23 so that the first power peak corresponds to 43.9 seconds (figure 17). The FPIN2 calculations show that fuel thermal expansion closed the fuel cracks at about 43.8 seconds. At this point the differential expansion between the fuel and the cladding rapidly increased the cladding stresses and caused plastic deformation as indicated in the figure. The maximum hoop strain reaches about 0.5 percent. However, fuel melting and creep allowed the cladding to deform back toward the fuel owing

to the high channel pressure (65 atm). The average cladding temperature during the time interval when differential thermal expansion was loading the cladding increased from 1000 to 1300K at a heating rate of 1000 K/s. These temperatures are beyond the cladding phase transformation temperatures so that significant weakening of the material would be expected. It is also known that oxidation of zirconium alloys in a steam environment may severely embrittle these materials in the β phase.[15] However, transient tube burst experiments on zircaloy in steam indicate that embrittlement would not occur for heating rates greater than 115 K/s and maximum temperatures less than 1600K because the time is too short for the oxidation kinetics to be important. Since the diametral strains measured at failure in the tube burst experiments were about 100 percent, it appears unlikely that the Chernobyl-4 pins would have failed early in the power transient prior to fuel melting.

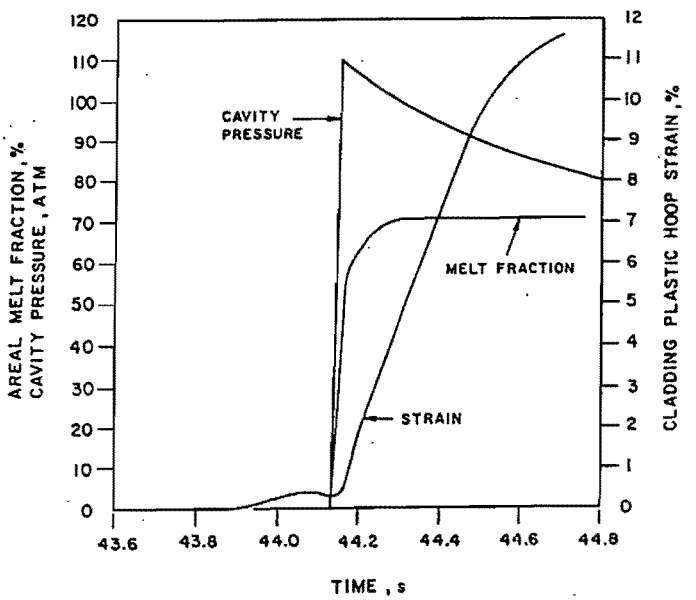

Figure 24. Fuel Pin Response for Case 2 with Adiabactic Heating

Once fuel begins to melt the available free volume inside the pin is rapidly consumed by the 10 percent increase in fuel volume and by the release of fission gas into coalescing bubbles. The pressure inside the pin increases to the point where any additional expansion must be accommodated by plastic deformation of the cladding. It has been our experience in FPIN2

calculations of numerous in-reactor fuel disruption experiments that if the pin is modeled using multiple axial segments, the volume expansion of the fuel in all of the axial segments is accommodated by rapid localized deformation of the hottest cladding. Cladding failure soon follows regardless of the failure criterion. The onset of this unstable deformation is indicated in the present calculations by the peak in the cavity pressure shown in figure 24. The reactor power and energy deposited in the fuel at the calculated time of failure are given in table 5 along with parameters of interest to the fuel disruption calculations. Also provided in table 5 are similar results for the case 1 calculations where maximum heat transfer to the coolant was assumed. In both cases, the fuel melt fractions at failure were about 50 percent (57-63 percent). However, the cavity pressures are much larger for the Case 1 FPIN2 calculations because the cladding is colder at the point where unstable plastic deformation begins.

Table 5.

FPIN2 - Calculated Pin Failure Conditions

	Case 1 Maximum Heat Transfer	Case 2 Minimum Heat Transfer
Time of Cladding Failure, s	44.3	44.2
Reactor Power, MWt	139,000	220,000
Energy Deposited in the Fuel Referenced to 298K, J/g	1316	1220
Average Cladding Temperature, K	712	1381
Fuel Area Melt Fraction, Percent	63	57
Average Temperature of Molten Fuel, K	3143	3139
Liquid Fraction of Molten Fuel, Percent	50	10
Cavity Pressure, Atmospheres	870	110

6.2.2.4 Post Cladding Failure

Upon cladding failure the pressure within the fuel elements exceeds the channel pressure. Hence fuel material is ejected from the pin into the channel according to this pressure differential. The fuel ejection process typically persists for the Chernobyl-type gassy fuel since retained fission gas is continually released from the fuel matrix and the bubbles

coalesce into larger ones which expand and expell the fuel. This involves both molten fuel from the central core of the fuel and the surrounding unmelted fuel annulus. The expulsion and downstream axial motion of the fuel causes rapid ablation of the cladding at the breach site and also causes ablation in the downstream direction. Hence the initial breach size which may be only one or two cladding diameters in length can rapidly enlarge to encompass a substantial fraction of the pin length. This is illustrated in figure 25 which is a photo of a failed irradiated fuel element from the H5 TOP test in TREAT.[16] This test sequence was programmed to terminate at the inception of cladding failure and therefore largely preserves the breach configuration. Within the initial breach shown in the upper photo, the central cavity from where molten fuel was ejected into the channel is visible. The surrounding unmelted annulus, part of which was blown into the channel, is also visible. In the lower photo, the downstream ablation of additional cladding (rotated from the original breach) is also evident. Rapid extension of the failure zone is typically expected. It should also be noted that the ejected molten fuel particularly from outer row pins may impinge on the zirconium-alloy channel wall. The combined transient heatup, ablation, and continued heat generation in plated out fuel have caused hot spots and channel wall failures in in-reactor tests, and this is also a potential failure mode of the Chernobyl-4 channel walls.

Although much of the fuel ejected from the pin into the coolant channel is liquid, a significant amount of solid fuel in the cavity has not absorbed the heat of fusion. The particle size of this material would be expected to be of the order of the grain size (~10μ) because melting would first begin at the grain boundaries. The particle size of any fuel ejected from the solid ring next to the failure site would also probably be of the order of grain sizes because this material is likely to have considerable grain boundary separation[13] from gas release during the severe transient heating of the gassy fuel.

H5 CENTRAL PIN FAILURE REGION

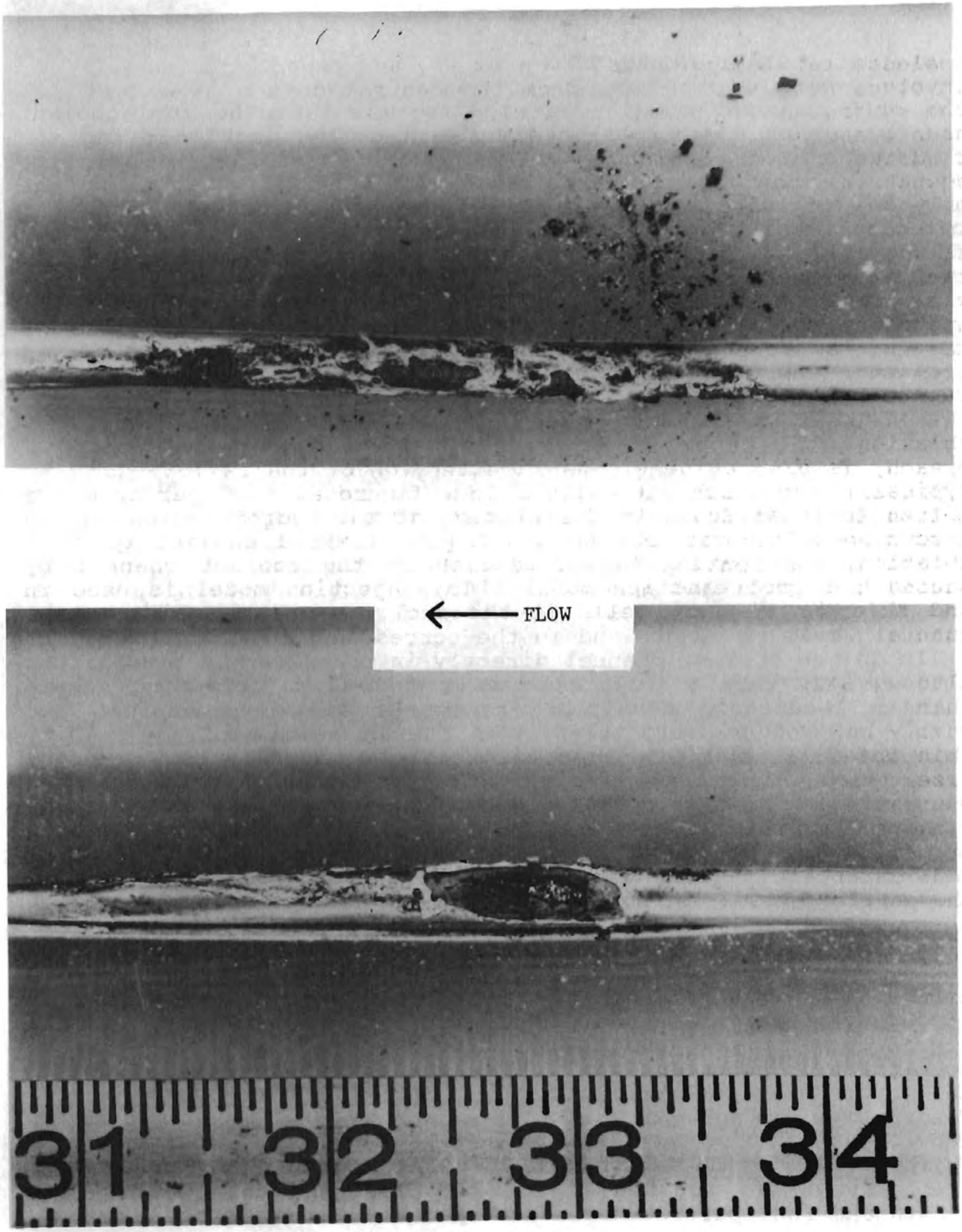

Figure 25.

6.3 FUEL-COOLANT INTERACTION

The EPIC computer code[17] was used to calculate the fuel-coolant thermal interactions and the fuel and coolant motion using the fuel conditions predicted by FPIN2 at the cladding failure time of 44.2 seconds. The EPIC model is generally based on the physical picture that there is a molten fuel cavity in the pin; the cladding breach allows ejection of molten fuel, unmelted fuel, and fission gas into the coolant channel, liquid coolant is present flowing through the channel at the breach elevation, and that the fuel pin structure remains nominally intact during the time scale of the fuel-coolant interaction. EPIC models the fuel bundle as a single, representative pin with its associated coolant. The results of base case calculations plus parametric variations of key parameters are presented in this section.

6.3.1 The EPIC Code

EPIC, shown schematically in figure 26, performs a one-dimensional Eulerian calculation of the hydrodynamics inside a molten-fuel cavity in the fuel pin, coupled explicitly to a one-dimensional Eulerian calculation in the coolant channel by means of a fuel ejection model. This ejection model is used in the Eulerian cell or cells in the fuel pin which delineate the cladding failure length and in the corresponding Eulerian cell or cells in the coolant channel directly in front of the pin failure cells. EPIC uses a full donor cell spatial differencing scheme with cell-centered densities, pressures and temperatures, and with cell-edge velocities. A combination of explicit, semi-implicit, and fully-implicit differencing in time is used. An explicit calculation is done to predict end of time step values; these are then used to compute average values over the step. The average values are in turn used to compute updated end-of-time-step values. There is an option in the EPIC model to make the time differencing strictly explicit after a specified time point, as, for example, when conditions are no longer changing rapidly. However, velocities in both the pin and channel are computed implicitly in time. These are computed on each pass which is semi-implicit for the rest of the variables besides velocity, or when the calculation is fully explicit in time for the variables besides velocity. A simple incompressible liquid slug model using a pressure gradient across the slug to accelerate it is used for the single phase liquid above and below the interaction zone where there is fuel in the coolant channel. To a large extent, EPIC is a parametric code. Our lack of knowledge of the precise physical processes requires this approach, particularly when coupled to the uncertainties that exist during an accident. For example, initial cladding rip length and fuel particle size are specified as input.

SCHEMATIC OF THE EPIC MODEL

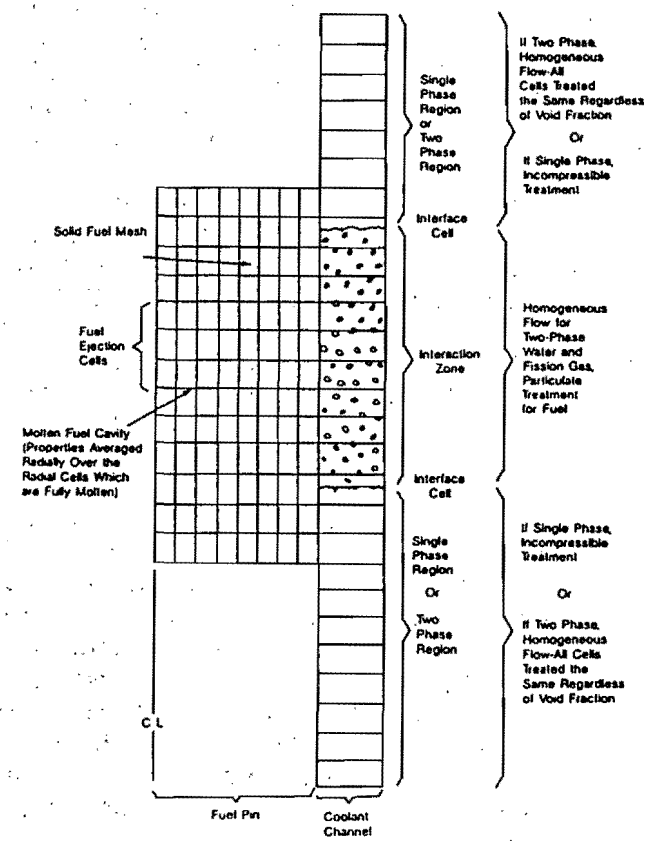

Figure 26.

EPIC was originally written to analyze postulated accident conditions in Liquid Metal Fast Breeder Reactors (LMFBRs). Therefore, the code had to be modified to be used for water reactor conditions. This primarily consisted of changing sodium properties such as specific heat, density, and saturation pressure as a function of coolant temperature to those appropriate for water. Also, considering that there were check valves at the inlet headers and taking into account the greater inertial constraints which exist below the location of pin failure than above, no coolant flow reversal was allowed during the 30-40 milliseconds of the EPIC calculation.

6.3.2 EPIC Reference Conditions

The reference conditions used in the calculations were as follows: Only the 3.5 millimeter long fuel element in the bottom of the core was assumed to fail, consistent with the RETRAN and FPIN results. The failure location extended from near the bottom

of this segment upwards. The reference breach length was 0.08 millimeters, and a failure length of 0.70 millimeters was also examined. A molten fuel cavity extending the 3.5 millimeters length of pin was assumed, consistent with the flat axial power variation (section 6.2). The cross-sectional area of the molten fuel was assumed equal to 50 percent of the fuel area; all the fuel in this area was at least undergoing melting at the failure time according to FPIN. Also, a temperature of 3150K was assumed for all the fuel in the molten fuel cavity again based on FPIN, which predicted very little temperature variation in this region. The pin pressure assumed initially at failure was 380 bar, a value roughly intermediate between the values predicted by FPIN cases 1 and 2.

The amount of free fission gas assumed in the cavity was 1.15 times 10^{-3} gm f.g./gm fuel which corresponds to 100 percent retention in the fuel of fission gas produced at 1 atm percent burnup. The effect of smaller fission gas retention was also examined. The fragmented fuel droplet size assumed when fuel was ejected into the coolant channel was varied parametrically, using values of 10 millimeters, 100 millimeters, 300 millimeters, or 600 millimeters radius. The heat transfer coefficient between fuel and water is k/r, where k is the fuel thermal conductivity, and r is the particle radius. In order to provide some perspective for these particle radius choices, the particle radius of 300 millimeters is the maximum stable droplet size using a critical Weber number criterion of 12, based on a coolant velocity of 3.5 milliseconds. Both larger and smaller droplet sizes were also used in the calculations, however. Also, for the relevant gassy fuel conditions and severe heating, solid fuel is predicted to fragment into grain sizes (~10 millimeters) due to microcracking during the transient. The effect of ejecting unmelted fuel with this very small size was also examined. An initial channel pressure of 68 atm was used in the calculations. Expansion of the FCI zone was allowed only in the upward direction due to check valves upstream and steam void downstream. The inertial constraint for upward acceleration was provided by the fuel/coolant mixture; this was represented in the calculation by an equivalent (collapsed) coolant mass of 5 millimeters effective length in the bundle.

6.3.3 Description of EPIC Results

Tables 6 and 7 summarize the six cases run with EPIC. Postponing discussion of case 6 for the moment, case 1 with the smallest particle size (100 millimeter radius) and therefore the most rapid and efficient heat transfer produced the highest FCI pressure in the channel (figure 27) and ejected the upper liquid slug the fastest (figure 28). The mass of fuel ejected from the pin was less in case 1 because the channel pressurization reduced the pin-to-channel pressure differential (figure 29). Cases 2

and 3 vary in a predictable fashion as the particle size was increased. However, the peak FCI pressure was nearly the same for 300 millimeter particles as for 100 millimeter particles. In case 3, the heat transfer to the water was so inefficient due to the large particle size that the channel pressure never exceeded 87 bar despite much more fuel ejected than in the other cases (due to less back pressure in the coolant channel). Case 4 can be compared with case 2 to determine the effects of fission gas retention in the fuel. With one-tenth the fission gas of case 2, case 4 ejects far less fuel, produces much lower channel pressures and accelerates the upper slug much more slowly. Hence, the gassy nature of the Chernobyl-4 fuel increases the severity of the fuel fragmentation. Case 5 can be compared to case 2 to determine the effect of a greatly increased breach length through which fuel may be ejected. The result is much more fuel ejected much earlier, although the channel pressurization cuts off fuel ejection later on. Case 6, which models the expulsion of micro-cracked fuel into the coolant channel, has about the same amount of fuel in the channel as case 1 but has a lower average interaction zone pressure because of more fuel penetrating the upper liquid slug. This causes more cold liquid to be mixed into the interaction zone and, therefore, a more rapid drop-off of pressure than in case 1 after 5-10 milliseconds. Much higher pressures immediately after pin failure produce the rapid acceleration of the upper slug seen in figure 27 but after about 15 milliseconds the velocity is relatively constant since the fuel in the vicinity of the upper slug interface has mostly reached thermal equilibrium with the water. Table 7 summarizes results of the six cases. The best estimates of channel pressurization and slug ejection velocity were 140-150 atoms and 40-50 milliseconds, respectively.

Table 6. Results of Parametric Cases

	Case No. 1	2	3	4	5	6
Peak pressure attained (bar)	150	140	87	114	142	150
Time peak pressure attained (ms)	20	27	21	20	30	2
Total fuel ejected (gm/pin)	125	150	200	36	150	112
Time by which fuel ejected (ms)	40	40	40	15	30	30
Coolant ejection velocity at end of calculation (m/s)	50	43	32	14	23	40

Table 7. Values of Parameters Varied By Case

Case No.	Cladding Breach Length, m	Particle Radius, μm	Retained Fission Gas
1	0.08	100	1.15×10^{-3}
2	0.08	300	1.15×10^{-3}
3	0.08	600	1.15×10^{-3}
4	0.08	300	1.15×10^{-4}
5	0.70	300	1.15×10^{-3}
6	0.08	10	1.15×10^{-3}

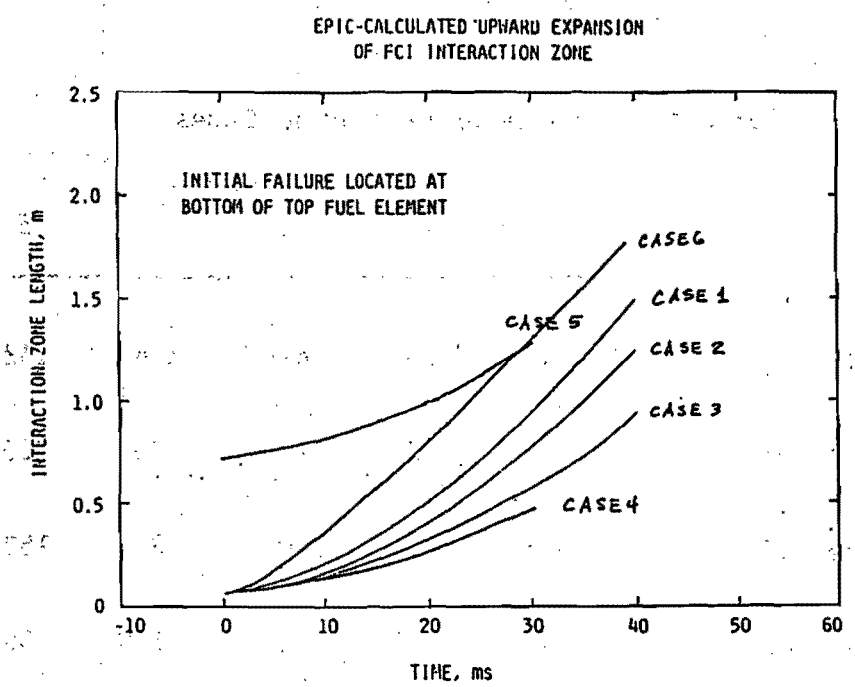

Figure 27.

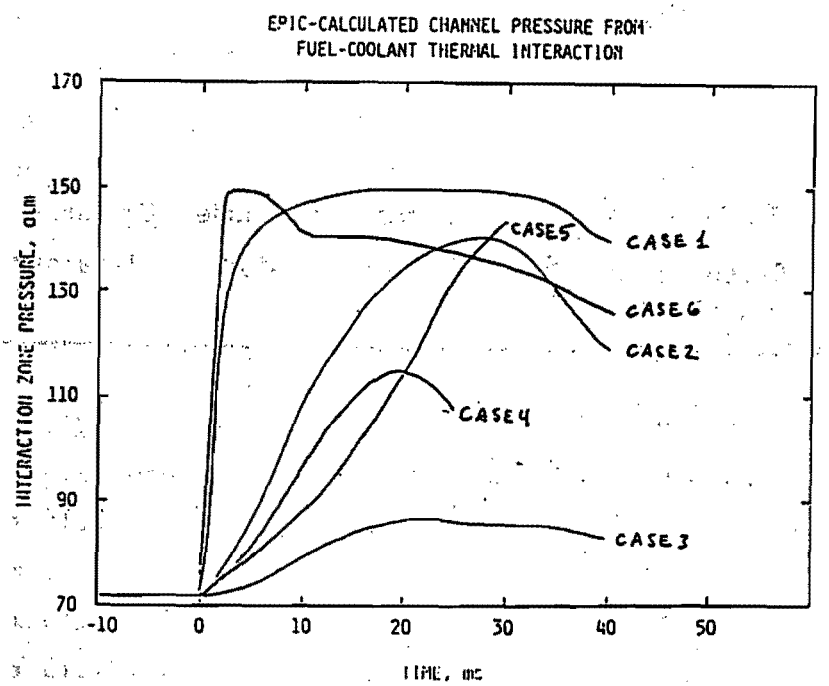

Figure 28.

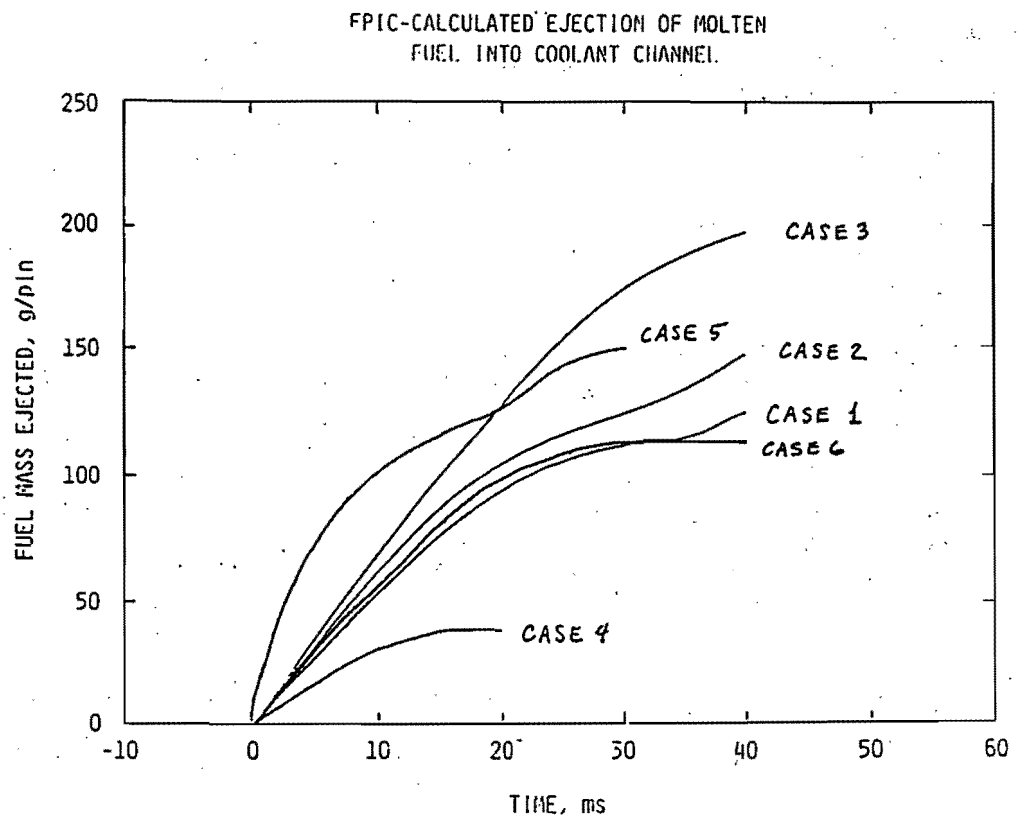

Figure 29.

The channel pressures reported are the saturation pressures corresponding to the average coolant temperatures in the interaction zone. Peak pressures in the interaction zone attained approximately 150 atom. This is not a matter of coincidence since the EPIC model requires that the coolant remain at saturation. The specific heat of the liquid phase to which the fuel transfers heat approaches an infinite value near the critical point as the water/steam mixture follows the saturation line toward the critical temperature. When the saturation pressure attained is approximately 150 atom, the specific heat rises to such a large value that a further rise in the temperature and pressure of the coolant becomes unlikely in this model.

6.4 STRUCTURAL RESPONSE EVALUATION

6.4.1 ALICE-II Analysis of Channel Pressurization

To provide a systematic analysis, responses of the Chernobyl-4 fuel-channel pressure tubes to three different FCI cases calculated by EPIC (section 6.3) analyzed with the ALICE-II fluid-structure interaction code. The ALICE-II code, Chernobyl-4 model, and results of the analyses are presented here. The

analysis is used to evaluate likely failure modes and locations of the pressure tube piping systems leaded by the fuel-failure-induced energetic fuel-coolant interactions.

6.4.1.1 Description of ALICE-II Code

The ALICE-II [18, 19] code was developed at Argonne National Laboratory for calculating the response of reactor structures in hypothetical core disruptive accidents. It is used to treat reactor vessels with complex internals such as internal thin shells, upper internal structures, perforated plates, core-support structure, shield baffles, and deflector plates.

The ALICE-II code uses a two-dimensional, hybrid Lagrangian-Eulerian finite-difference technique to calculate the compressible hydrodynamics and fluid-structure interactions, together with a purely Eulerian finite-difference approach to analyze the free-surface and material interface motions. Numerical calculations for the hydrodynamic solutions are separated into three phases. The first phase consists of an explicit Lagrangian calculation. The second phase, which is optional, contains an implicit iteration. The third phase, which is also optional, rezones the mesh vertices to prescribed positions. The structural response is computed by two nonlinear, elastic-plastic, finite-element modules formulated in corotational coordinates. The first employs two-dimensional, thins-hell and quadrilateral continuum elements to model the reactor vessel and axisymmetric elastic-plastic solids. The second module utilizes a three-dimensional pipe element to calculate the response of the support columns that connect the internal structure to the reactor vessel or head. All elements are capable of treating both material and geometric nonlinearities.

The ALICE-II code has been validated against the SRI rigid and flexible vessel experiments and the SRI complex vessel experiments.[20, 21]

6.4.1.2 Pressure Tube Model

The fuel channel pressure tube was considered to be a thin shell in the calculations. The tube has an inside diameter of 80 mm and a wall thickness of 4.0 mm. The top closure head is located 6.5 m above the top of the core. It was modeled simply as a closed end of the thin-walled tube. In the core the tube material is a Zr2.5 Nb alloy; above and below the core, in the regions of the steel shield blocks, there are Zr-to-steel transitions. The tube was allowed to deform radially under internal pressurization without constraint imposed by the graphite heat transfer rings or moderator blocks. At the top, the end cap can move axially under impact loading. The internal

hardware was omitted in the model. The presence of internals would reduce somewhat the velocity of the water slug. Thus strains in the wall near the closure head may be somewhat overestimated in the present analysis. Details of the configuration of the closure head region are not known. Failure of the tube wall may thus be conservative if the actual weak point were in the closure itself.

The response of the pressure tube was analyzed by a finite-element structural dynamic routine in which the tube wall was discretized into 20 elements. The nonlinear temperature-dependent elastic-plastic characteristic of the tube wall was simulated by several piece-wise straight line segments, based on the material data at approximately 600K. More specifically, for the Zr alloy, the stress (σ) and strain (ϵ) relationship was approximated by four straight line segments. In the plane, the stress and strain corresponding to the higher valued end point of each straight segment are:

σ_1 = 220 MPa ϵ_1 = 0.28 percent,

σ_2 = 292 MPa ϵ_2 = 1.92 percent,

σ_3 = 350 MPa ϵ_3 = 6.93 percent,

σ_4 = 418 MPa ϵ_4 = 40 percent.

For the stainless steel, the stress-strain relationship was simulated by two straight line segments. The corresponding higher valued end points are:

σ_1 = 129.7 MPa ϵ_1 = 0.074 percent,

σ_2 = 453.3 MPa ϵ_2 = 28 percent.

The stress and strain of the last end point represent the ultimate values of the material. Thus, the ultimate stresses of the Zr alloy and steel are 418 and 453 MPa, respectively. The ultimate strains of zircaloy and steel are 40 percent and 28 percent, respectively. For convenience, both ultimate stresses and strains are used as the failure criteria. If the predicted stress and/or strain exceeds the respective ultimate values, failure is assumed to occur.

Due to the lack of available property information regarding the zirconium alloy and the stainless steel used in the pressure tube (O8Cr18Ni10Ti steel), properties of zircaloy and stainless steel 316 were used in the analysis. Since the stainless steel 316 may be stronger than the actual material used for the Chernobyl-4 pressure tube, the ALICE-II predicted stress and strain near the

closure head might be underestimated. It is believed that the difference is small.

6.4.1.3 Results of ALICE-II Analysis

Three calculations were performed, corresponding to fuel particle diameters of 0.20, 0.60, and 1.20 mm, respectively. The FCI zone pressure and slug acceleration calculated by EPIC (section 6.3.3) were used as the loading function. In each of the three cases studied, the numerical calculation was terminated approximately at 100 ms, at which time the major event due to slug impact was essentially terminated. Also, at this time, the tube wall has reached its dynamic equilibrium.

To illustrate the analysis, results pertaining to reference Case 2 (fuel particle diameter = 0.60 mm, peak pressure = 14 MPa) are given here. Figure 30 shows the pressure history on the closure head generated from the impact of the water slug. This pressure history is slightly oscillatory due to propagation of the incident compression wave originating from the expanding interaction zone and the waves reflected from the surrounding structures. The total force acting on the top closure head is presented in figure 31. It represents the sum of the forces in each of the hydrodynamic zones underneath the cover. The hoop stress of the tube wall near the closure head is given in figure 32. The maximum stress generated from the slug impact is about 760 MPa, which exceeds the ultimate stress of 450 MPa. In figure 33, which gives the corresponding hoop strain, it can be seen that the maximum strain is about 39 percent, as compared with the material ultimate strain of 28 percent. This obviously would lead to tube failure in the circumferential direction near the closure head. Pressure history near the outlet tube for the steam-water mixture is given in figure 34. This pressure pulse can be used to analyze the response of the outlet tube system.

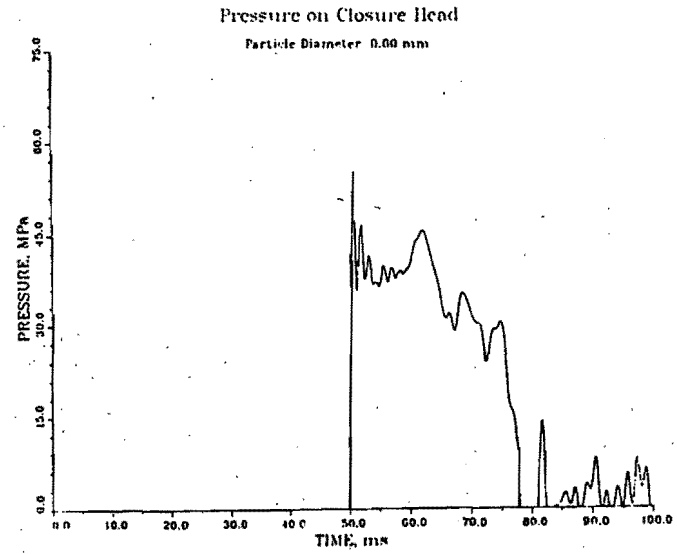

Figure 30. Pressure Under Closure Head as a Function of Time

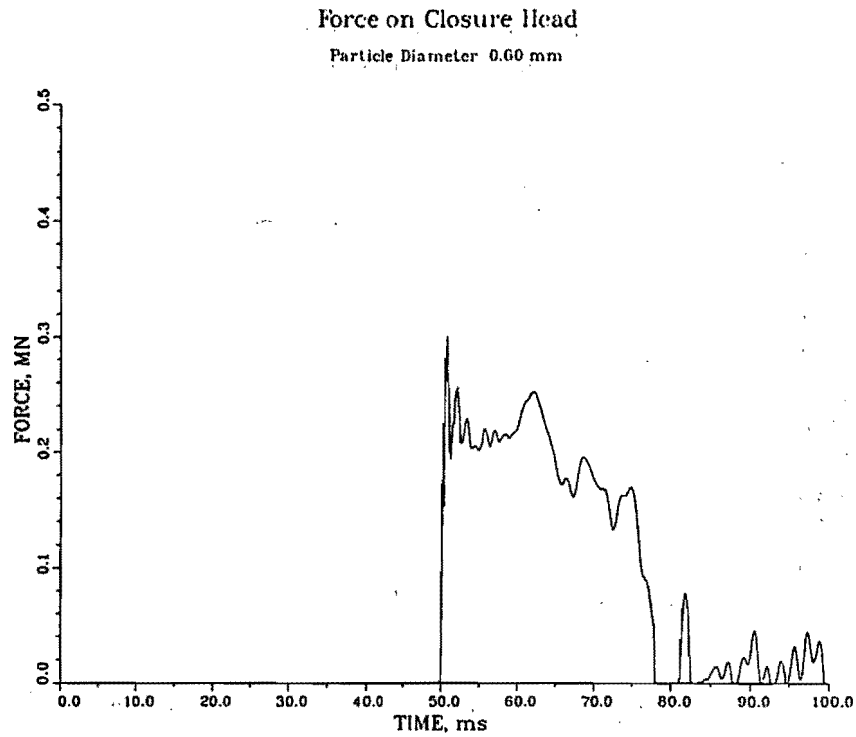

Figure 31. Force on the Closure Head as a Function of Time

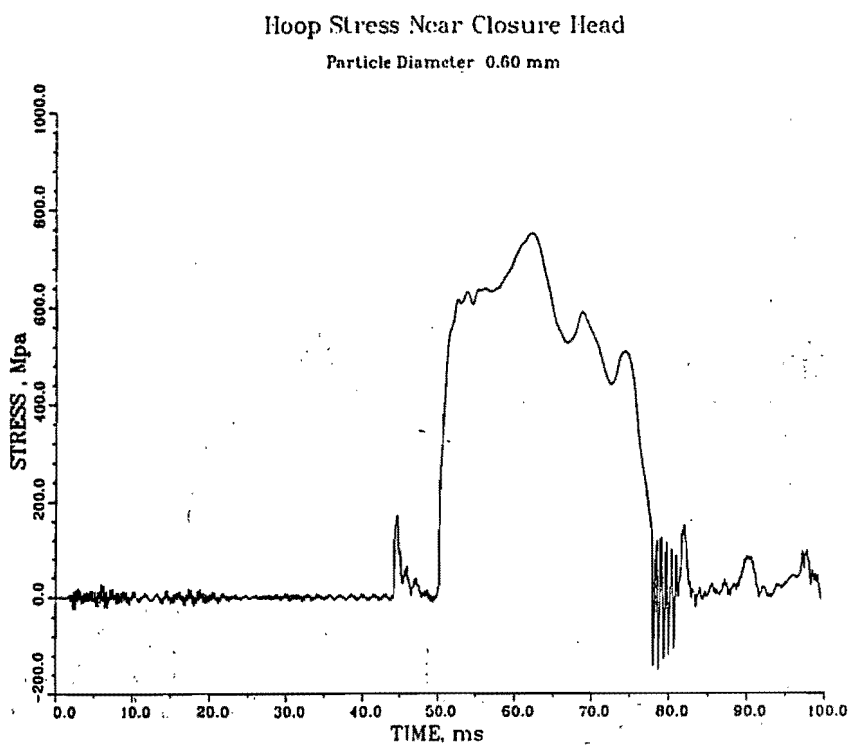

Figure 32. Hoop Stress of Tube Vessel Near the Closure Head

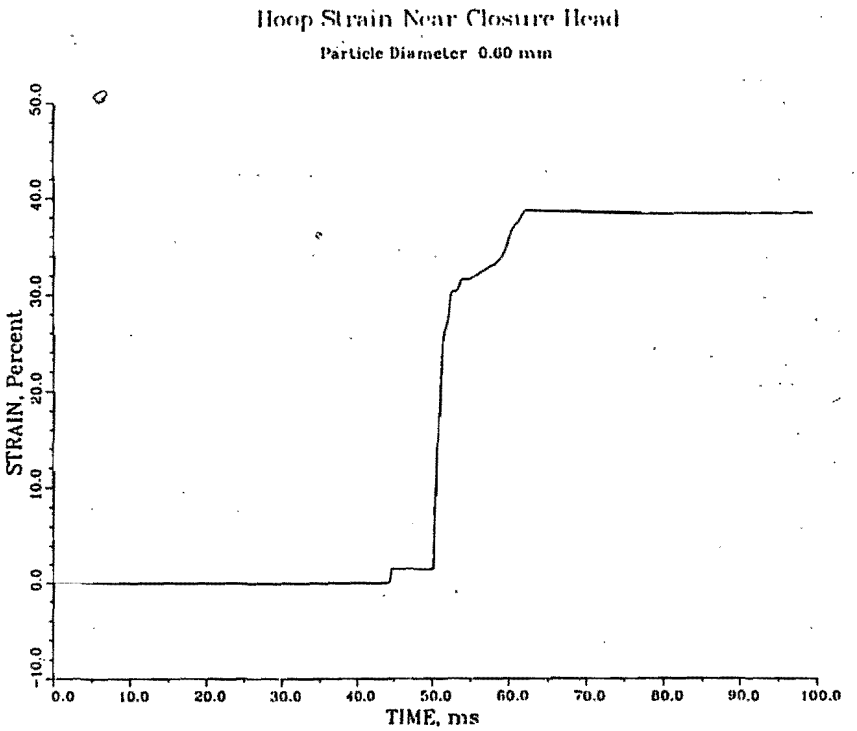

Figure 33. Hoop Strain of Tube Vessel Near the Closure Head

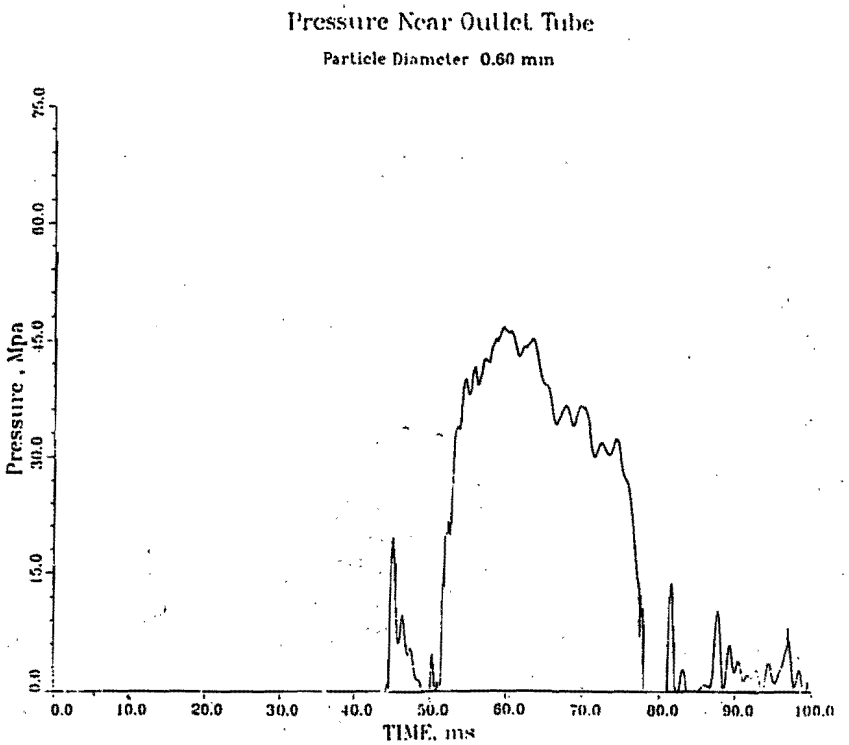

Figure 34. Pressure History Near the Outlet Tube

Figures 35 and 36 provide the radial displacements at vessel nodes 2 and 5 in the vicinity of the FCI zone. The displacement of node 2 reaches a value of 0.015 cm immediately following the interaction, whereas a slight time delay occurs at node 5, which is located away from the interaction zone. Since the displacements of these two tube nodes are very small and their strains are within the elastic range, tube failure caused solely by channel pressurization in the FCI region is not predicted. However, the possible effects of fuel impingement on the wall could still cause thermal-induced failure. Axial stress at element 15 near the welded junction between stainless steel and Zr alloy is given in figure 37. Again, the results reveal that during the early stages of excursion, the stress generated from the incident wave propagation of the interaction zone is small, thus leading to the elastic response of the element. However, at later stages of the excursion, the axial stress gradually increases due to the reflection of the strong pressure wave caused by the slug impact. Figure 38 further provides the pressure at the region of the diffusion weld. A strong pressure pulse created from the coolant impact is quite evident. This loading, combined with the temperature transient calculated in the joint (see following section) suggests that the upper weld is also a likely failure location.

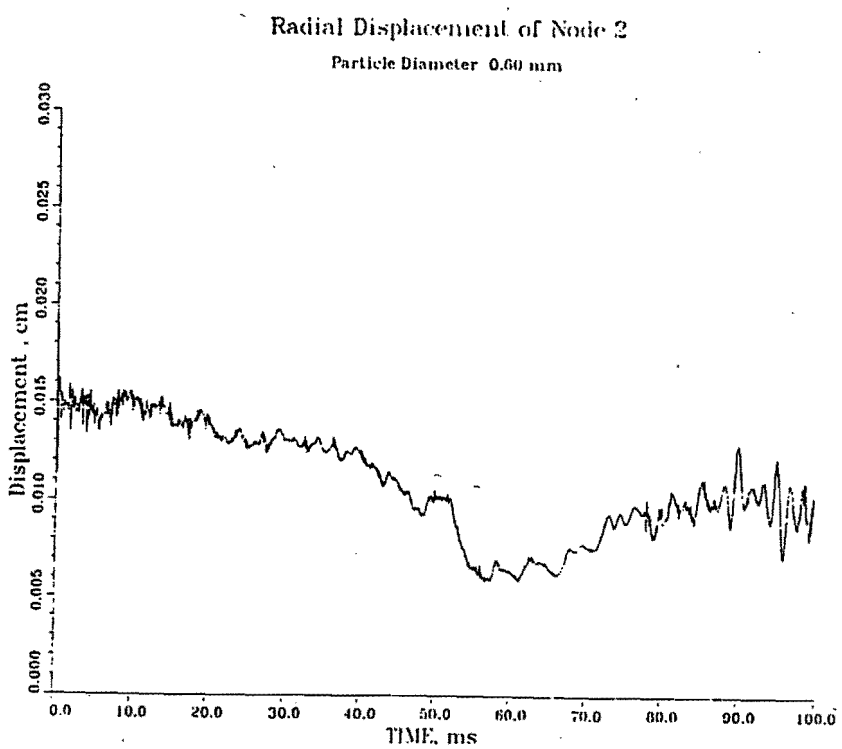

Figure 35. Radial Displacement of Tube Node 2

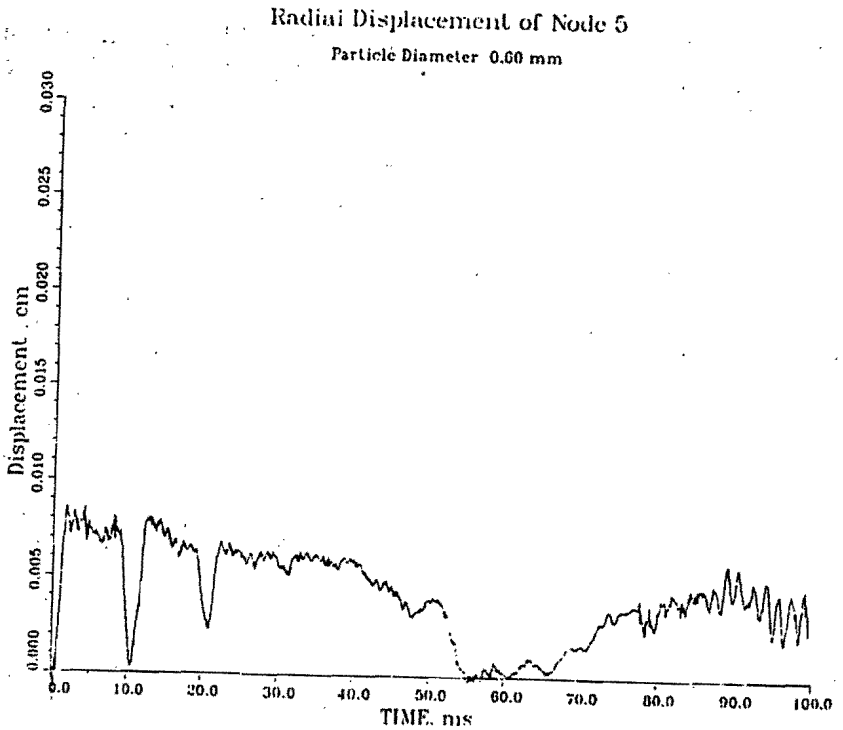

Figure 36. Radial Displacement of Tube Node 5

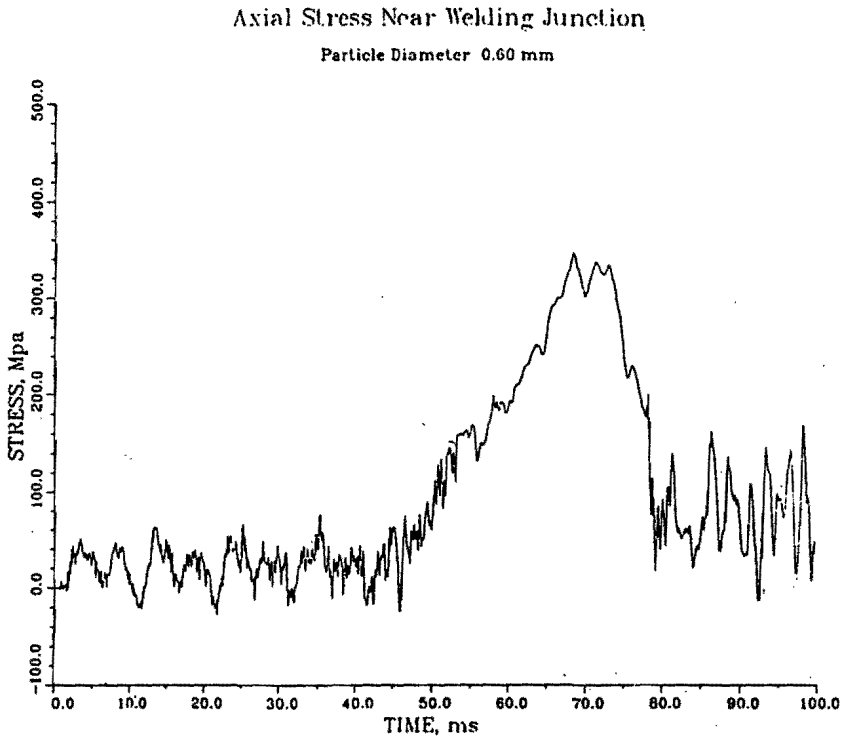

Figure 37. Axial Stress at Element 16 Near the Steel-Zircaloy Welded Junction

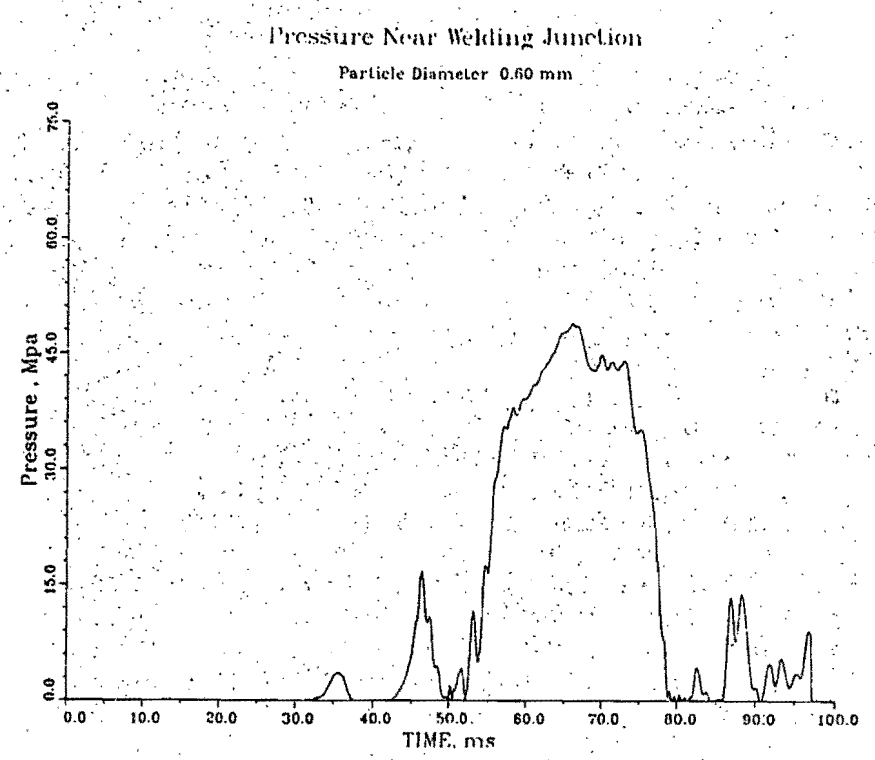

Figure 38. ALICE-II Predicted Hydrodynamic Pressure Adjacent to the Welded Junction

Results of the analyses indicate that channel failure would occur for all three cases, i.e., for fuel-particle diameters of 0.20, 0.60, and 1.20 mm, respectively. However, the third case (fuel particle diameter = 1.20 mm) represents a marginal failure case since the calculated maximum strain of 34 percent is only about 20 percent greater than the material ultimate strain of 28 percent. Since the effect of the outlet tube and internals were not considered in the analysis, the predicted strain might be overestimated. It was found that channel failure occurred near the closure head due to slug impact hammer pressure owing to the FCI expansion. Such failure not only could lead to the missile generation of the closure head and floor slab, but could also cause blowdown of coolant and possible ejection of fuel and cladding material into the reactor building. Failure of the pressure tube solely due to the FCI pressurization was not indicated, although local failures in the core region due to fuel impingement effects would be anticipated.

6.4.2 Transient Heating of the Transition Welds

The heatup of the upper transition weld region of the pressure tubes during the core steam formation and voiding transient was predicted with the INCIRT thermal hydraulics computer program[22] previously developed at Argonne National Laboratory. The code was used to perform a multicell, radial, finite difference calculation of thermal conduction within the 8 mm thick wall of the pressure tube in the transition region where the zirconium

alloy and steel segments are diffusion welded together. The model included the 9.5 mm thick graphite spacer ring surrounding the pressure tube, and the surrounding steel shield blocks.[1] The pressure tube wall, spacer rings, and shield blocks were each nodalized with twenty numerical grid cells. Idealized perfect thermal contact was assumed between the pressure tube outer surface and the spacer rings as well as between the spacer rings and the shield blocks. Flow and temperature conditions of water and steam exiting from the core and flowing through the weld region were obtained from the results of the RETRAN calculation described in section 6.2.1. During the heatup and voiding transient, the fluid flowing past the pressure tube inner surface in the weld region changes from all liquid water to a two-phase water-steam mixture and finally to single-phase steam. The heat flux from the fluid to the pressure tube inner surface was determined using the Dittus-Boelter heat transfer correlation. The thermal conductivity and viscosity employed in the evaluation of the heat transfer coefficient were specified using temperature and density dependent universal ASME expressions for water encompassing both liquid and vapor phases.

The predicted temperature averaged over the full pressure tube thickness in the upper transition weld region is shown in figure 39, together with the temperature of the water and steam flowing through the weld region. The weld average temperature is calculated to rise by 55 degrees K between 43.9 and 44.9 seconds. The predicted heatup rates over this interval thus correspond to an average value of 55 degrees K/seconds and attain a maximum of 95 degrees K/seconds which exceeds by four orders of magnitude the Soviet operational limitation of 10 to 15 degrees K per hour. As a result of the indicated heatup rates, differential thermal expansion of the dissimilar zirconium alloy and steel materials might be expected to lead to failure of the pressure tube boundary within the upper transition region.

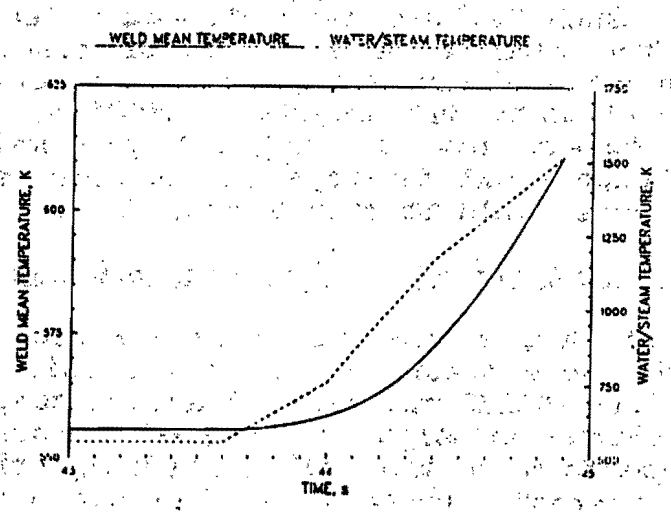

Figure 39. Calculated Heatup of Upper Transition Weld

6.5 BEST ESTIMATE OF ACCIDENT EVENTS

6.5.1 Noncoherence of Fuel Failures

The approach described in section 2 for the fuel failure calculations was based on average channel conditions and uniform axial power, consistent with the Soviet core-wide average approach in calculating fuel failures, and necessitated by the current lack of information regarding suspected gross shifts in the axial power variation during the power excursion. Actually, there is variation in the power-to-flow among the multitude of process channels, and there is additionally axial power peaking. These two effects cause there to be a time variation in the actual fuel failures in the channels, and correspondingly regarding the incremental void reactivity insertion. The effects of noncoherent failures were investigated in a set of scoping calculations using the EPIC code. Results presented here are only illustrative of the physical processes; many of the details needed to make definitive calculations are not presently known. The reactor core was divided into 10 groups of equal numbers of pressure channels which will hereafter be referred to as "channel groups." The Soviet calculations for the reactivity and power history of the reactor were used until fuel failure was calculated in the highest power channel. The Soviet reactivity history was used as input for a point kinetics calculation, and the neutron lifetime was adjusted to match the Russian power history up to this point. After this, the reactivity level at this time was used as the initial condition for the subsequent calculation when reactivity effects of fuel-failure-related coolant voiding plus the Doppler effect were calculated explicitly and used subsequently to determine the changing reactor power. From the time of first fuel failure, Doppler reactivity was calculated in all channels assuming adiabatic heating of the fuel. Coolant voiding reactivity was added according to a calculated ramp rate beginning in each channel as that channel failed.

Table 8 summarizes the parameter values used. For the point kinetics parameters, the precursor data was presumed to be that for U-235 with adjustments in the group's to account for the fact that β_{eff} was taken to be 0.0048 (since there was probably a mixture of U-235 and Pu in the core). The lifetime was adjusted to fit portions of the Soviet calculation. The value arrived at was 7.75×10^{-4} seconds. Reactivity coefficients required for the point kinetics calculation consisted of the Doppler coefficient which was taken to be 1.2×10^{-5} $\Delta k/k/\Delta C$ (Soviet value) and the void reactivity coefficient for which there is a considerable amount of uncertainty among different best estimates. A constant value of 0.03 $\Delta k/k/\Delta \alpha$ was used. This value implies a residual void reactivity of 1.8×10^{-2} millik/k ($3.75) at a void fraction of 40 percent which is the void

fraction at which the Soviet calculations indicate fuel failures. This residual value of $3.75 appears to be consistent with the void reactivity inserted during fuel failure in the Soviet calculations. To weight these reactivity coefficients on a channel-by-channel basis when incoherence is introduced, a parabolic radial power profile with a peaking factor of 1.43 was used. The normalized radial profile for the 10 channels is shown in table 9. In order to calculate the rate of void reactivity introduced after pin failure, an axial profile assuming a tent function was used with a peaking factor of 1.4. (An axial cosine distributed worth function was used as well with little change in results.) Then a simplified velocity versus time function was assumed (based upon EPIC mechanistic calculations) such that the remaining coolant in the core for a given channel after pin failure was expelled with an initial velocity of 4 m/s which increased linearly to 40 m/s by 45 msec after failure and remained constant thereafter.

Table 8. Neutronics Data

β_{eff} = 0.0048

ℓ = 7.75×10^{-4} secs

Precursor Group	λ, sec^{-1}	$\beta i/\beta$
1	0.0124	0.033
2	0.0305	0.219
3	0.111	0.196
4	0.301	0.395
5	1.14	0.115
6	3.01	0.042

Doppler $\alpha = 1.2 \times 10^{-5}$ $\Delta k/k/°C$

Void α = 3×10^{-2} $\Delta k/k/\Delta\alpha$

Axial peaking factor = 1.4

Radial peaking factor = 1.43

Table 9. Radial Power Profile

Channel No.	Power Factor
1	0.143
2	0.133
3	0.124
4	0.114
5	0.104
6	0.094
7	0.085
8	0.075
9	0.066
10	0.056

The Doppler feedback was calculated as follows. At the time of first fuel failurein the highest power channel group, all changes were assigned an average enthalpy based on the radial power profile. The power history after first fuel failure determined the subsequent energy deposition according to the radial power shape, and the Doppler contribution for each channel was based on the temperature difference between the current time and that at first fuel failure.

The calculation for the 10 channel groups of the reactor proceeded as follows. First, as was stated above, the Soviet reactivity versus time function was assumed up to the time of the first fuel failure. This function was simplified and linerlized as shown in table 10 (zero time is 1:23:00). The time of first fuel failure was determined by assuming (based on FPIN calculations) that the failure occurred at an enthalpy corresponding to 50 percent fuel melt fraction at the peak axial location, 1286 J/g. With an axial peaking factor of 1.4, the corresponding average enthalpy of the peak channel was 919 J/g, and the average enthalpy of the average channel was 642 J/g. This enthalpy for the average pin in the whole core occurred at an integrated power of 138 x 10^3 MW seconds, which occurred at about 43.8 seconds in the Soviet calculated power excursion (just

prior to the peak power). Therefore, at 43.8 seconds the first channel group is assumed to fail. Both the Doppler feedback from all channels and the void reactivity feedback for channel 1 were calculated after 43.8 seconds and added to the existing reactivity level at the time (0.00553). The pin failure times for all channels are given in table 11. The void reactivity feedbacks for each channel group were added to the total feedback beginning at the time of each channel's failure. The resulting reactivity and power history versus time are shown in figure 40. There is obviously a discontinuity at the point of first pin failure where the slope of the reactivity down since the power level is still relatively high. However, it is apparent that the calculated power transient is significantly different from that calculated using a coherent fuel failure model as in the Soviet analysis.

Table 10. Assumed Reactivity with Time

Time (sec)	Reactivity ($\Delta k/k$)
35.	0
41.	0.00231
42.	0.00357
42.6	0.00504
43.0	0.00714
43.37	0.00987
44.4	-0.00052
44.7	-0.0022

Table 11. Pin Failure Times for ten Channels

Channel No.	Failure Time (sec)
1	43.800
2	43.832
3	43.865
4	43.908
5	43.955
6	44.004
7	44.047
8	44.095
9	44.141
10	44.203

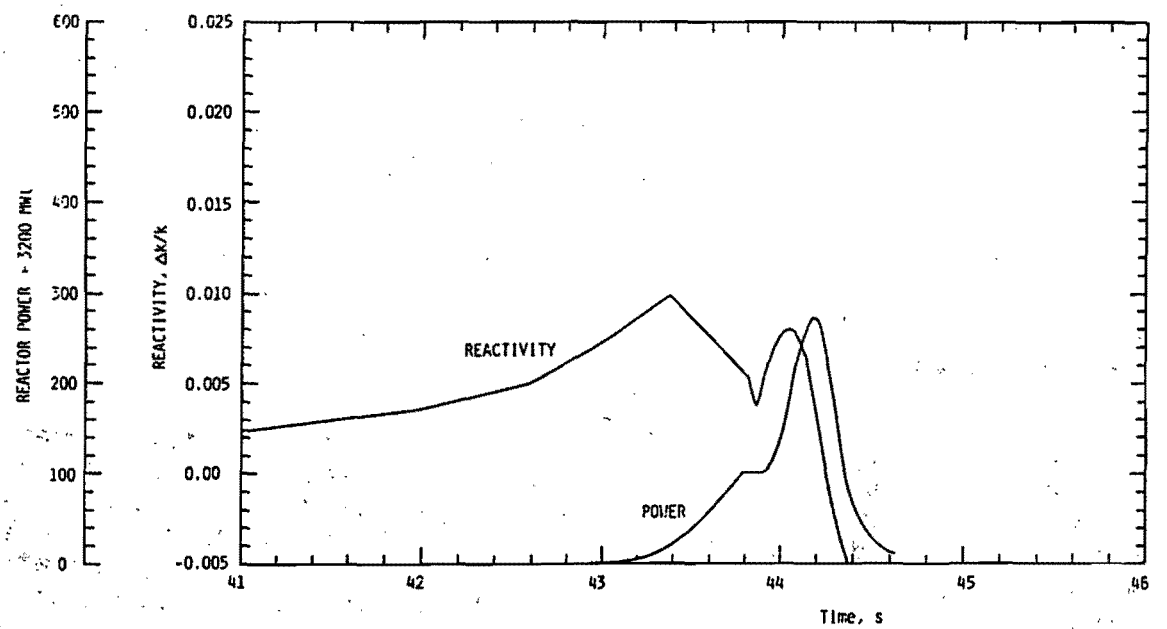

Figure 40. Normalized Power and Reactivity vs. Time for 10 Channel Case

It is apparent that the effect of introducing incoherency into the addition of the reactivity feedback produces a much milder transient since the Doppler feedback can then mitigate the voiding reactivity more effectively. The average core temperature in the 10-channel case was 4825K. Table 12 shows average fuel temperatures and the corresponding fuel vapor pressures for each of the 10 channel groups. It is seen that half the fuel in the core has a vapor pressure high enough to produce significant material motion potentially contributing to the severity of the destructive events.

Table 12. Final Temperatures and Fuel Vapor Pressures in Ten-Channel Case

Channel No.	Average Temperature °K	Vapor Pressure at Average Temperature (MPa)
1	6764.	>50.0*
2	6312.	>40.0*
3	5906.	29.2*
4	5454.	14.7*
5	5002.	6.3
6	4551.	2.2
7	4144.	0.7
8	3693.	0.1
9	3286.	-
10	3138.	-

*Extrapolated values

In summary, the scoping calculation has illustrated the general trend expected when the fuel failures are spread out in time according to relative power-to-flow amongs the various channels. Failures in the lead channels were predicted to occur at 43.8 s, before reaching peak power condition in the Soviet calculated power excursion. Accounting for both the reactivity insertion of channel voiding as the channel groups failed progressively, as well as the fuel Doppler effect, the reactor power is calculated to escalate from the peak of the "first" burst directly into a larger event. Overall, the single, larger power excursion

calculated here is less severe in terms of peak power, energy deposition, fuel temperature, and fuel vapor pressure than the double-peaked excursion calculated by the Soviets. However, even in this calculation, the fuel vapor pressure in high-power channels is predicted to significantly augment the destructive event. The Soviet double-peaked power excursion is seen to be a consequence of assumed coherent fuel failures.

6.5.2 Fuel Failures

An unfortunate limitation of the present analysis has been the unavailability of information pertaining to the variation in the axial power profile during the power excursion. The axial power distribution is of major importance in determining the initial fuel failure elevations in the channel during a severe TOP accident. From information furnished by the Soviets, we know that at 1:22:30 the shape was axially double-humped with the larger peak in the upper region. However, at the start of the power excursion when the scram was initiated (1:23:40), there was positive reactivity insertion at the bottom region of the core, and subsequently negative reactivity was added to some unknown extent in the upper region. The overall effect of the scram action is thought to have shifted the power peaking to the bottom region of the core during the power excursion, although this has not been quantified. If this premise is qualitatively correct, the major energy deposition in the fuel would have occurred in the lower region of the core initially, certainly in the lower set of fuel elements. The RETRAN thermal-hydraulics calculations (section 6.2.1) indicated that the cladding axial hotspot is also located in the bottom region of the core. Therefore, the cladding is already weakest and most likely to fail in that lower region. The combination of peak energy deposition and cladding hotspot both occurring in the lower region of the core would make that the inevitable origin of the initial fuel failures in the c-hannel. Since there is still a substantial presence of water flowing up through this lower core region, fuel-coolant interaction events would be predicted as described in section 6.3.

The FCI causes a transient pressurization, including slug impact pressure, which may cause failure of the channel with consequences described in the following section. In any event, the power excursion (figure 40) continues to cause energy deposition in the fuel beyond the time of initial fuel failures, particularly for the high power channels. Once there is a loss of intact fuel geometry, phenomena in the channels become complex. The melting of fuel and cladding progress and materials move in the channels driven by the forces of expanding fission gas, increasing fuel vapor pressure, and the overall channel pressure gradient provided by the pump head, including the effects of high velocity steam flow. The flow direction remains

upward. Molten fuel and cladding material typically contact relatively cold surfaces available such as the channel wall and spacer grids. In doing so the structural surfaces experience transient heatup and possibly cause melting at the interface upon contact; the wall will not remain a viable pressure boundary for very long under these conditions. The upper set of fuel elements will eventually fail, releasing more fuel into the channel. Eventually the geometry becomes so disrupted that the molten material and debris largely bridge the channel passages, blocking the channel. In this extreme, the pump head is localized as a pressure drop across the accumulated materials. The materials tend to flow upward under such conditions, and it is typically found in in-reactor tests that the molten core materials freeze out and cause plugging in the colder structure region above the top of the active fuel. This cuts off upward gas and vapor flow. By this time the channel wall has likely failed by thermal attack. If the power excursion continued beyond this time (as for lead channels) or if there were a subsequent power excursion with the channel largely plugged by frozen debris, pressure would build up in the channel, failing the channel wall in the core region if that hasn't already occurred, and causing blowdown into the graphite space.

The above picture is based in part on results of in-reactor TOP tests. There has been no attempt to quantify the processes described since events beyond the time that intact geometry was lost are regarded as highly uncertain.

6.5.3 System Structural Response

In previous sections there have been descriptions of three plausible failure mechanisms of the pressure channels. The FCI channel pressurization is capable of accelerating the water/fuel mixture above the interaction zone. Because of the Chernobyl-4 pressure tube design for online refueling from the top end closure, the water slug impacting the closure is predicted to cause stress in the channel wall immediately below the top cap which exceeds the material ultimate strength. This part of the Chernobyl-4 piping system has no containment whatsoever. If end caps failed in this manner, they, along with the overlying floor slabs, would be ejected upward directly into the refueling building. A blowdown of high pressure steam upward into the building would ensue from failed channels which may explain the multiple shock sounds heard by the operators. It is likely that fuel and cladding material would be ejected during the blowdown, including possibly the fuel assembly itself. It is not known for certain that this type of failure actually occurred. The recovery of physical evidence from among the debris such as the top caps or large fuel and cladding segments has not been reported.

Failures of the upper transition weld joints are strongly suspected due to the combined effects of channel pressurization and transient heatup which far surpassed the design limitation. Failure of this weld joint would have caused steam blowdown into the sealed reactor space. Since the weld is located in the region of the massive steel shield blocks (above and below the graphite blocks) and since the steel blocks are attached to the underside of the massive reactor cover assembly,[23] it is unlikely that there would have been any significant compliance of the structure due to blowdowns in this region. Failures of the Zr-alloy pressure tubes are predicted in the core region owing to the transient heating and ablation of the channel wall by molten core materials. High channel pressure increases the severity of the loading although the channel would not be predicted to fail by FCI pressurization alone. Failure of the channel wall in the core region would also cause blowdown into the sealed reactor space. Specifically, the blowdown would occur amongs the graphite heat transfer rings and graphite moderator blocks. The compliance of these blocks to the blowdown forces is uncertain, as is the tightness of the packing. The blocks appear to be interlocked and prevented from any significant upward motion (at this stage) by the secured steel shield blocks. Hence the blowdown rate into this tightly packed region is uncertain.

One matter is unmistakable about this accident. Channel failures did occur in the sealed reactor space, and this caused steam blowdown and subsequent overpressurization. Although this region is regarded as "contained," it has shortcomings in criteria of effective containment. The design overpressure rating of the region is 0.18 MPa (26 psig), the free volume is exceedingly small, and the provision for steam condensation (based on rupture of a single channel) was certainly inadequate for this accident. As a result of multiple channel failures, the steam pressure increased in the sealed space and the vault failed catastrophically. The 1000 tonne reactor cover assembly was lifted and tilted in the process of failing. In doing so it destroyed the pressure tube outlet piping which ran horizontally above the cover. Hence, massive steam blowdown of the reactor system through nearly all the channels would have ensued. It is likely that the channel piping separated at the weld joints or in the core so that the blowdown would have occurred via the vault/graphite space. It is also likely that piping was ripped apart above the cover so that blowdown would also have occurred directly into the refueling building. If there had still been water in the core at this time, channel voiding would now have been complete. This would have been accompanied by insertion of any remaining void reactivity, literally as a step insertion.

The abrupt release of stored energy when the cover failed plus continued blowdown into the graphite region caused an upward dispersal of materials from this region through the roof of the

refueling building. The ejection consisted of a steam/water mixture, numerous graphite moderator blocks, and fuel and cladding debris. Figure 41 shows a picture of the cover and the core region after the accident. It was reported that about 25 percent of the graphite was ejected from the vault. This would have included blocks from the topmost layer which are largely reflectors above the top of the core (at lower temperature than the blocks below) plus additional blocks from the upper part of the core region. There is no report that steel shield blocks fastened to the underside of the cover on a length of piping were also ejected. It was reported that the mass of fuel ejected amounted to 3-4 percent of the total. Following the blowdown, air eventually entered the vault region permitting the subsequent graphite fire.

When the reactor cover was lifted and tilted during structural failure, control rod structural members which are attached to the cover were also lifted. We know that certain of the rod drives had been disengaged in an attempt to drop the rods by gravity into the core, but the rods were still attached by cable to the structure. Depending on details of the attachments and actual rod positions at this stage of the accident, it may be speculated that upward motion of the control structures attached to the cover may have had some influence to withdraw rods. At the elevated initial temperature of the fuel, an ensuing rod-ejection power excursion could have particularly high energetics potential if high fuel vapor pressure is reached.

6.5.4 Explosions

It was reported that two explosions were heard, separated by a time interval of 2 or 3 seconds. One event which can be clearly established to cause an "explosion" was the catastrophic breach of the sealed reactor vault and the ensuing release of stored energy and core materials. The origin of another explosion-type sound is not so clear. Based on the present analysis it could have been attributable to the near simultaneous failures of top end caps involving high power channels owing to the FCI energetics. This would have led to high-pressure steam blowdown from numerous channels which would have caused an initial explosion-like sound. (The blowdown sound would have persisted, especially to individuals inside the building.) Both the end cap failures and the vault failure would have been accompanied by upward-directed missiles. Other possibilities include a secondary power excursion, if lifting the vault cover did in fact pull control rods.

6.5.5 Fireworks

The explosion(s) were reported to have caused burning lumps of material and sparks to shoot into the air above the reactor, some of which fell onto roofs and started fires. Tests were performed to examine whether the ejection of the graphite blocks could account for the "fireworks" observed above the plant at the time of the explosions. Graphite specimens were heated to 700, 800, and 900 degrees C to observe their luminescence and their behavior when a high velocity jet of air was directed onto them. In one case the graphite was a solid block of reactor-grade materials of about the same density as used at Chernobyl-4; in the second case the block was crushed into chunks of 1 cm characteristic size. At ~700 degrees C the graphite had become slightly luminescent, but both the block and chunks were quickly "quenched" by the air jet. The luminescence increased at 800 degrees C but the result was the same when the air jet was applied. At 900 degrees C the graphite was brightly luminescent and slowly burned with application of the air jet. The graphite at Chernobyl-4 was reported to be 700 degrees C during normal operation. Due to the low power, overcooled conditions of the test, the graphite may have been at even lower temperature. The 0.5 m of graphite in the upper axial reflector was at lower temperature and would have been among the first blocks ejected from the vault. Five percent energy deposition in the graphite during the first Soviet calculated power burst would have raised the graphite temperature by less than 10 degrees C. Hence, based on the test results, it is unclear that the graphite alone could have accounted for the observed fireworks. Views of the graphite debris show large chunks lying closely together on the reactor building roof in regions where there was no fire. Elsewhere, however, fires were started. While this may be explained by the temperature differences of the blocks, there is also the suspicion that other reactive materials may have been ejected. In particular, upward ejection of fuel and cladding segments would have been brightly luminescent due to their very high initial temperature and rapid oxidation in air. Such segments may have been ejected when the vault failed, but large segments capable of starting fires could well have come from the channels, supporting the notion that top end caps may have been blown off some of the channels and fuel and cladding ejected upward.

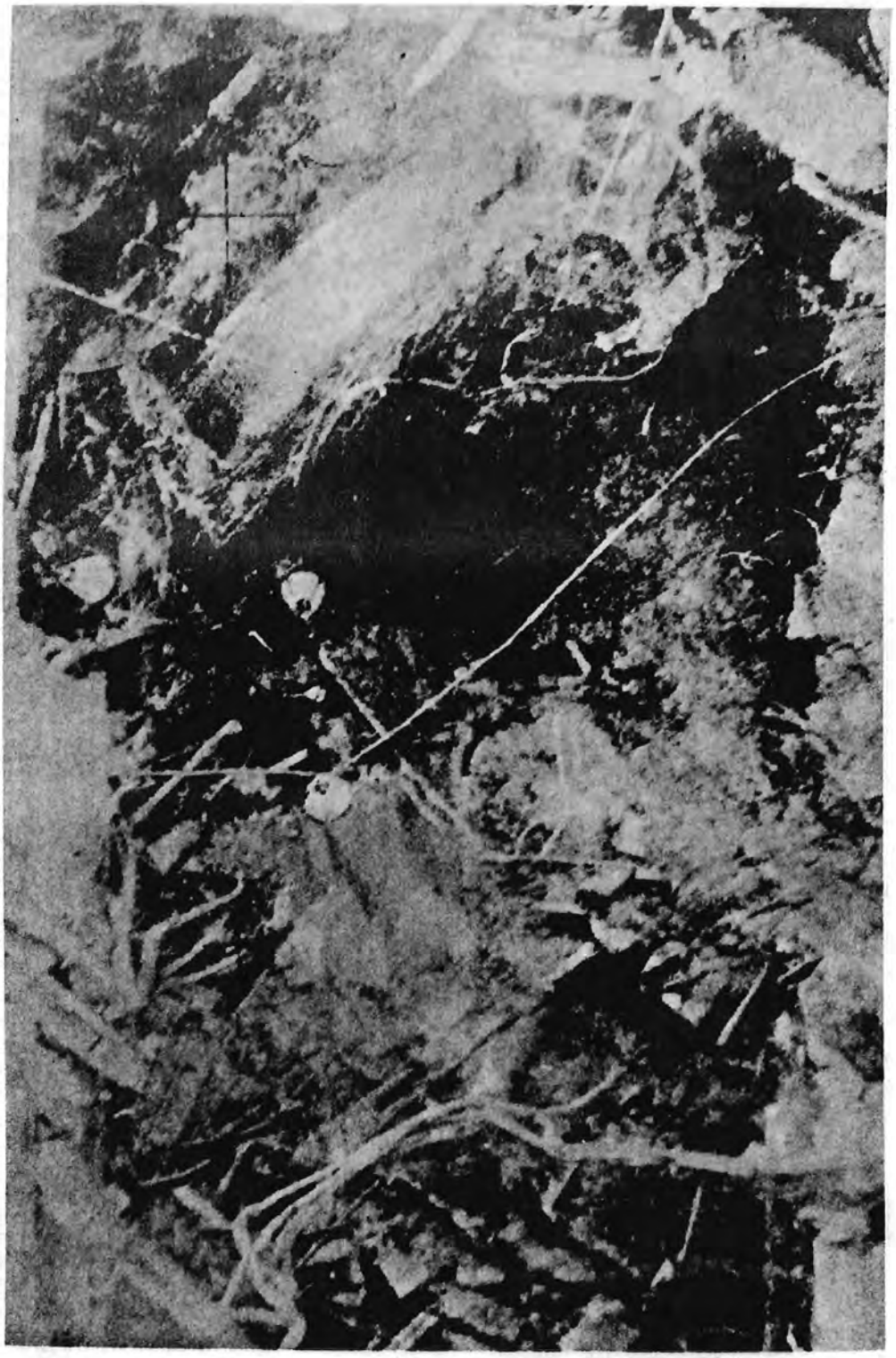

Figure 41. Picture of the Cover and the Core Region After the Accident.

References

1. U.S.S.R State Committee on the Utilization of Atomic Energy, The Accident at the Chernobyl-4 Nuclear Power Plant and Its Consequences (information compiled for the IAEA Experts' Meeting, Vienna, 25-29 August 1986), Parts I and II, August 1986.

2. R. T. Lahey and F. J. Moody, The Thermal-Hydraulics of a Boiling Water Reactor, ANS Press, Hinsdale (1977).

3. G. C. Slovic, et al., "RAMONA-3B Application to Browns Ferry ATWS," Proceedings of 12th LWR Safety Research Information Meeting, NBS, Gaithersburg, MD, October 22-26, 1984.

4. Argonne National Laboratory, Chemical Engineering Division Semiannual Report, ANL-7425 (1968).

5. R. W. Miller, The Effects of Burnup on Fuel Failure; I. Power Burst Tests on Low Burnup UO2 Fuel Rods, IN-ITR-113 (1970).

6. L. W. Deitrich, et al., Summary and Evaluation of Fuel Dynamics Transient-Overpower Experiments: Status 1974, ANL-77-44 (1977).

7. R. Simms, et al., Transient Overpower Test E8 on FFTF-Type Low-Power-Irradiated Fuel, ANL-77-93 (1977).

8. P. E. MacDonald, et al., "Assessment of Light-Water- Reactor Fuel Damage During a Reactivity-Initiated Accident," Nuclear Safety, 21, No. 5 (1980).

9. M. S. El-Genk, R. R. Hobbins, and P. E. MacDonald, "Molten Fuel-Coolant Interaction During A Reactivity Initiated Accident Experiment," Nucl Eng. and Des., 66 (1981).

10. RETRAN-02, A Program for Transient Thermal Hydraulic Analysis of Complex Fluid Flow Systems, EPRI NP-1850-CCM (4 volumes).

11. T. H. Hughes and J. M. Kramer, "The FPIN2 Code-An Application of the Finite Element Method to the Analsyis of the Transient Response of Oxide and Metal Fuel Elements," Proceedings of the Conference on Science and Technology of Fast Reactor Safety, Guernsey, May 12-16, 1986.

12. V. G. Adon, et al., "Fuel Elements of the RBMK-1000 Reactor," Atomnaya Energiya, 43, pp. 235-239 (1977).

References (Continued)

13. S. M. Gehl, Comparison of Fission-Gas Release and Mechanical Behavior During Transient Nuclear and Electrical Heating of Light-Water-Reactor Fuels, NUREG/CR-1001, ANL-78-60, June 1979.

14. MATPRO-Version 11 (Revision 2), A Handbook of Materials Properties for Use in the Analysis of Light Water Reactor Fuel Rod Behavior, G. A. Reymann, ed., TREE-NUREG-1280, August 1978.

15. H. M. Chung and T. F. Kassner, Deformation Characteristics of Zircaloy Classing in Vacuum and Steam Under Transient Heating Conditions: Summary Report, NUREG/CR-0344, AND-77-31, July 1978.

16. A. E. Wright, Personal Communication, Argonne National Laboratory, September 1986.

17. Pizzica, P. A. Garner, P. L. and Abramson, P. B. "A User's Guide to EPIC," NUREG/CR-1504, ANL-80-47.

18. C. Y. Wang and W. R. Zeuch, "A Multi-Dimensional Arbitrary Lagrangian-Eulerian Method for Dynamic Fluid-Structure Interaction," Fluid Transients and Fluid-Structure Interaction, 1982 ASME Special Publication, PVP64, Book No. H00221, pp. 289316 (June 1982).

19. C. Y. Wang and W. R. Zeuch, "Recent Developments of the Arbitrary Lagrangian-Eulerian Containment Code ALICE-II," Trans. 7th Int'l. Conf. on Structural Mechanics in Reactor Technology, paper E 4/8, Vol. E, Chicago (August 1983).

20. J. L. Ku, C. Y. Wang, and W. R. Zeuch, "Comparison of ALICE-II Code Predictions with SRI Complex Vessel Experiments," Trans. 7th Int'l. Conf. on Structural Mechanics in Reactor Technology, paper E 4.5, Vol. E, Chicago (August 1983).

21. C. Y. Wang, J. L. Ku, and W. R. Zeuch, "Analysis of Complex Vessel Experiments Using the Hybrid Lagrangian-Eulerian Containment Code ALICE-II," Advances in Fluid-Structure Interaction, 1984 ASME Special Publication, PVP-Vol. 78 (AMD-Vol. 64) Book No. H00292 (June 1984).

22. J. J. Sienicki, Private Communication, Argonne National Laboratory, Reactor Analysis and Safety Division.

APPENDIX A

ANALYSES PERFORMED PRIOR TO THE VIENNA CHERNOBYL-4 POST ACCIDENT REVIEW MEETING IN AUGUST 1986

PRELIMINARY ANALYSIS OF CHERNOBYL POWER EXCURSION EVENT

BEGINNING 4/26/86 AT 1:23:04 A.M.

GREGORY J. VAN TUYLE

DEPARTMENT OF NUCLEAR ENERGY

BROOKHAVEN NATIONAL LABORATORY

AUGUST 21, 1986

INTRODUCTION

- IN MAY, USED MINET TO SIMULATE STATION BLACKOUT
- AFTER O'HARE MEETING, BEGAN TO LOOK AT REACTIVITY TRANSIENTS FROM 7% POWER
- ON TUESDAY, 8/19/86, RECEIVED TRANSLATION OF RUSSIAN DOCUMENTATION OF ACCIDENT FOR IAEA
- SIMULATION OF ESSENTIAL FINAL MINUTE OF ACCIDENT BASED ON REPORT AND BEST ESTIMATES
- CAN IDENTIFY ESSENTIAL BOUNDARY CONDITIONS - KEY QUESTIONS FOR VIENNA

MINET

- FLEXIBLE THERMAL-HYDRAULIC SYSTEMS CODE USED FOR LWR, LMR, HTGR SYSTEMS
- MODULAR CODE - USER CONSTRUCTS REPRESENTATION FROM BASIC MODULES, SPECIFYING OPTIONS FOR EACH
- TWO PHASE FLOW BY HEM OR DRIFT
- REACTOR MODEL HAS MANY OPTIONS
- CHERNOBYL MODEL:
  - REACTOR - POINT KINETICS, 4 AXIAL NODES, 1 RADIAL FUEL NODE, GRAPHITE NEGLECTED
  - HEM USED (DRIFT FLUX IN RESERVE)
  - PUMPS, PIPING, SEPARATORS STANDARD

ACCIDENT DESCRIPTION

- FROM 7% POWER AND HIGH FLOW (8 PUMPS ON), 4 PUMPS BEGAN COASTDOWN, CAUSING POWER EXCURSION
  - VARIOUS SAFETY SYSTEMS DEFEATED BY OPERATORS
  - OPERATOR DEPARTED FROM PLANNED EXPERIMENT
  - UNCERTAINTY IN FEEDWATER AND STEAM FLOWS:
    - FEEDWATER PROBABLY LOW
    - STEAM FLOW PROBABLY UNKNOWN
  - UNCERTAINTY IN PUMP COASTDOWN RATE
- APPROXIMATELY 35 SECONDS AFTER PUMPS BEGAN COASTDOWN, VERY SEVERE CONDITIONS DEVELOPED

FIGURE 1: MINET Representation of Chernobyl System for Dry-Out Analysis

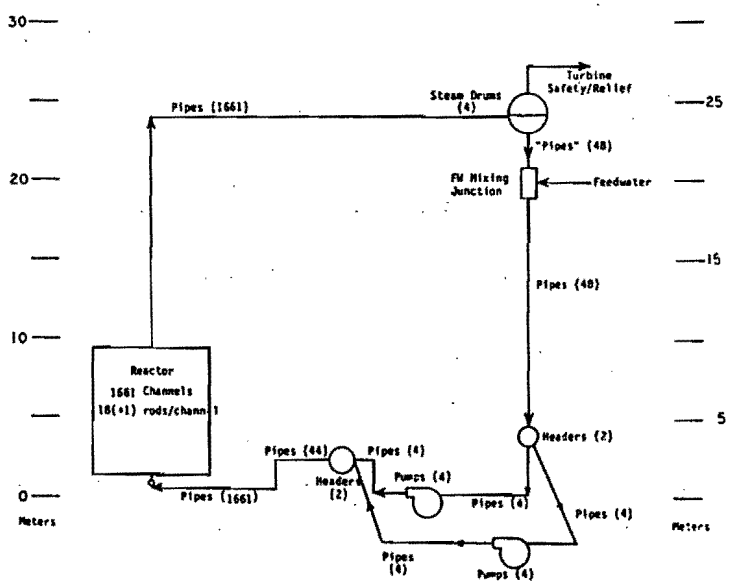

ESTIMATED INITIAL CONDITIONS

- REACTOR GENERATING 200 MW_T
- FEED AND STEAM FLOW APPROXIMATELY 100 KG/SEC
- HIGH FLOW THROUGH REACTOR - 12,000 KG/SEC
- DRUM LEVEL HIGH - ASSUME 0.6 RELATIVE
- 8 PUMPS ADDING 1.2 MW_T HEAT EACH
- ESTIMATE BACK PRESSURE AT 6.5 MPA

TRANSIENT BOUNDARY CONDITIONS UTILIZED

- FW FLOW DROPS TO 50 KG/S AS 2 FW PUMPS COAST DOWN
- 4 MAIN PUMPS COAST DOWN
  - ASSUME 65% SPEED AT 10 SECONDS
- ASSUME W_{STEAM} AT 100 KG/SEC (7% POWER PRODUCTION)
- ASSUME NO CONTROL ROD ACTION - ONLY VOID AND DOPPLER

DOPPLER = 1×10^{-5} $\Delta K/°C$

VOID :

α	ρ $\Delta K/\Delta\alpha$
0.0	+ 0.032
0.49	0.0

(VOID CONVERTED FROM FIGURE 1 OF 7/19/86 REPORT)

MINET Analysis of Chernobyl Power Excursion of 4/26/86

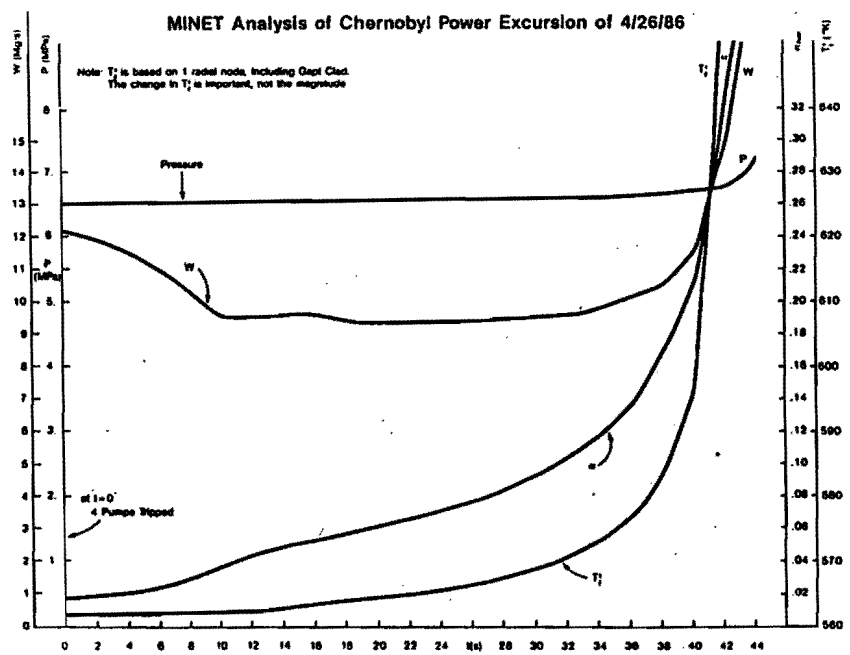

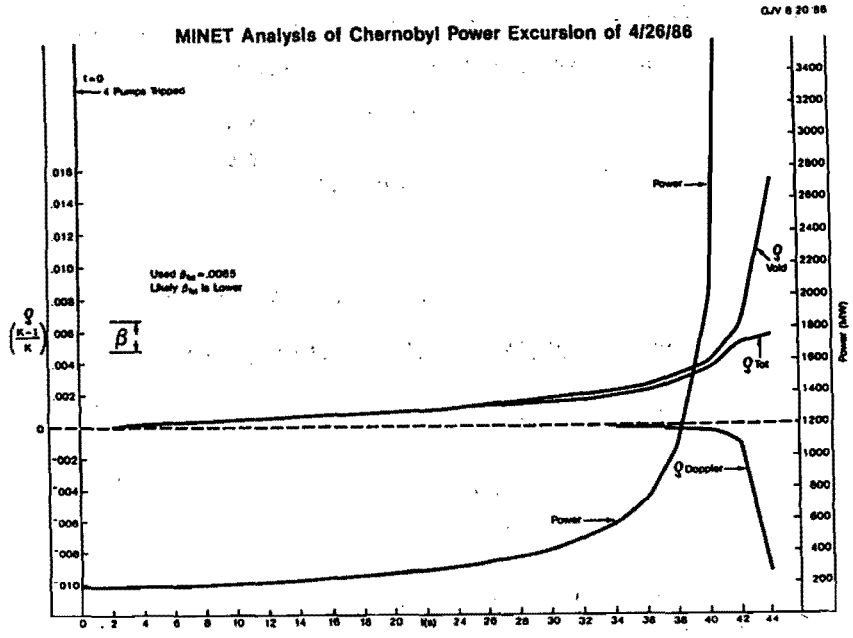

KEY UNCERTAINTIES

PARAMETER	IMPORTANCE	HOW ESTIMATED FOR THIS ANALYSIS
STEAM FLOW RATE	HIGH	7% POWER PRODUCTION
FORM LOSS FACTORS	MEDIUM	BACKFIT FROM FLOW RATE
FEEDBACK COEFS	HIGH	FULL POWER VALUES
PUMP COASTDOWN	HIGH	100% TO 65% IN 30
FEEDWATER FLOW	LOW	7% POWER + TRIP 2

CONCLUSIONS TO DATE

- SOVIET DESCRIPTION OF ACCIDENT PLAUSIBLE, ALTHOUGH SOMEWHAT INCOMPLETE, ESPECIALLY BALANCE OF PLANT
- KEY BOUNDARY CONDITIONS ARE STILL UNKNOWN
- SCOPING ANALYSIS ESSENTIAL PRIOR TO HEAVY EFFORT, E.G., RAMONA
- LARGE EXPERIMENTAL UNCERTAINTIES
- QUITE PROBABLE THAT VOID SUPPRESSION DUE TO PRESSURE INCREASE LIMITED THE EXCURSION

SUMMARY

- MINET ANALYSIS REVEALS LARGE UNCERTAINTIES IN ESSENTIAL BOUNDARY CONDITIONS --- MUST BE RESOLVED BEFORE ADDING DETAIL
- FEEDBACK PARAMETERS UNDER 7% POWER AND 12,000 KG/SEC FLOW NOT WELL KNOWN - NEED TO CALCULATE (OR ACQUIRE?)
- REFINED BOUNDARY CONDITIONS MAY ....
  - LEAD TO UNDERPREDICTIONS FROM SIMPLE ANALYSIS
  - FORCE AND FACILITATE USE OF RAMONA TO SIMULATE TRUE TRANSIENT

NOTE:

MODELING THE CHERNOBYL SYSTEM

In order to perform an initial analysis of the Chernobyl acccident scenario, we utilized the MINET Code, a highly modular thermal-hydraulic systems transient analysis program. The reactor was modeled using point kinetics, and a flat power profile. System design details were estimated as best as possible.

The computer simulation was initialized to correspond to conditions in the plant at the time the turbine generator coastdown was begun. It was assumed that the water level in the separators was 0.6 relative, and the pressure in the separators was 6.5 MPa (from the Soviet briefing report).

In developing boundary conditions for the transient calculations, we assumed that the feedwater was reduced by 50% in the first 30 seconds (two of four pumps coasting down), that the steam flow was maintained at 7% of full power (i.e., 100 kg/sec), and that the four affected primary pumps coast down to 65% speed in 30 seconds (lower speeds are not important). Feedwater temperature was held constant. Control and/or scram rod movements were neglected.

THE TEST TRANSIENT

At 1:23:04 AM, the operators closed off steam to one of the turbines, thereby causing a reduction in the power being used to drive several of the pumps in the system. This caused a slow reduction in flow rate (value of core outlet is plotted) in the core. As the flow decreased, more water was converted to steam (as opposed to being heated to the boiling point), and the void fraction increased. This added reactivity to the core, so the power increased as shown. There were two compensating effects. First, as the power increased, the pressure increased, which suppressed some of the voiding (but obviously not enough). Second, the fuel got hotter which tends to decrease the reactivity ("Doppler"). Unfortunately, the fuel heatup lags the voiding, so its negative reactivity contribution ("Doppler") is too late to prevent the large power excursion. The plotted power peak is low by a factor of four (approximate) because of the way it was calculated (composite of prompt-jump in systems calculations plus exact stand-alone calculation). (This problem was corrected in 9/86 by adding exact solution to MINET.)

GJV 11/86

MINET Analysis of Chernobyl Power Excursion of 4/26/86

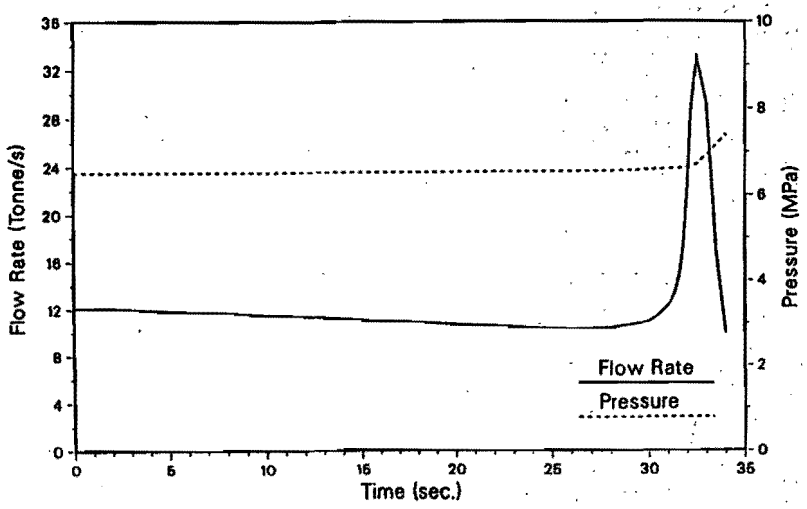

MINET Analysis of Chernobyl Power Excursion of 4/26/86

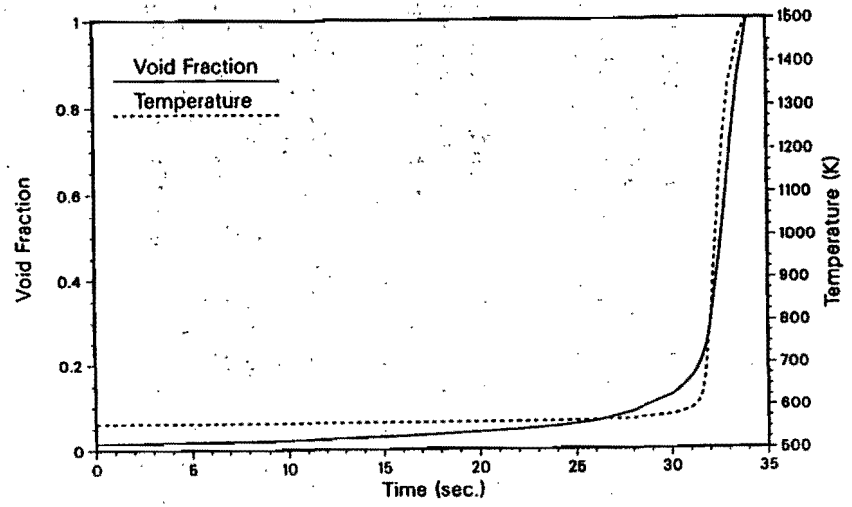

MINET Analysis of Chernobyl Power Excursion of 4/26/86

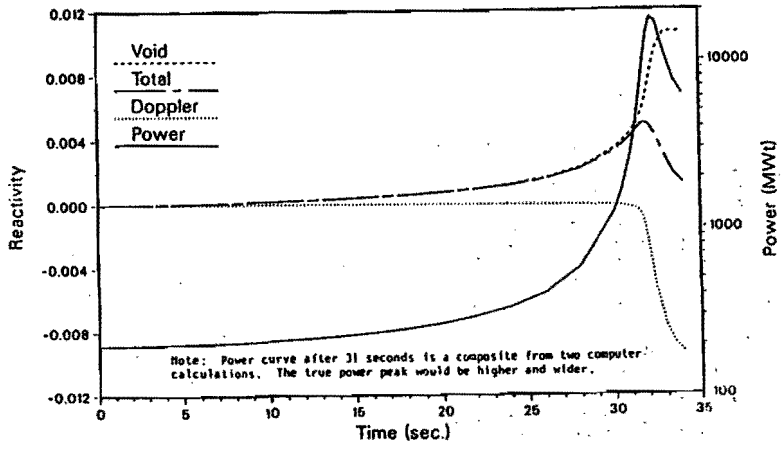

8/24/86

IMPORTANT NOTE ABOUT THE POWER TRACE

It should be noted that the power excursion shown in Figure 4 is very probably an underestimate of the true excursion at the Chernobyl plant. That is because the plotted power is the result of two calculations that were combined in a way that tends to reduce the power transient. The MINET Code uses the "prompt jump" approximation for reactor kinetics, which predicts overly fast power increases when the reactivity approaches one dollar (ρ = 0.0055 in this case). Thus, after completing the MINET systems analysis, we repeated the kinetics calculation using a point kinetics code with a more exact solution methodology. The two calculations were in perfect agreement until 31 seconds. After that time, the point kinetics code predicted a lower power excursion, and that is the power trace plotted in Figure 4. However, the separate point kinetics calculation relied on MINET for the time-dependent reactivity, and the MINET calculations had a bigger power peak (74,000 MW_t) and thus very hot fuel and a high Doppler feedback. Thus, the plotted power peak is likely significantly lower in magnitude and narrower in time than the one we will ultimately calculate when we get the two computer calculations properly coupled. As a footnote for those trying to perform severe accident analysis, the integrated energy burst in the MINET calculation was about 40 full power seconds (128,000 MJ) over 3 seconds. An estimate of such an energy release over 5 seconds is probably reasonable.

Gregory J. Van Tuyle

INITIAL SIMULATION OF THE APRIL 26, 1986 ACCIDENT AT CHERNOBYL-4

S. J. BALL
R. M. HARRINGTON*

Instrumentation and Controls Division
Oak Ridge National Laboratory

INITIAL SIMULATION OF THE APRIL 26 ACCIDENT SEQUENCE IS COMPLETE

- QUICK RESULTS POSSIBLE BECAUSE:
  - USE OF SIMULATION LANGUAGE
  - USE OF EXISTING PROGRAM ROUTINES
    FROM NRC SPONSORED BWR SEVERE ACCIDENT SEQUENCE
    ASSESSMENT RESEARCH
- PARAMETERIZED ON SHAPE, MAGNITUDE OF VOID FEEDBACK, AND ON INITIAL CORE INLET SUBCOOLING
- THE PRELIMINARY RESULTS SUBSTANTIATE THE PLAUSIBILITY OF RECENTLY RELEASED RUSSIAN INFORMATION

A SIMPLIFIED MODELING APPROACH WAS USED

- NO SEVERE FUEL DAMAGE
- 6 GROUP POINT KINETICS
- ONE FUEL NODE - NO DNBR CALCULATION
- COOLANT DENSITY PROFILE FOR ONE AVERAGE CHANNEL
- MASS, ENERGY BALANCES FOR STEAM DRUM LIQUID
- MASS, ENERGY BALANCES FOR STEAM LINE/STEAM DRUM STEAM
  --- STEAM TABLE LOOK-UP TO DETERMINE PRESSURE
- CRITICAL FLOW THROUGH STEAM RELIEF ORIFICES

INITIAL CONDITIONS FOR ORNL RUNS

POWER = 7% OF 3140 MW

CORE FLOW = 112%

STEAM DRUM PRESSURE* = 942 PSIA

STEAM DRUM LEVEL = 100%

SUBCOOLING, STM DRUM = 1 BTU/LB

INITIAL STEAM PRODUCTION = 119 LB/S

INITIAL CORE AVG. VOID = 1.6%

BOUNDARY CONDITIONS

CORE INLET FLOW: DECREASES TO 70% OVER 20 SECONDS

TURBINE/BYPASS SYS: CONSTANT ORIFICE OPENING

NO CONTROL ROD MOTION

*COOLANT IN FUEL CHANNELS IS ASSUMED TO BE 25 PSI HIGHER.

FIGURE 1 VOID COEFFICIENTS USED FOR ORNL CALCULATION CASES 1 -- 8

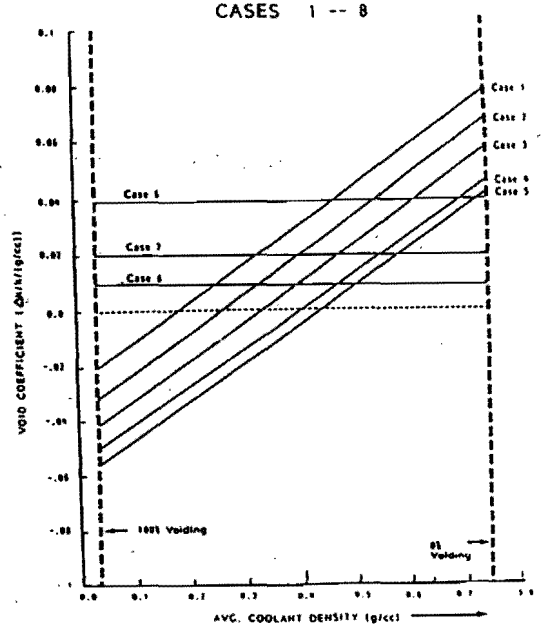

RESULTS: VOID FEEDBACK SENSITIVITY

CASE NO.*	PEAK PROMPT POWER (MW)	TIME OF PEAK POWER (S)	MINIMUM PERIOD (S)
NOTE: FOR CASES 1-5 VOID COEFF DEPENDS ON COOLANT DENSITY			
1	55,000	21.5	0.46
2	38,650	26.0	0.67
3	24,460	32.0	1.01
4	11,963	41.0	1.99
5	7,065	48.5	3.25
NOTE: FOR CASES 6-8 VOID COEFF IS CONSTANT WITH COOLANT DENSITY			
6	31,100	45.5	1.06
7	8,230	91	5.23
8	2,730	227	42.2

FOR VOID FEEDBACK CURVE, SEE FIGURE 1

RESULTS: COOLANT SUBCOOLING* SENSITIVITY

INITIAL SUBCOOLING (BTU/LB)	PEAK PROMPT POWER (MW)	TIME OF PEAK POWER (S)	MINIMUM PERIOD (S)
1	55,000	21.5	0.46
5	60,450	25.0	0.42
10	59,350	31.5	0.44
20	61,000	50.0	0.39
40	59,000	91.0	0.43
60	59,800	132.5	0.39

SUBCOOLING SPECIFIED IN STEAM DRUM

CONCLUSIONS

- RUSSIAN EXPLANATION OF ACCIDENT AS SEVERE POWER SPIKE IS PLAUSIBLE
- STRONG POSITIVE VOID FEEDBACK CAN CAUSE SEVERE TRANSIENT OVERPOWER
  - SHAPE OF VOID COEFFICIENT VS DENSITY IS IMPORTANT
- LIMITING MAXIMUM VOID REACTIVITY TO LESS THAN ONE DOLLAR OF REACTIVITY WOULD:
  - DECREASE PROMPT POWER BY FACTOR OF ~ 10
  - INCREASE MINIMUM PERIOD BY FACTOR OF ~ 6
  - MAKE MITIGATION BY CONTROL ROD INSERTION MORE FEASIBLE

APPENDIX B

THE CHERNOBYL-4 ACCIDENT ANALYSES WORKSHOP HELD ON SEPTEMBER 16, 1986

Workshop Report

Date and Place of Workshop: September 16, 1986
Dulles Airport Marriott

Workshop Topic: Analysis of Chernobyl Event

Purpose: To present and discuss the results of analyses of the Chernobyl accident.

Agenda:

Introduction	Edward E. Purvis, DOE
Hinet Analysis of Chernobyl Power Excursion As Compared With Soviet Figure 4	Gregory J. VanTuyle, BNL
Chernobyl Modeling Activities	James P. McNeece, PNL
Analysis of the Chernobyl-4 Accident	Syd J. Ball, ORNL
Evaluation of Accident Events	Bruce W. Spencer, ANL
Video of Roof	Edward E. Purvis, DOE
Review of INSAG Report	Herbert Kouts, BNL

Comments and general discussion took place during the course of the various agenda items.

Participants:

DOE	NEA	
Ed Purvis Frank Tooper D. McPherson Bruce Bingham	Kunimiso Soda, JAERI Gianni Petrangeli, ENEA/DISP-Italy Harry Teague, SRD/UKAEA	
FAI	**Bechtel**	**B & W**
Ariel Sheron Phillip G. Ellison	Raphiel Daniels Allen Vieira	Jim Smotral
IT	**SWEC**	**W**
Mario Fontana	Mike Donahue	Aladar Stohmar L. E. Hochreiter
MPR	**EPRI**	**GA Technologies**
Theodore Rockwell	Jack Berge	A. H. Baxter
NUS	**NRC**	**ANL**
John Trotter William Greenaway	Brian Sheron Cardis L. Allen H. Wayne Hodges Howard Richings F. Odar	A. H. Tardiff Bruce Spencer
BNL	**ORNL**	**PNL**
Herbert Kouts Walter Kato John Caren Gregory J. VanTuyle	Syd Ball	Laurin Dodd James P. McNeece

4 Attachments

ORNL ANALYSES OF THE CHERNOBYL - 4 ACCIDENT

R. M. HARRINGTON

S. J. BALL *

INSTRUMENTATION AND CONTROLS DIVISION
OAK RIDGE NATIONAL LABORATORY

SEPTEMBER 16, 1986

* SPEAKER

ORNL'S C R A S - 1 CODE WAS DEVELOPED IN ABOUT 2 WEEKS

(CHERNOBYL REACTOR ACCIDENT SIMULATOR-1)

- USED SIMULATION LANGUAGE (CSMP)
- USED EXISTING MODULAR ROUTINES FROM NRC-SPONSORED SAFETY RESEARCH PROGRAMS
- USED USSR & PNL-DERIVED INPUT DATA FOR SIMPLIFIED PRIMARY SYSTEM MODEL
- SENSITIVITY STUDIES WERE RUN TO:
  - SHOW EFFECTS OF UNCERTAINTIES IN MODEL
  - SHOW EFFECTS OF VARYING INITIAL CONDITIONS AND INITIATORS

A SIMPLIFIED MODELING APPROACH WAS USED

- NO SEVERE FUEL DAMAGE
- 6 GROUP POINT KINETICS
- ONE FUEL NODE - NO DNBR CALCULATION
- COOLANT DENSITY PROFILE FOR ONE AVERAGE CHANNEL
- MASS, ENERGY BALANCES FOR STEAM DRUM LIQUID
- MASS, ENERGY BALANCES FOR STEAM LINE/STEAM DRUM STEAM
  --- STEAM TABLE LOOK-UP TO DETERMINE PRESSURE
- CRITICAL FLOW THROUGH STEAM RELIEF ORIFICES

SEVERAL IMPORTANT DANGEROUS FEATURES OF ACCIDENT'S INITIAL CONDITIONS:

- HIGH FLOW (112%) AND LOW POWER (7%) GAVE LOW QUALITY & LOW VOID FRACTION:
  - LARGE +REACTIVITY "AVAILABLE" FROM MASSIVE VOIDING
  - STEEP SLOPE OF VOID/QUALITY CURVE LEADS TO RAPID INITIAL INSERTION

VOID FRACTION VS FLOW QUALITY (990 PSIA)

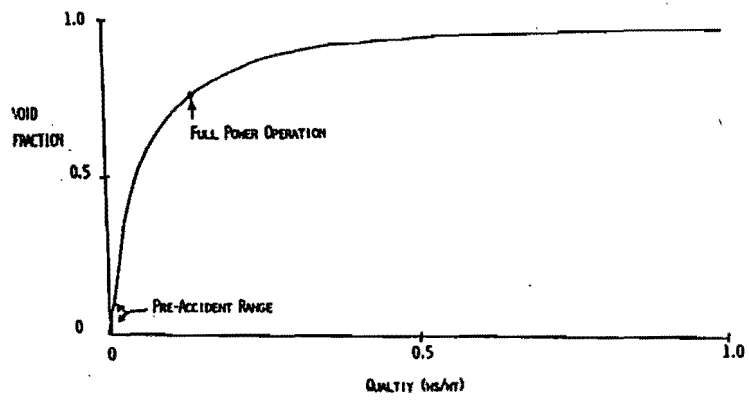

- LOW "CORE REACTIVITY" LED TO MOST RODS BEING APPROX. FULLY WITHDRAWN, INEFFECTIVE EARLY IN SCRAM

  (APPROX. 20 SEC. FULL TRAVEL)

  - HIGH XENON POISON FROM POWER MANEUVERS
  - LOW INITIAL VOID FRACTION GIVES LOW REACTIVITY

REFERENCE CASE

- PNL VOID COEFF FOR 10.3 MWD/KG FUEL
- RECIRC FLOW DECREASES BY 20% IN 30 SEC
- BETA-TOTAL = 0.005
- DRYOUT H FOR HIGH (140%) THERMAL POWER
- TURBINE/BYPASS SYSTEM - CONSTANT ORIFICE OPENINGS
- NO CONTROL ROD MOTION

Calculated RBMK Void Coefficient for 2 W/O U-235 Fuel

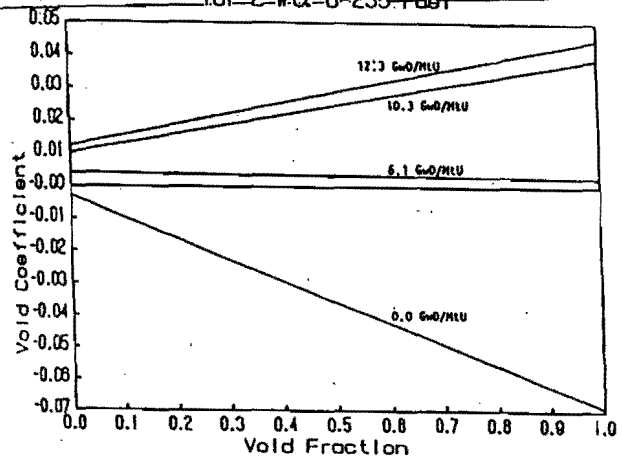

From Jim McNeece
PNL Studies

INITIAL CONDITIONS - REFERENCE CASE

- POWER = 7% OF 3140 MW
- CORE FLOW = 112%
- STEAM DRUM PRESSURE* = 942 PSIA
- STEAM DRUM LEVEL = 100 %
- STEAM PRODUCTION = 277 LB/S
- CORE AVG. VOID = 1.8%

---

*COOLANT IN FUEL CHANNELS IS ASSUMED TO BE 25 PSI HIGHER

SENSITIVITY STUDIES RUN ON:

- VOID COEFFICIENT OF REACTIVITY
- BETA-TOTAL
- CORE INLET SUBCOOLING
- INITIAL POWER LEVEL
- CHANNEL DRYOUT HEAT XFR COEFF
- RECIRC FLOW DECREASE
- PRESSURE RELIEF
- CHANNEL CHARACTERISTIC TIME CONSTANT

** MAJOR CONCLUSIONS **

- USING SIMPLE PRIMARY SYSTEM MODEL W/VARIETY OF PLANT PARAMETERS & INITIATORS - USSR SCENARIO IS APPROX. REPRODUCED.
- POINT KINETICS MODEL NON-CONSERVATIVE FOR LARGE THERMAL CORE.
- USSR ACCOUNT (CRITICAL OF OPERATORS AND DESIGN) IS PROBABLY ACCURATE.

Pacific Northwest Laboratory

Chernobyl Modeling Activities

Reactor Physics Parameters

- Effect of Fuel Enrichment
- Reactivity Coefficients
  - Fuel Temperature
  - Graphite Temperature
  - Coolant Temperature
  - Coolant Void
- Reactor Kinetic Parameters

Pacific Northwest Laboratory

Benchmarking and Validation

- Soviet Literature
  - Experimental Results from Leningrad RBMK's
  - Mock-up Facilities
  - Calculations
- Independent Calculational Tools

Pacific Northwest Laboratory

Delayed Neutron Fraction

Exposure	Fuel Enrichment 2.0%	2.4%
0.0	0.0065	0.0065
10.3	0.0048	---

Pacific Northwest Laboratory

Temperature Coefficients

Exposure	Fuel Coefficient Calculated	Fuel Coefficient Reported	Graphite Coefficient Calculated	Graphite Coefficient Reported
0.0	-1.3×10^{-5}/°C	---	-0.1×10^{-5}/°C	---
10.3	-1.2×10^{-5}/°C	-1.2×10^{-5}/°C	$+3.6\times10^{-5}$/°C	$+6.0\times10^{-5}$/°C

Pacific Northwest Laboratory

Calculated RBMK Void Coefficient for 2 wt% ^{235}U Fuel

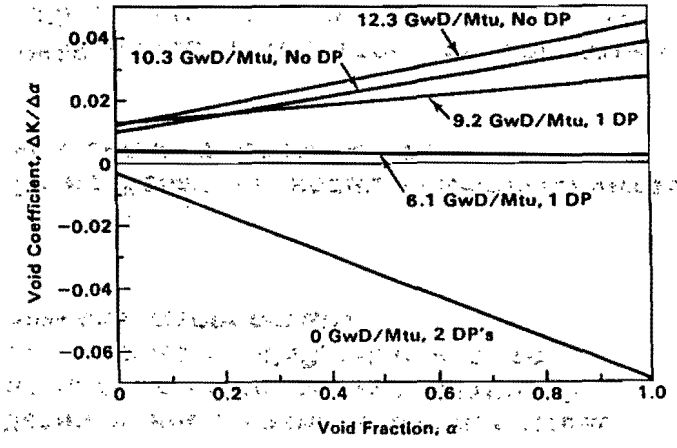

Pacific Northwest Laboratory

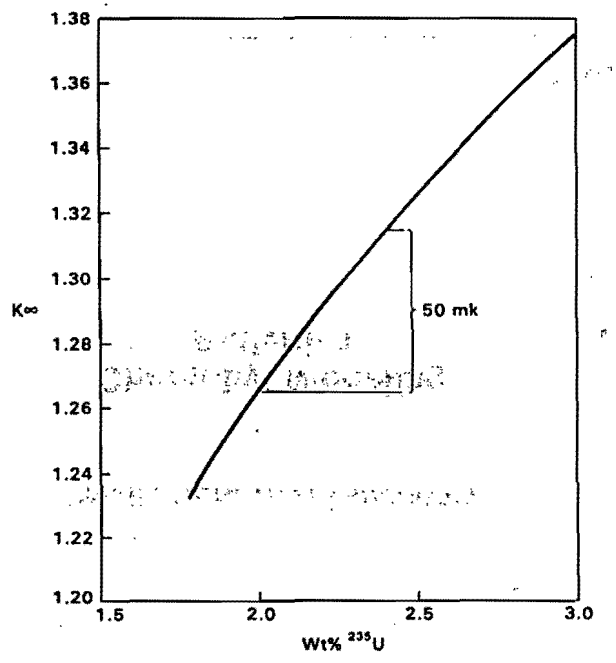

Pacific Northwest Laboratory

MINET ANALYSIS OF CHERNOBYL POWER EXCURSION
AS COMPARED WITH SOVIET FIGURE 4

GREGORY J. VAN TUYLE
DEPARTMENT OF NUCLEAR ENERGY
BROOKHAVEN NATIONAL LABORATORY

SEPTEMBER 16, 1986

MINET

- GENERALIZED MODULAR SYSTEMS CODE DEVELOPED BY BNL FOR NRC
- REACTOR MODULE
  - POINT KINETICS
    - SIX GROUP DELAYED NEUTRONS
    - PROMPT JUMP TO 50 CENTS
    - EXACT SOLUTION ABOVE 50 CENTS
  - SINGLE CHANNEL (4 AXIAL NODES FOR CHERNOBYL)
  - RADIAL CONDUCTION (1 RADIAL NODE FOR CHERNOBYL)
- STANDARD MINET MODULES USED FOR PUMPS, PIPES, DRUMS

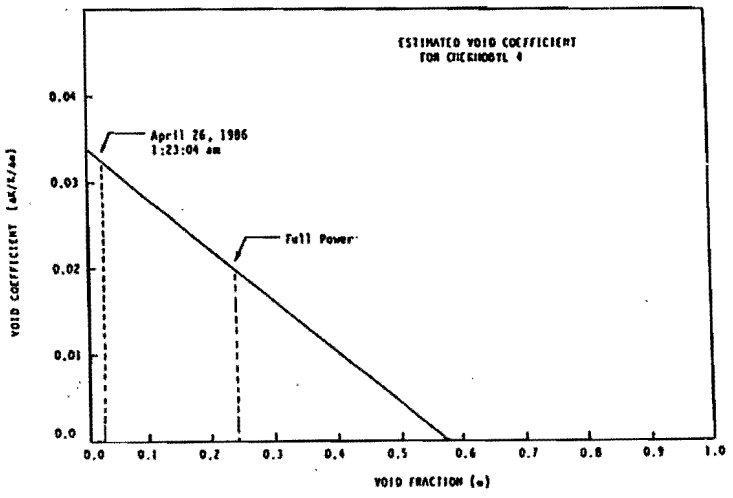

USE OF FIGURE 4

CURVE	PARAMETER	HOW USED?
A	POWER	COMPARED
B	REACTIVITY	COMPARED
C	SD PRESSURE	COMPARED
D	POWER	COMPARED
E	RODS AP-1	*REACTIVITY BOUNDARY CONDITION
G	RODS AP-2	NEGLECTED
H	RODS AP-3	NEGLECTED
K	CORE FLOW	COMPARED
L	FW FLOW	*FLOW BOUNDARY CONDITION
M	TG#8 FLOW	NOT USED
N	FUEL TEMP	COMPARED
O	STEAM FLOW	*FLOW BOUNDARY CONDITION
P	OUTLET VOID	COMPARED
S	SD LEVEL	*INITIAL CONDITION + COMPARED

*USED AS INPUT FOR MINET CALCULATIONS

MINET Analysis of
Chernobyl Power Excursion
of 4/26/86

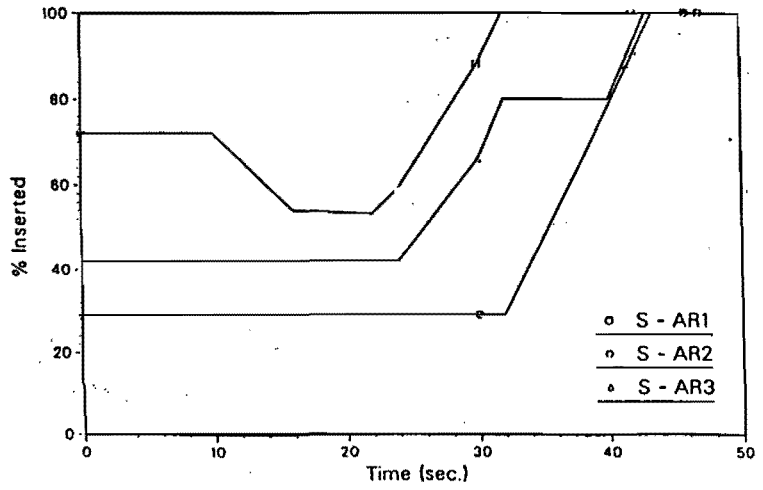

MINET Analysis of
Chernobyl Power Excursion
of 4/26/86

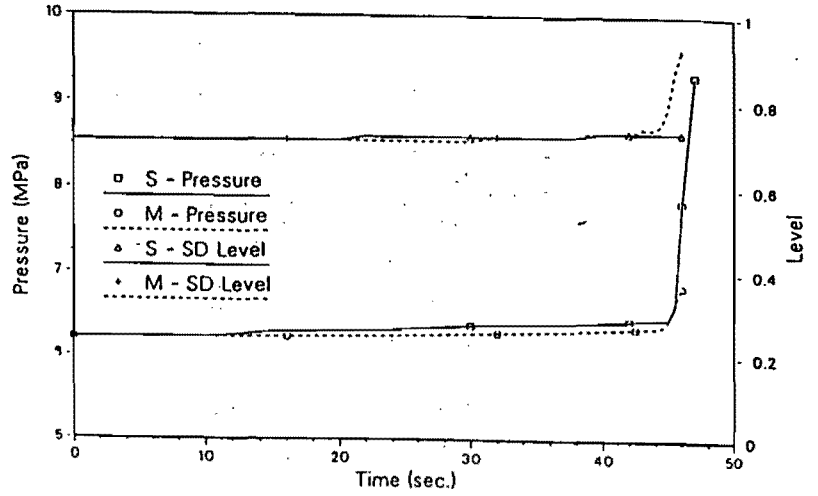

MINET Analysis of
Chernobyl Power Excursion
of 4/26/86

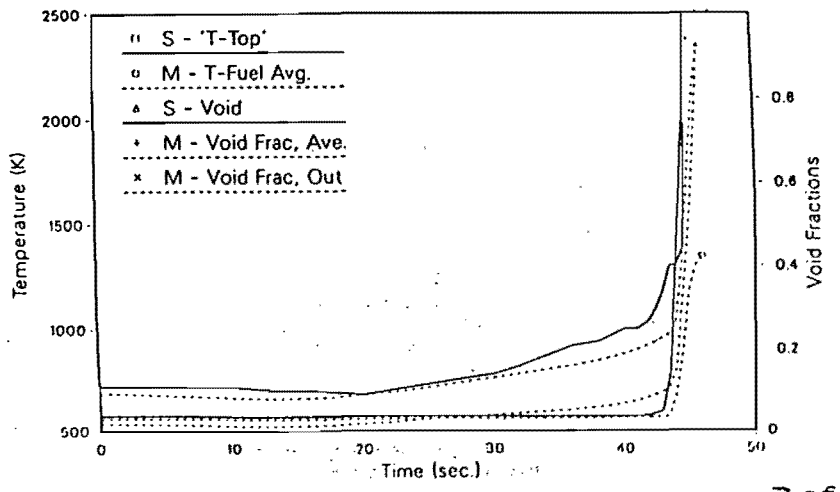

Chernobyl Power Excursion
of 4/26/86

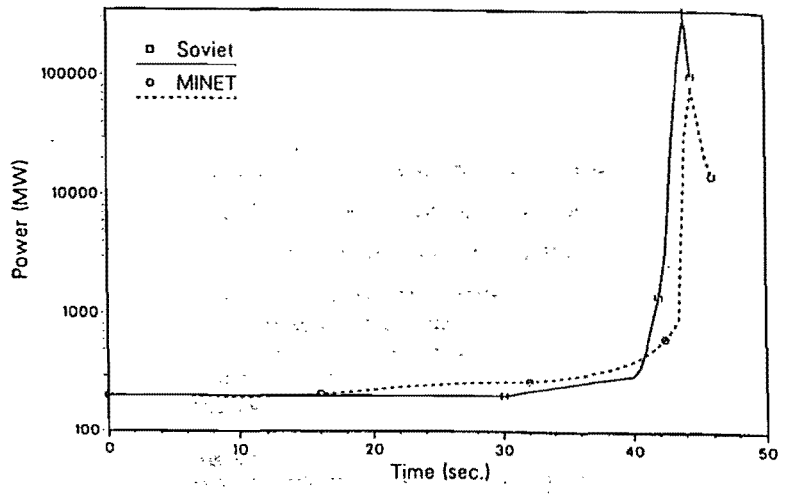

CONCLUSIONS

- BROAD AGREEMENT IN ANALYSIS SUPPORTS SOVIET EXPLANATION
- WITH CURRENT VOID COEFFICIENT, CORE WIDE POWER PEAK MARGINALLY LARGE ENOUGH FOR SEVERE DAMAGE. MAY NEED RAMONA CALCULATIONS TO DETERMINE LOCAL PEAKS
- MANY MYSTERIES NOW RESOLVED, SOME REMAIN - SUCH AS WORTHS OF AP-2 AND AP-3

EVALUATION OF ACCIDENT EVENTS

PRESENTATION TO
CHERNOBYL ANALYSIS WORKSHOP
SEPTEMBER 16, 1986

B. W. SPENCER

ARGONNE NATIONAL LABORATORY
REACTOR ANALYSIS AND SAFETY DIVISION
9700 S. CASS AVE.
ARGONNE, IL 60439

OUTLINE

I. ESTIMATE OF RUSSIAN-CALCULATED FUEL FAILURE CONDITIONS

II. APPLICATION OF ANL ACCIDENT ANALYSIS CODES
- FPIN - FUEL BEHAVIOR
- EPIC - FCI PRESSURIZATION
- ALICE - STRUCTURAL RESPONSE

III. TRANSIENT OVERPOWER DATA BASE
- TREAT
- PBF

IV. BEST ESTIMATE OF ACTUAL EVENTS

THE ENERGY RELEASE DURING THE TRANSIENT OVERPOWER EVENT "EXCEEDED 300 CAL/G" WHICH INDICATES THAT UO_2 FUEL WAS AT LEAST MELTED IN THE INITIALLY INTACT FUEL ELEMENTS ACCORDING TO UO_2 PROPERTY DATA.

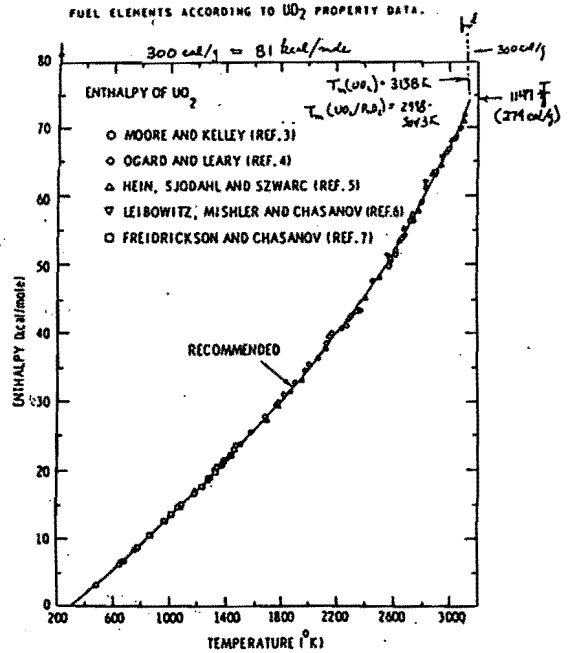

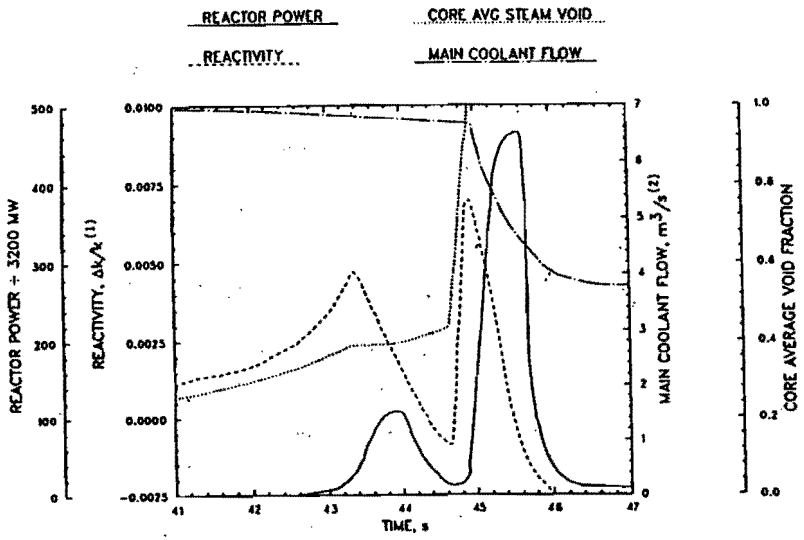

RUSSIAN CALCULATIONS OF REACTOR PARAMETERS AT TIME OF CHERNOBYL-4 ACCIDENT EVENTS

(1) Scale factor reduced by factor of 2 per ORNL analysis and recommendation.
(2) Coolant flow per loop; two loops total.

RUSSIAN-CALCULATED POWER AND FUEL ENERGY DEPOSITION FOR CHERNOBYL-4 TRANSIENT OVERPOWER ACCIDENT

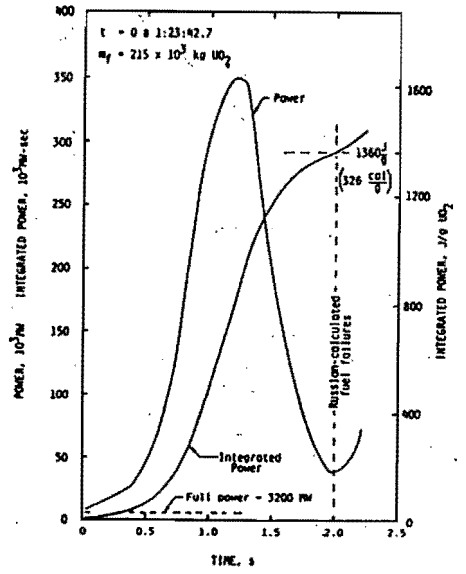

Estimate of Fuel Enthalpy at Time of Fuel Failures[1]

	Enthalpy, J/g (cal/g)	
1. Enthalpy at initial low power operation	67	(16)
2. Estimated energy release in power burst to time of fuel failures	1360	(326)
3. Estimate of energy transferred to coolant during power burst ($q'' \sim 1 \times 10^6$ BTU/hr ft^2 ~ 3 MW/m^2)	-185	-(44)
4. Estimated enthalpy at time of fuel failures	1242	(298)

[1]Enthalpy referenced to zero at 300K

Use Efficiency Model to Estimate Plausible Magnitude of FCI Energetics

Fuel mass = 130 kg UO_2 per operating channel

Avg enthalpy at failure = 1.24 MJ/kg

Assume:

- 10% of fuel participates in interaction
- Thermal-to-mechanical energy conversion is 5% efficient (~ 40% thermodynamic maximum efficiency for expansion to ambient conditions)

For above assumptions, overall energy conversion is 0.1 x 0.05 = 0.005 (0.5% efficient)

Mechanical energy = $1.24 \frac{MJ}{kg}$ x 130 kg x .005 = 0.8 MJ

Conclude of the order of 1 MJ of mechanical energy is available to damage individual operating channels.

Integrated Analyses of Chernobyl Transient Overpower Event -- Fuel Behavior and Consequences

FPIN	Provides detailed calculation of fuel thermal behavior such as failure temperature, melt fraction, and internal pressure under transient overpower conditions; power-time history input from separate source.
EPIC	Provides calculation of fuel-coolant thermal interaction producing channel pressurization events under conditions that FPIN calculates for fuel element failure into water in the RBMK operating channels.
REXCO/ALICE	Provides calculation of slug acceleration and pressure-wave propagation in piping system for EPIC-calculated pressurization event. Determines likely modes and location of piping failures.

ARGONNE NATIONAL LABORATORY

FPIN2 Fuel Failure Calculations

- FPIN2 Code
  - Transient heat transfer analysis
  - Finite element mechanical analysis
- Adaptation of FPIN for Chernobyl transient overpower analysis
  - Fuel structure similar to low-power LWR fuel
    - Unrestricted
    - Essentially 100% fission gas retention
- UO_2 and zircaloy properties
- Power burst period set at 0.65 s
- Failure strain of 5% for irradiated α-zircaloy at 573K

Comparison of Fuel Types

	Chernobyl	DEH-Tested PWR Fuel
Density, % TD	91	92
Enrichment, %	2	2.55
Pellet dia., mm	11.5	9.32
Cladding OD, mm	13.5	10.7
Cladding thickness, mm	0.9	0.61
Peak/Ave power	1.4	1.3
Average linear power, Kw/m	15.3	20
Average specific power, W/g	17	29
Fast fluence, n/cm^2	[A]1.75×10^{21}	4.2×10^{21}
Average burnup, a/o	1	2.4
Percent fission gas retention	[A]100	100

[A] Estimated from burnup and PWR data

FPIN2-CALCULATED FUEL AND CLADDING TEMPERATURES AT THE TIME OF PIN FAILURE

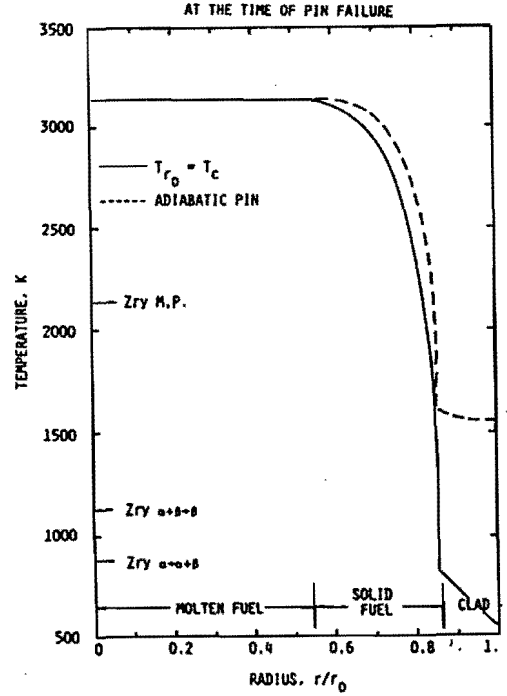

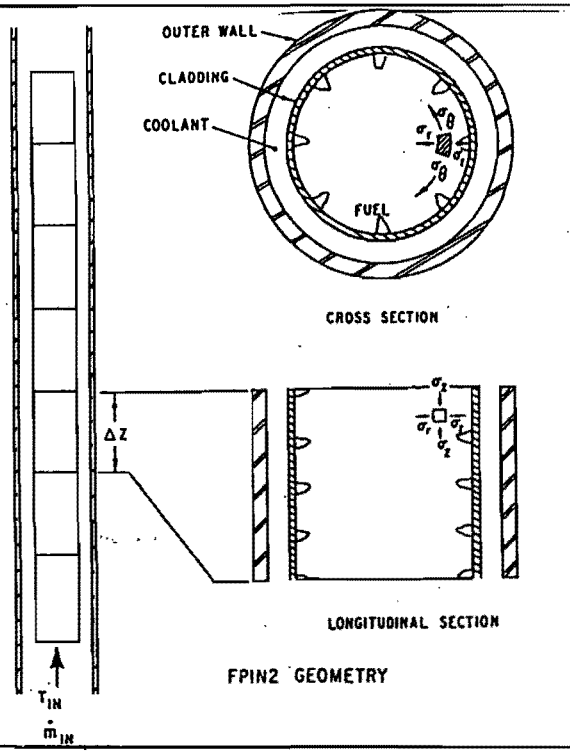

FPIN2 GEOMETRY

FPIN Cases Studied

- Cladding failure at about 50% areal melt fraction
- Case 1
  - Maximum heat transfer to coolant
  - Cladding outer surface remains at saturation temperature (573K)
- Case 2
  - Zero heat transfer to coolant
  - Cladding provides substantial heat sink (consistent with TREAT reactor F-series tests on fuel segments
  - Cladding reaches phase transformation (where there is a large reduction in strength) prior to fuel melting

FPIN2 - Calculated Thermal Events in Fuel Elements

Event	Case 1 Maximum Heat Transfer Energy, J/g (cal/g)	Case 2 Minimum Heat Transfer Energy, J/g (cal/g)
Start of transient from 7% full power	67 (16)	67 (16)
Cladding phase transition	A	201 48
First fuel melting	1198 (286)	1147 (274)
50% areal melt fraction (approximate cladding failure point)	1320[B] (315)	1181[B] (282)
Cladding melting	A	1981 (473)
100% fuel liquid fraction	3390 (810)	2538 (606)

A) Cladding remains at 573K

B) Internal pin pressure at this point is between 40-80 MPa (400-800 atm)

Cladding Failure under Transient Overpower Conditions

- Fuel melting leads to internal pin pressurization
  - 10% fuel expansion on melting
  - Fission gas bubble coalescence
- Expansion initially accommodated by available void space
  - Local fabricated porosity
  - Local crack volume
- Cavity pressure increases rapidly when void space becomes exhausted, usually at about 50% peak areal melt fraction
- Cavity pressure then dictated by yield strength of the weakest cladding segment along the cavity length
- Deformation becomes unstable and localized in the form of a bulge
- Initial cladding failure quickly follows at the bulge site

Fuel Behavior upon Cladding Failure under Transient Overpower Conditions

- Chernobyl-4 fuel had high burnup at low power operation
  - Burnup of 12-15 GWD/T in 75% of channels at time of accident (original core load)
  - Average linear power ~ 15 KW/M
- Internal pin pressurization of 400-800 atm ejects molten fuel into coolant channels
- Due to microcracking of "gassy" fuel under rapid top conditions, expect "dust cloud" mode of breakup of unmelted fuel to grain size particles (~ 10 μ)
- Expect rapid enlargement of pin disruption zone due to:
  - Continued top heat generation
  - Fission gas bubble coasescence
  - Cladding ablation
  - Multiple failures prior to depressurization

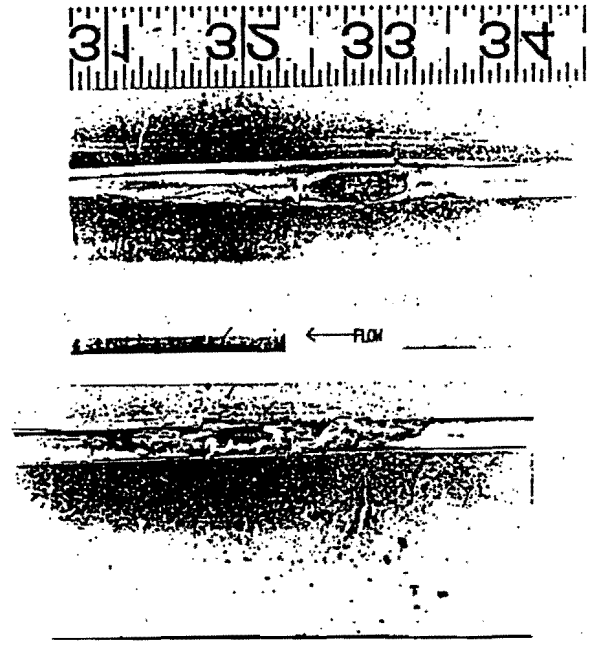

H6 CENTRAL PIN FAILURE REGION

Application of the EPIC Code to the Chernobyl Reactor Accident

- The EPIC computer code provides a framework for making parametric variations on fuel-to-coolant heat transfer efficiency, fuel failure location and extent, initial coolant channel void fraction, etc., in order to predict fuel and coolant motion and energy transfer after failure.
- The effects of fuel particle size and local coolant voiding can be taken into account in predicting fuel-to-coolant heat transfer.
- The time-dependent system pressurization is characterized based upon the fuel pin pressure and upon the coolant pressure resulting from energy transfer from the fuel.
- Reactivity feedbacks from fuel and coolant motion can also be calculated if worth data are available.

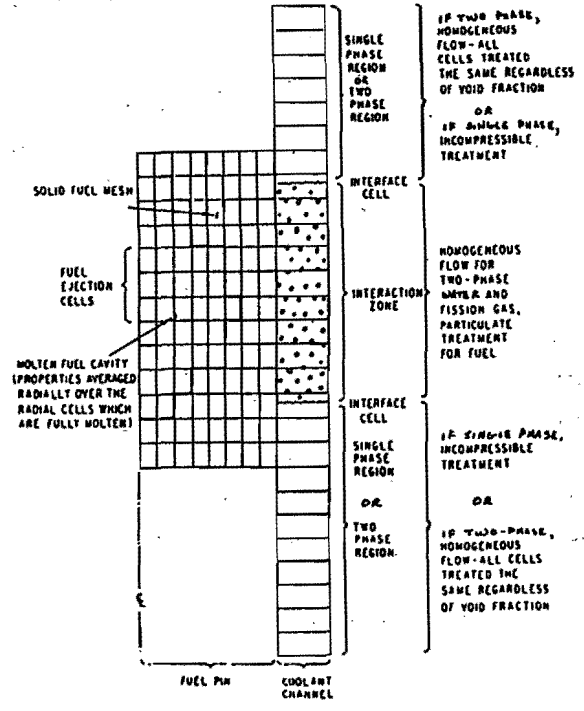

SCHEMATIC OF THE EPIC MODEL

EPIC-CALCULATED EJECTION OF MOLTEN FUEL INTO COOLANT CHANNEL

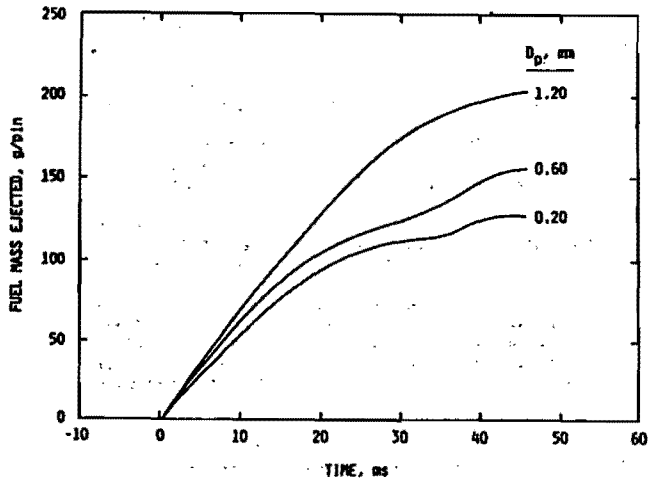

CONDITIONS FOR THE EPIC CALCULATIONS OF THE CHERNOBYL-4 ACCIDENT

• AXIAL POWER DISTRIBUTION	CHOPPED COSINE
• INITIAL PIN PRESSURE	400 ATM
• MAX FUEL MELT FRACTION	0.50 AREAL
• LENGTH OF MOLTEN FUEL CAVITY	2.7 M
• LOCATION OF CLADDING FAILURE IN CORE	3.5 M[1]
• INITIAL CLADDING RIP LENGTH	8, 70 CM
• LOCAL VOID FRACTION	0
• FUEL PARTICLE SIZE	0.2, 0.6, 1.2 MM

[1]BOTTOM OF TOP FUEL ASSEMBLY

EPIC-CALCULATED CHANNEL PRESSURE FROM FUEL-COOLANT THERMAL INTERACTION

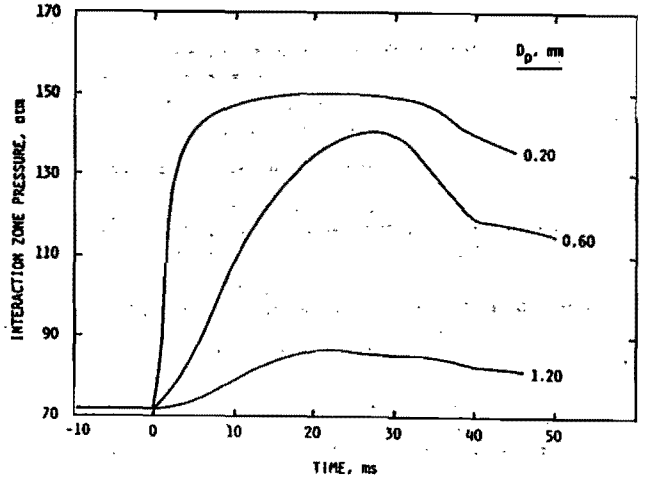

EPIC-CALCULATED UPHARD EXPANSION OF FCI INTERACTION ZONE

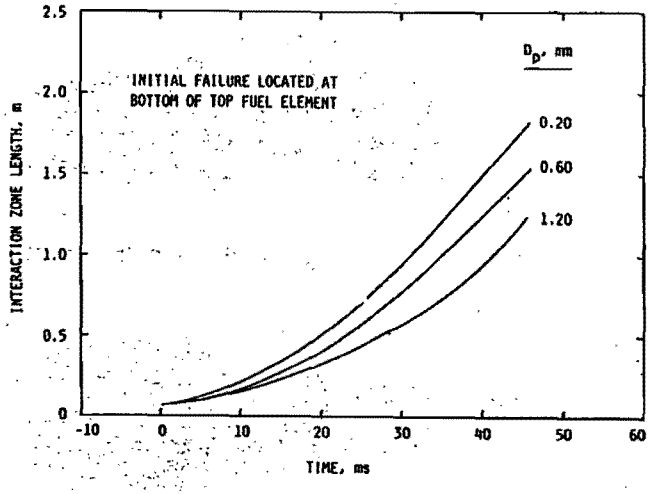

Results of ALICE Code Calculations

Case No.	FCI Pressure (ATM)	Max. Pressure at Impact (10^2 MPa)	Max. Axial Stress, σ_z (10^2 MPa)	Ultimate Stress, σ_{ULT} (10^2 MPa)	σ_z/σ_{ULT}
1	70+300 = 370	4.68	24.5	4.5*	5.4
2	70+150 = 220	3.35	16.8	4.5*	3.8
3	70+75 = 145	2.33	11.6	4.5*	2.6

*Steel

Consequence Of Channel Pressurization Events*

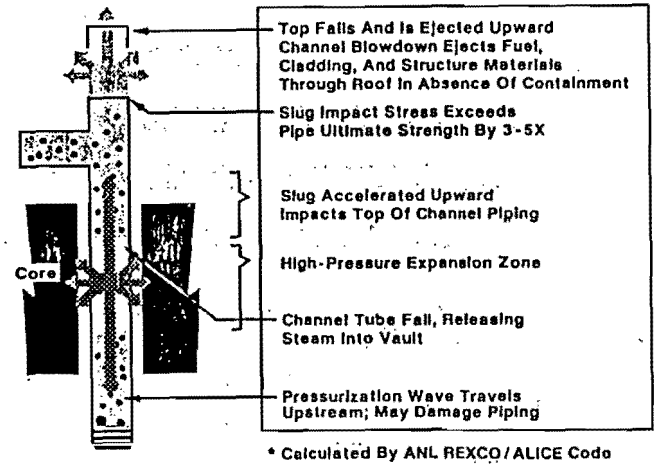

* Calculated By ANL REXCO/ALICE Code

Transient Overpower Tests in TREAT and CDC with LWR Fuel in Water

- Natural power bursts in TREAT and in SPERT IV (CDC Facility) were used for fuel failure/metal-water reaction tests in the 1960's
  - TREAT period (min) 40 ms
  - CDC period (min) 3 ms
- Zircaloy-2 clad uranium dioxide fuel pins
  - Fuel temperature threshold for Zr-water reaction
    - 2800C in TREAT
    - 2500C in CDC
  - Energy threshold for fuel failure and fragmentation
    - 280 cal/g in TREAT
    - 260 cal/g in CDC
  - Fragmentation to Sauter mean diameters from 0.1 to 1.0 mm

Transient Overpower Tests in TREAT with Zircaloy-2 Clad Uranium Dioxide Fuel Pins (Pins Submerged in Water in Sealed Capsules)

Fission Energy Input cal/g	No. Fuel Pins	Fuel Pin Length cm	CEN Run No.	Reactor Period ms	Mean Particle Diameter mm	Percent Metal-Water Reaction
250	9	14.3	2028	117	(DAMAGED)	4
287	1	1.3	181	72	1.4 (1.8)	24
290	1	14.3	230T	108	(PIECES)	11
330	1	14.3	225T	107	(PIECES)	21
368	1	14.3	231T	104	(PIECES)	18
375	1	1.3	214	73	0.6	13
450	1	14.3	224T	80	(FINES)	37
450	1	1.3	173	52	0.7 (0.9)	63
485	9	14.3	209S	87	-	24
595	1	1.3	215	49	0.5	21
675	1	1.3	216	42	0.3	68
771	1	1.3	173	39	0.6 (1.2)	80

IN-PILE (TREAT) MELTDOWN EXPERIMENT
CEN-231T; 360 cal/g

Rod-Axe

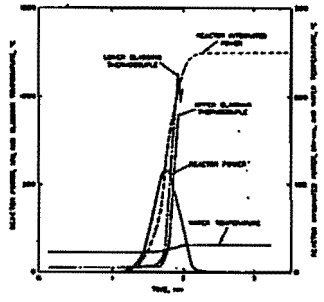

Oscillograph Record

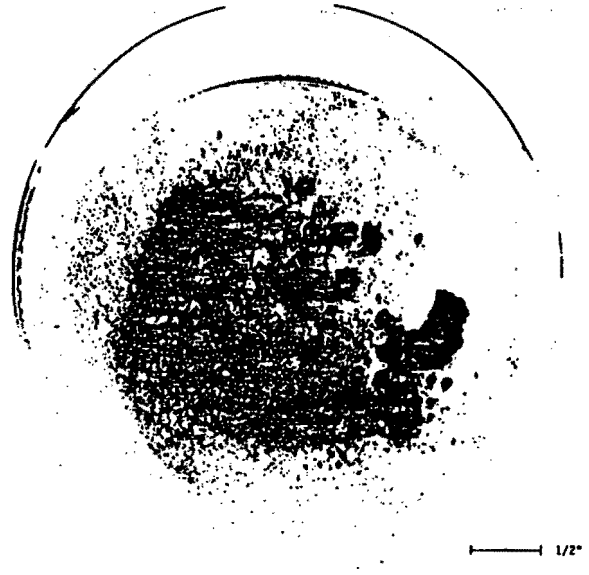

IN-PILE (TREAT) MELTDOWN EXPERIMENT CEN-178; 360 cal/g

TREAT TRANSIENT CEN-209S: UO_2-CORE, Zr-2 CLAD FUEL PINS
485 cal/g

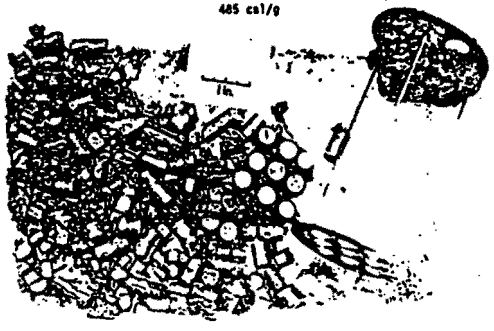

Cheese after Transient

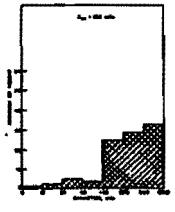

Particle Size Distribution

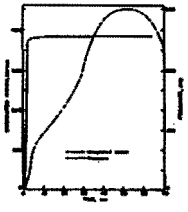

Oscillograph Record

Transient Overpower Fuel Testing at TREAT

- In-Pile simulations of fuel performance under severe accident conditions - test to melting, disruption and resulting fuel and coolant motions.
- Support development and validation of severe accident fuel performance codes such as FPIN and EPIC.
- Features:

  Test Fuels: Multi-pin bundles, including irradiated UO_2 fuel exceeding Chernobyl burnups.

  Channel Conditions: Fuel failures span the range from full coolant flow to fully voided channels.

  Power Bursts: Controlled bursts rise on exponential periods ranging from 15s to 0.1s.

  Melt Fractions: Cladding failures have been achieved with fuel melt fractions ranging up to 80%.

Recent TREAT Tests Bearing Relevance to Chernobyl Transient Overpower Event

Tests L04, L05, L06, L07

Tested low-power irradiated oxide fuel under varying degrees of transient undercooling, followed by an overpower burst.

Measurements included fuel failure threshold, fuel motion, coolant motion, and channel pressurization.

Tests L01, L02, E7, E8, AX1

Tested irradiated fuel under transient overpower conditions at full flow.

Measurements included fuel failure thresholds, fuel motion, coolant motion and channel pressurization. As above. Measured energetics of molten-fuel coolant interaction.

PBF Reactivity-Initiated Accident Test Series

Test	Fuel Rod Type	Fuel Enrichment (% U-235)	Burnup (MWd/kU)	Power Peaking Factor	Radial Average Total Energy Deposition (cal/g UO_2)	Radial Average Peak Fuel Enthalpy (cal/g UO_2)	Maximum Local[a] Fuel Enthalpy (cal/g UO_2)	Comments
RIA-ST-1 Series 1	17 x 17 PWR	3.3	0	1.076	330	183	301	Did not fail; first test on RIA-ST-1 rod
RIA-ST-1 Series 2	17 x 17 PWR	3.3	0	1.076	330	230	275	10% of fuel washed out; second test on RIA-ST-1 rod
RIA-ST-2	17 x 17 PWR	3.3	0	1.076	345	268	290	15% of fuel washed out
RIA-ST-3	17 x 17 PWR	3.3	0	1.076	300	175	230	Did not fail
RIA-ST-4	15 x 15 PWR	30	0	1.400	693	190[b]	530	Completely destroyed; pressure pulse of 35 MPa measured
RIA 1-1	Two Samples Two Sections	3.7 3.6	4600 0	1.130 1.079	365 365	315 293	130 315	Complete flow blockage Series failure; partial flow blockage
RIA 1-2	Four Samples	3.7	3000	1.130	340	183	315	One rod failed; three rods did not fail
RIA 1-4	Nine Samples	3.7	1300	1.130	293,270,345[c]	237,251,214[c]	340,300,345[c]	3 x 3 bundle all failed

a. The maximum fuel enthalpy at the axial and radial peak locations.

b. The fuel enthalpy at the time of failure (~1 ms after the time of peak power).

c. Values for corner, side, and center fuel rods in bundle, respectively.

RIA-ST-4 Summary*

(Reactivity Insertion Accident)

- Initial Condition
  - Similar to BWR Hot Startup
  - Coolant Pressure = 6.45 MPa
  - Coolant Temperature = 538 K
  - Coolant Flow Rate = 0.085 L/S
- Test Condition
  - 20% Enriched, Unirradiated, Single-Pin UO_2 Clad with Zircaloy-4 (Pin O.D. = 10.73 mm, Pin Length = 0.914m)
  - Single 75-ms Power Burst
  - Energy Deposition at Failure = 1550 J/g UO_2 (510 cal/g)
    (Radial Average at Axial Peak)
- Test Results
  - Extensive Melting and Fragmentation
  - Peak Pressure = 35 MPa
  - Coolant Temperature = In Excess of 940 K
  - The Results are Attributed to a Vapor-Explosion Type of Molten Fuel-Coolant Interaction
  - Estimated Thermal-to-Mechanical Conversion = 0.3% (Based on the Total Thermal Energy of the Fuel Pin)

*From NUREG/CR-1900, EGG-2080, March 1981.

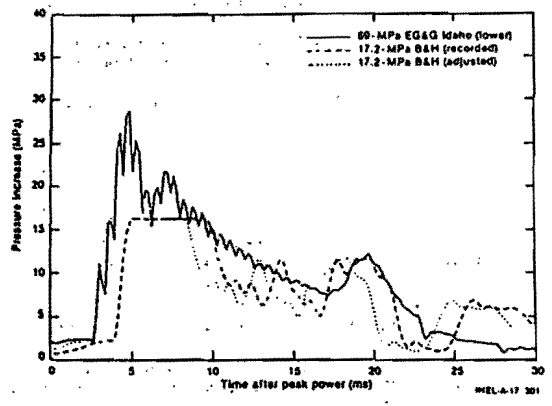

Figure 5. Recording of coolant pressure in the flow shroud.

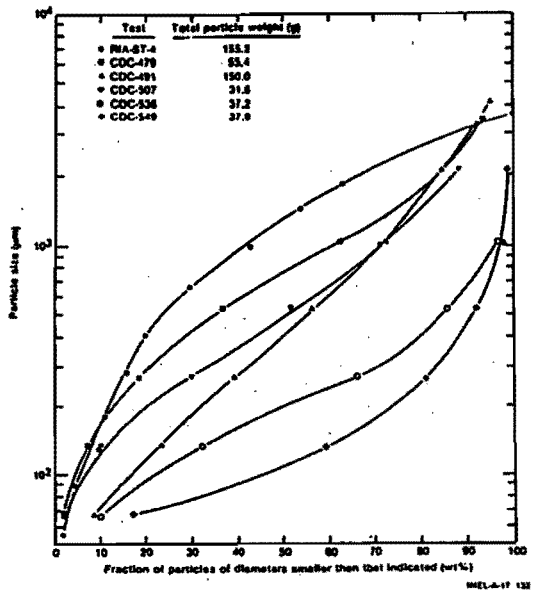

Figure 12. Comparison of particle distribution in RIA-ST-4 experiment with that during CDC power excursion tests.

Best Estimate of Actual Events

1. Channel-to-channel noncoherence of fuel failures
   - Failures occur according to relative power-to-flow ratios in the various channels
   - Peak-to-avg channel power at Chernobyl may be as high as 1.7
   - Russian analysis was based on average fuel behavior (i.e., complete coherence)
   - Changes void reactivity and power behavior from that depicted in Russian analysis
   - "300 cal/g" may have been far surpassed in some channels
2. Effect of axial power distribution
   - RBMK has separate 3.5-m long upper and lower fuel assemblies
   - Separate fuel failures for upper and lower elements
   - Initial, double-humped axial distribution peaked at upper region; initial failures predicted to be in upper region
   - Subsequent failure of lower elements probably caused greater energy release than failures of upper elements

Best Estimate of Actual Events (cont.)

3. Various modes of piping failure
   - Slug ejection and impact on top cap of pressure tube; calculated to be plausible failure mechanism. Causes upward blowdown into refueling building.
   - Failures of transition welds. Causes blowdown into reactor vault.
   - Local failures at FCI zone. Causes blowdown into reactor vault.
   - Pressure wave propagation upstream; hammer-type overpressures.
     Possible failures into lower piping areas.
4. The actual events probably involved all of the first three modes of piping failures listed above, and perhaps others. The vault rapidly overpressurized due to the pressure tube failures, and the upper shield was displaced upward causing massive destruction of the upper piping and opening the graphite-filled area to the atmosphere.

Best Estimate of Actual Events (cont.)

5. What were the observed "fireworks" above the reactor?
   - Experiments in our laboratory show that a block of reactor-grade graphite is only slightly luminescent at 700C and is "extinguished" by a blast of air. The same is true of fragments of ~ 1 cm characteristic size.
   - Fuel and cladding at their high temperatures would oxidize upon being ejected into air and would be highly luminescent.
   - Graphite blocks were found dispersed around the reactor site.
   - Fuel is also reported to have been dispersed around the reactor site.

APPENDIX C

SUMMARY PAPER ON THE POSSIBILITY OF CHERNOBYL-4 TYPE TRANSIENT OVERPOWER ACCIDENTS IN U.S. REACTORS

Summary Paper on the Possibility of Chernobyl-4 Type Transient Overpower Accidents in U.S. Reactors

August 25, 1986
Revised October 15, 1986

Argonne National Laboratory
Reactor Analysis and Safety Division
Applied Physics Division
9700 South Cass Avenue
Argonne, IL 60439

SUMMARY

This report addresses whether an accident of the Chernobyl type could occur in a nuclear power reactor in the United States. The best estimate of the sequence of events at Chernobyl-4, after studying the report released by the U.S.S.R., is that while testing the performance of new electrical equipment under turbogenerator rundown conditions, during which most of the safety systems had been rendered inoperable, the reactor coolant flow reduction caused coolant heatup and increasing steam bubble formation in the core. The Chernobyl-4 reactor design has a positive void coefficient of reactivity which under normal circumstances is automatically compensated by control rod motion. Under the conditions of this test, the compensation was inadequate and the increasing steam formation led to a worsening reactivity insertion which resulted in a severe power excursion which destroyed the reactor.

Specifically, the question which this report addresses is whether a reactor in the U.S., subjected to a loss of flow or loss of coolant accident (with the equivalent safety systems disabled, however improbable that might be) would experience a power excursion of the type that happened at Chernobyl-4. The results of our investigation indicate that while reactors in the U.S. may be damaged they would not experience a severe power excursion as happened at Chernobyl-4. The basic reason is that all U.S. reactors are designed to be "undermoderated," and as a result a decrease in coolant density (as caused by temperature rise or steam formation) produces the equivalent of a poisoning effect (negative reactivity) which causes the reactor power to decrease. The reactor inherently shuts itself down under these conditions.

Severe accidents to U.S. reactors have been postulated as part of extensive studies of reactor risk, beginning with the Reactor Safety Study (WASH 1400), and these studies of reactor risk are constantly being updated as new information becomes available. As part of these risk studies, accident sequences which postulate power excursions have been studied. Because of the characteristics of U.S. reactors, these accidents cannot follow the type of accident sequence which occurred at Chernobyl-4.

1. Introduction

The purpose of this report is to address the power behavior of a U.S. reactor when subjected to increased coolant void fraction in the core, whether by coolant flow reduction or by loss of coolant inventory (LOCA), with the reactor emergency protection (scram) systems disabled, as improbable as that may be.

Chapter 2 contains a summary description of the accident at Chernobyl-4 including a description of RBMK design features which contributed to the severity of the consequences of the accident. Chapter 3 contains a description of the significance of the various reactivity coefficients and their meaning in determining transient reactor power behavior. Chapter 4 provides applications to U.S. commercial light water reactor (LWR) designs. Chapter 5 provides applications to U.S. liquid metal reactor (LMR) designs. Chapter 6 covers the U.S. military production reactors. Chapter 7 covers the High Temperature Gas-Cooled Reactor (HTGR).

2. Description of Chernobyl-4 Accident

A. Turbine-Generator Test

The accident at Chernobyl-4 occurred during a planned test which was being conducted at low power as Unit #4 was being taken out of service for maintenance. In the test, it was desired to verify the ability of a turbogenerator (TG) to continue to provide electric power for internal operation of ECCS equipment, such as feedwater pumps, during a turbine rundown. This is interpreted to mean during loss of offsite power, where continuous power to vital safety equipment is needed until the emergency diesel generators become operational. This test repeated a similar previous test at Chernobyl-4 in which the busbar voltage dropped much faster than the turbine rundown. In the present test, an electrical engineer was directing testing of a special generator field regulator designed to maintain higher busbar voltage for a prolonged time. The reactor power operation was needed only to provide steam for initial turbine operation. The TG was being loaded primarily by four primary coolant pumps of the reactor; four additional pumps were being powered from outside sources so that even upon complete turbine rundown there would still be substantial coolant flow through the reactor for heat removal.

The test procedure prescribed that ECCS be disengaged for the duration of the test. The procedure also prescribed that one of the two TGs powered by Unit #4 be taken out of service as an initial condition. After a delay of about 9 hours, the test was initiated by shutting down steam flow to the remaining TG, initiating the rundown. According to the Soviet report, shutdown

of the second TG should have automatically scrammed the reactor which would have been appropriate since neither the reactor power norcontinued steam generation should have played any further role in this test. However, this particular reactor scram signal actuated by shutoff of steam flow to both TGs had been blocked during the previous day "to have the possibility of repeating the test, if the first attempt proved unsuccessful." (They were concerned about Xe buildup.)

> **Hence the test was entered into with the reactor continuing to generate power rather than automatically scrammed as planned.**

The reactor was manually scrammed 36 seconds (1:23:40) later when the operators observed the increasing power. By that time scram was too late in the RBMK, the damaging power excursion was under way, fed by the positive reactivity insertion due to the increasing coolant boiling with the reactor producing power and the coolant flowrate coasting down.

B. Conditions Contributing to the Accident

The accident might still have been avoided, or considerably less severe, except for other circumstances. The local automatic power regulating rods (LAR) had been disengaged per standard operating procedure for low power operation, and hence were not available to counteract the voiding reactivity insertion. The global automatic power regulating rods (AR) were operational and were automatically inserted by the plant diagnostics and computer control system, partially compensating for the power rise but apparently without sufficient worth. Other absorber rods had been completely withdrawn previously to counteract Xe buildup and overcooling effects. When finally scrammed, these rods were too far out of the core to be of immediate worth and moved at too slow insertion speed (0.4 meters per second; about 20 seconds full insertion time) to terminate the overpower excursion.

> **The Soviets use the phrase "operating reactivity margin" expressed as a number of effective control rods capable of protecting against plant transients. The number available at the time of the test (6-8) was far below the normal required number (30), requiring shutdown of the reactor. "Nevertheless, this did not stop personnel, and the test began."**

Due to the particular design of the Chernobyl-4 control rod assemblies, when the absorbers were fully withdrawn the control assembly duct contained 5 meters of graphite displacer centrally located in the 7 meters core with 1 meter of water above and below the graphite at the axial extremes of the core. In this configuration, it is calculated that the initial scram effect was

not negative but positive reactivity insertion due to displacement of water, particularly at the bottom of the core. This circumstance probably caused a significant power shift to the bottom of the reactor.

Additionally, the reactor was at very low power (7 percent) and very high coolant flow (> 100 percent). Hence, the initial steam void in the core was exceedingly small, about 2 percent average. The Soviet report emphasizes that in this condition a small change in power causes the volumetric steam content to increase "many times more sharply than at nominal power". It is also believed that the void coefficient of reactivity is itself a function of void fraction, being larger for smaller void condition. These two factors would combine to cause the void reactivity insertion to be particularly severe under the conditions during which the test was run.

Immediately prior to the test, the operator "sharply reduced the feedwater flowrate." Hence, the temperature of water to the main coolant pumps and to the core inlet was increasing since suction was now primarily from the steam separator drum. Increasing water temperature at the core inlet may have exacerbated the steam generation in the core.

In summary, the circumstances leading to the accident were as follows: (1) the reactor was operating (though it should have been scrammed from the onset), (2) the coolant flow rate was decreasing leading to additional steam generation in the core, (3) coolant inlet temperature was increasing, leading to more rapid steam generation in the core, (4) the initially overcooled core with close to zero steam content was in a particularly severe state with regard to void related reactivity insertion, (5) the automatic power regulating system was incapable of counteracting the void reactivity insertion, (6) the rods available for scram were located fully out of the reactor core in a region of low initial worth, and (7) the scram itself is calculated to have caused a sizeable reactivity insertion initially.

C. Transient Overpower Excursion

Under the conditions described, a net positive reactivity due to increasing coolant boiling in the core, resulted in a power rise. At first the rate of power rise was slow. At 1:23:40 the reactor was manually scrammed, but without the desired shutdown effect. At 1:23:43 the power was reported to have exceeded 530 MW (up from 200 MW at beginning of test), and the "runaway period came to be much less than 20 seconds." Actually the reactor was already experiencing a prompt critical power excursion at that time. It is stated that "only the (fuel) Doppler effect partially compensated for the reactance introduced at this time."

The power transient calculated by the Soviets had a peak power of 350,000 MW (110 x full power) and a full width at half maximum (FWHM) of 0.8 seconds. The Soviets indicate that the energy release in the fuel "exceeded 300 cal/g."

The effect of the power burst is described in the Soviet report as follows:

> "[The power rise] led to an intensive steam formation and then to nucleate boiling, overheating of the fuel, melting of the fuel, a rapid surge of coolant boiling with particles of destroyed fuel entering the coolant, a rapid and abrupt increase of pressure in the fuel channels, destruction of the fuel channels, and finally an explosion which destroyed the reactor and part of the building and released radioactive fission products to the environment."

D. Consequences of the Overpower Transient

The above description suggests that fuel-coolant thermal interactions (FCIs) occurred from the sudden mixing of hot UO_2 fuel and coolant in the channels, and that the subsequent pressurizations caused channels to rupture. (The plausibility of this was subsequently confirmed through application of ANL accident analysis codes.) Rupturing the channels would initiate blowdown of steam and flashing water from about 6.5 MPa pressure to the surrounding volume(s). The Soviet's report is silent on the suspected locations of ruptures. There are thought to be four principal locations. Upward slug expulsion from the pressurization zone has been shown to be capable of breaching the top end cap of the operating channel at the refueling machine attachment, initiating upward blowdown and fuel dispersal into the uncontained region immediately below the removable refueling floor slabs. The zirconium-to-steel weld joints immediately above and below the active fuel zone of the core are thought to be weak points; failures of the piping at either or both of these locations would cause steam blowdown into the region of graphite blocks in the sealed reactor space. The zirconium-alloy pressure tube is likely to fail locally at the region of the pressurization event due both to the overpressure itself and to thermal effects of fuel impingement on the pressure tube-wall. This failure location would cause steam blowdown into the central zone of graphite blocks in the sealed reactor space. It is also possible that shockpressures and hammer pressures propagated upstream as a result of the pressurization events in the operating channels and damaged piping at the inlet side of the reactor; blowdown of steam and flashing water would enter the containment cell (65 psig) designed to vent to the pressure suppression pool. Any or all of these types of ruptures could have occurred from the initial fuel failure events. The ruptures

of the top end caps would have caused the immediate blowdown and discharge of fuel debris upward into the refueling building and possibly directly into the atmosphere. Multiple tube ruptures into the reactor space would quickly overpressurize this region since its overpressure relief protection is sized for failure of only one channel. Upon overpressurization this region would fail structurally, as is known to have occurred. Some of the graphite blocks were ejected, and air subsequently entered this region.

It is reported that two explosions were heard, "one after another," and that "hot fragments and sparks" flew up above the plant, described elsewhere in the report as "fireworks of flying hot and glowing fragments." The mechanism for this dispersal may have involved the upward-directed channel ruptures at their tops, the overpressurization failure of the reactor vault and subsequent blowdown of that region, or a subsequent explosion of some other origin. There are statements in various parts of the report attesting that fuel debris was ejected into the atmosphere; e.g., "As a result of explosions in the reactor an ejection of core fragments heated to a high temperature... (occurred)." The report also speculates that a chemical explosion could have occurred "after unsealing of the reactor space." These statements are not necessarily contradictory; they indicate uncertainties in the actual sequence and consequences of multiple events.

E. <u>Chernobyl Plant Features that Exacerbated Accident Consequences</u>

Although the Soviets place heavy blame for the accident on the individuals who planned and carried out the turbine-generator rundown test and on the reactor operators rather than on equipment failures or design shortcomings, it is clear that features of the RBMK reactor design contributed to the severity of the accident.

1. The speed of insertion of the scram rods (AZ) appears too slow to provide adequate protection against emergency situations such as arose during the accident. The Soviet approach is that large numbers of rods compensated for their slow rate of insertion. The insertion rate is stated to be 0.4 meters per second, and since the the total core height is 7 meters, it takess about 18 seconds for complete scram rod insertion.

   The comparable scram time for U.S. PWR and BWRs range from 3 to 5 seconds.

2. There was no positive stop on the absorber rods to limit their withdrawal. The rods were so far out of the core that they did not immediately insert negative reactivity as

depended upon when the reactor was scrammed. To the contrary, the rod design and initial position caused a "positive scram;" i.e., there was a major reactivity insertion upon scram, rather than shutdown.

The "positive scram" appears to be unique to the RBMK and to the particular state of the reactor; there is no positive scram in U.S. reactors.

3. Many parts of the reactor piping system pass through areas where there was no containment whatsoever. This includes the top sections of the operating channels, steamwater lines (PVK), steam line piping, and parts of the feedwater and returnline piping. It is indicated that fuel debris was released directly to the atmosphere at Chernobyl-4 as a result of pipe ruptures and blowdown into uncontained regions.

   U.S. PWRs and BWRs all have substantial containments as one of a series of barriers to prevent accidental release of radioactive materials into the atmosphere.

4. The pressure relief line from the sealed reactor space was sized to handle blowdown from only one channel rupture. Hence, multiple ruptures into this sealed space did not have adequate relief to prevent over pressurization. Furthermore, the free volume of the reactor space was very small so that with inadequate pressure relief the volume would rapidly overpressurize and the region would become "unsealed" by structural failure.

   U.S. containments are designed with combinations of features involving large volume, high containment strength, and large-capacity pressure suppression systems to maintain containment integrity for accident conditions.

5. The zirconium-to-steel transition welds are throught to be weak points in the RBMK piping system, although it is uncertain whether this played any role during the accident. The welds have a heatup rating limited to 15 degrees C/hour which may have been exceeded during the accident. Since rupture of the piping at the welds would cause blowdown into the sealed reactor space, they are a potential cause of failing the vault during the accident involving multiple ruptures.

   There are no comparable weld joints in U.S. BWRs or PWRs. Even if such joints existed, their failure would not pose a threat to vessel integrity

which is a unique characteristic of the pressure tube reactor design.

3. Reactivity Coefficients and Reactor Transient Behavior

A. Reactivity Effects of Power and Flow Conditions

It is often convenient to characterize the dynamics or safety properties of a nuclear reactor in terms of reactivity coefficients associated with the measurable (and controllable) reactor variables, power, coolant flow rate, and coolant inlet temperature and pressure. Thus, in terms of a power coefficient of reactivity, α_P, a power to flow coefficient, $\alpha_{P/F}$, an inlet temperature coefficient, α_{in}, and a primary system pressure coefficient, α_p, the incremental change in reactivity associated with a change from equilibrium of the process variables is given by a simple summation of the process variable incremental changes times their reactivity coefficients:

$$\delta\rho = \alpha_P \, \delta P + \alpha_{P/F} \, \delta P/F + \alpha_{in} \, \delta T_{in} + \alpha_p \, \delta p$$

This simple expression prescribes the reactivity change which results from the change in process variables.

That reactivity increment will lead to a subsequent change in reactor power level; a positive reactivity, $\delta\rho$, will cause the power to increase; a negative $\delta\rho$ will cause it to decrease. This inherent reactivity increment may be overcome by movement of control rods during normal operation of the reactor to follow load changes prescribed by the balance of plant. Alternately, in the event of severe accident sequences in which control devices are inoperative, the signs (positive or negative) and the relative magnitudes of the reactivity coefficients and the relative time delays between the incremental changes in the process variables determine the course of the reactor response in the accident.

The case at hand is a loss of coolant flow without control rod scram (LOF/WOS). In that case, the coolant inlet temperature and coolant pressure initially remain constant, and the reactivity expression simplifies to:

$$\delta\rho = \alpha_P \, \delta P + \alpha_{P/F} \, \delta P/F$$

Upon loss of flow (for example from loss of electric power to the pump drive motors) the coolant flow rate (F) begins to decrease so that $\delta P/F$ is positive. Thus for the LOF/WOS accident sequence, a negative power to flow coefficient of reactivity, $\alpha_{P/F}$, is sufficient to cause a negative reactivity which will

lead to a power decrease. (While the power to flow mismatch may cause the core components to overheat and experience severe damage, the reactivity is negative, nonetheless, and a power excursion is avoided.)

Even if the power/flow coefficient is zero or slightly positive, the reactor may still be controllable and safe if the power coefficient, α_p, is sufficiently negative and sufficiently prompt. As the power increases, the uranium and/or plutonium fuel itself rises in temperature faster than does the coolant because the heat is deposited directly in the fuel, whereas it must be conducted to the coolant from the fuel. The incremental temperature rise of the fuel relative to the temperature of the coolant introduces a reactivity component of α_p which is prompt and negative for every existing reactor type (the fuel Doppler coefficient).

Thus, even in a reactor for which the power/flow coefficient is zero or slightly positive, the power increase will always be ultimately limited by the heating of the fuel, and it only remains to determine the amount of energy deposited in the fuel to heat it enough to terminate the power rise. This depends on the engineering details which control the introduction of the positive and negative reactivity components such as the time delay of transferring heat from the fuel to the coolant and the speed with which the pumps coast down (i.e. decrease coolant flow rate).

To assess these details requires identification of the specific physical components of the power and power to flow reactivity coefficients--which is the subject of the subsequent section.

To summarize the simple results of this section:

a) If the reactor is designed with a negative power to flow coefficient of reactivity, it is evident by inspection that a loss of flow without scram will lead to a negative reactivity and will avoid a power excursion.

b) Alternately, if the power/flow coefficient of reactivity is positive, but the prompt component of the power coefficient is sufficiently negative, a severe power excursion can still be avoided.

An examination of the reactor types deployed in the U.S. shows that they all have a negative power/flow coefficient of reactivity (because they are designed to be undermoderated) and so, in conformance with item (a), they are immune to a power burst upon loss of flow without scram.

B. Physical Components of the Reactivity Coefficients

Reactor core designers have consciously selected core configurations which will lead to desirable reactivity coefficients, α_P, $\alpha_{P/F}$, α_{in}, and α_p. In order to understand the implications of these design choices it is useful to identify the physical components which make up the reactivity coefficients. These physical components derive from density and temperature changes of the three generic components of a reactor core--fuel, coolant, and moderator. Further, they are qualitatively categorized as prompt (associated with fuel temperature or coolant pressure), fast (associated with coolant temperature) and delayed (associated with moderator temperature).

B.1 Coolant Inlet Temperature Coefficient Components

The coolant inlet temperature coefficient is described first. At constant power, flow rate, and coolant pressure, an incremental change in coolant inlet temperature will lead to that same temperature increment in all core components. When the fuel temperature increases, the two principal reactivity effects derive from fuel axial expansion and Doppler broadening of the U238 capture resonances. Both effects are negative reactivities, and the Doppler effect is the more important in large commercial and military production reactors.

When the reactor-average coolant temperature increases, the coolant becomes less dense, its neutron slowing down properties are diminished, and its neutron transmitting properties are increased permitting neutrons to more easily move away from the fuel. The net effect on reactivity involves a balance of neutron leakage and neutron spectrum related effects, some of which are positive and some of which are negative and all of which depend not only on the lattice geometry and core size but also on the instantaneous values of fuel burnup, burnable and soluble poison concentration, xenon concentration, and control rod pattern. Several generalities can be stated, however. First, the neutron leakage effect is always negative--leading to loss of neutrons out of the core or into more absorptive parts of the lattices (such as parked control rods). Second, the soluble poison effect is always positive--less poison density, less neutron absorption. Third, if the lattice is designed to be undermoderated at all operating burnup and poison levels, then the spectral component will also be negative, as a reduction in coolant density will lead to still further undermoderation. Finally, in those reactor designs which have a moderator which is separate from the coolant, when the moderator temperature increases, again, like the coolant, both spectral and leakage effects come into play. And, again as in the case of the coolant, these effects can be designed to be negative if the lattice is undermoderated at all operating burnup and poison states.

In general, the penalty paid for undermoderation is higher enrichment, shorter refueling interval, or the need for a physically larger core with more fuel inventory. There may be a reactivity effect associated with thermal dilation of core support structures. This is generally small, but would be positive in undermoderated lattices.

The components of the coolant inlet temperature coefficient which derive from fuel and coolant are associated with a time constant comparable to the coolant residence time in the core. In cases with separate moderator regions, the components due to heating or cooling the moderator are delayed because of the bulk and low cooling surface to volume ratio of the moderator regions. The component associated with thermal expansion of core support structures is slow in that it requires heatup of massive structural members.

Table C-1 summarizes the several components comprising the coolant inlet temperature reactivity coefficient.

Table C-1

Summary of Reactivity Coefficient Components*

Reactivity Coefficient	Fuel Doppler	Fuel Axial Expansion	Coolant Density	Steam Fraction	Moderator Temperature	Structural Temperature
Coolant Inlet Temperature	F	F	F	F	D	D
Coolant Depressurization			P	P		
Power	P	P				
Power/Flow	F	F	F	F	D	D
Sign of Coeff. Component	always negative		can be made negative by undermodulation		may be positive, but very slow acting	

*P = prompt
F = fast
D = delayed

} qualititative time constants of reactiviy effects

B.2 Coolant Pressure Coefficient Components

At constant power, flow rate, and coolant inlet temperature, a decrease in coolant pressure will decrease the coolant density, and in the case of water cooled reactors will lead to increased steam fraction, which strongly decreases effective coolant density. The effects are as discussed above for coolant temperature. In general, design of an undermoderated lattice will lead to a negative reactivity upon pressure decrease.

This coefficient is fast in the sense that a pressure change is effective throughout the core on a time scale of the core height divided by the speed of sound in the coolant. Table 1 summarizes these effects.

B.3 Power Coefficient Components

At constant flow rate, coolant inlet temperature, and coolant pressure, an increase in power leads to an increased heat flux out of the fuel pins and an increased coolant temperature rise across the core. The second effect will be discussed in the following section with the power/flow coefficient; the increased heat flux from the fuel to coolant leads to an incremental increase in the fuel temperature relative to the coolant temperature. The higher fuel temperature leads to two negative reactivity components--fuel Doppler and fuel axial expansion. Both of these are prompt in that they respond with a time characteristic of the fuel pin thermal diffusivity.

B.4 Power/Flow Coefficient Components

At constant power, coolant inlet temperature, and coolant pressure, a decrease in coolant flow rate leads to an increased coolant temperature rise across the core, as is also the case for increased power at constant flow. It is convenient to combine both effects into a power/coefficient flow whose reactivity effect derives from an increased average core temperature and (as appropriate) an increased steam volume fraction. The reactivity components are identical to those discussed for the coolant inlet temperatures coefficient. The components associated with the coolant and fuel temperatures (and steam volume fraction) have a time constant characterized by the coolant residence time in the core; the component associated with separate moderator region heating is delayed.

B.5 Summary of Reactivity Coefficient Components

Table 1 summarizes the components and their characteristic time constants of each of the reactivity coefficients described above. As seen, the power to flow and coolant depressurization (void) coefficients are made negative by design of an undermoderated lattice. As discussed below, this is the case for all U.S. reactors.

C. Validation of Predictions of Reactivity Coefficients

While the predictions of reactivity coefficients and of the time evolution of accident scenarios are based on calculational models, the veracity of the physical effects rests on a vast history of experimental tests. The calculational models must be shown to the satisfaction of the NRC to correctly reproduce the

values and trends seen in the experiments in order to be accepted as a basis for licensing. The measured results include not only critical experiments and specifically designed thermal hydraulics and system tests (such as LOFT) but also actual reactor operating data.

In the areas of validation of lattice physics code predictions of the reactivity effects of coolant density, metal to water ratios, etc., each individual reactor vendor has provided the utilities and the NRC with evidence of the validation of his in-house (proprietary) codes based on comparison with the lattice critical experiments and operating reactor plant data.

Utilities often undertake to specify reload cores, often using a different set of computer codes than was used by the original vendor. Again, the utilities must provide evidence to the NRC of the ability of their analysis procedures to correctly predict reactivity effects. Examples of utility validation of physics analysis methods can be found in references 6 through 13.

4. U.S. Commercial LWRs

United States commercial light water reactor plants are (with the exception of a few very early plants) in the 500 to 1300 MWe range and are of two reactor types; pressurized water reactors (PWRs) manufactured by Westinghouse, Combustion Engineering, and Babcox and Wilcox, and boiling water reactors (BWRs) manufactured by General Electric Company. In both types the coolant is the moderator and no separate moderation region exists.

A. PWR Reactivity Coefficients

All PWR vendors design their lattices to be undermoderated so as to yield negative power/flow and depressurization coefficients. Enrichments of 3 to 4.5 percent are required depending on refueling interval. Soluble poison is used in the moderator to reduce control rod requirements; this positive component reduces the magnitude of the negative power/flow and depressurization coefficients. In older designs this formerly led to a small positive coefficient early in core life. Modern designs make use of fixed burnable poison in rods to lessen the soluble poison requirement and thereby to assure negative power/flow and depressurization coefficients throughout life. The prompt power coefficient is always negative. A negative power coefficient is now an NRC requirement.

For modern PWRs, the sufficient condition for avoiding a power burst in a LOF/WOS accident (i.e. negative power/flow coefficient) is met by the undermoderated lattice design and the use of fixed burnable poison. A loss of flow would introduce a negative reactivity, and the power would decrease.

B. BWR Reactivity Coefficients

The BWR lattices are undermoderated so as to yield negative power/flow and depressurization coefficients. The lattice employs enrichment grading with enrichments ranging from natural to 4.2 percent. Core-average enrichments are in the range 2.0 to 3.4 percent. The void (steam volume fraction) reactivity coefficient is strongly negative leading to favorable features such as spatial xenon stability, use of coolant flow to load follow, and flattening of the radial power distribution through local void poisoning.

The negative void coefficient dominates a small positive subcooled coolant temperature coefficient which develops late in core life as the withdrawal of control rods increases the coolant volume fraction in the nonboiling length of the channel to a slightly overmoderated level. The prompt component of the power coefficient (fuel Doppler) is always negative.

The sufficient condition for avoiding a power burst in a LOF/WOS accident (i.e., negative power/flow coefficient) is met by the undermoderated lattice design of BWRs in the U.S. A loss of flow would introduce a negative reactivity, and the power would decrease.

C. Analysis of Chernobyl Scenario for U.S. LWRs

C.1 PWR

All PWRs in the U.S. are required by NRC technical specifications to have a negative moderator coefficient. With the power coefficient established as being negative, it would require the insertion of rods rather than the withdrawal of rods to establish the steady state of 7 percent power with the fixed speed reactor coolant pumps running at the 100 percent conditions and in the absence of a buildup of xenon resulting from a delay in conducting the test. If the same sequence had been applied to a PWR in the U.S. and the turbine trip test had been initiated with the scram system bypassed, then the following scenario would have occurred. Upon turbine trip the turbine stop valves would close momentarily reducing the steam flow out of the steam generator. This reduction in steam flow would lead to a heating up of the primary side which would be alleviated by the opening of the turbine bypass valves to the condenser. At the low power there would be ample bypass capacity. In this sample scenario, the trip of the reactor coolant pumps as the test proceeded and the resulting loss of flow in the core would add to the heatup of the primary side. The moderator coefficients, primary coolant heatup, and any voiding would all act together to decrease the rate of power production. The power would stabilize, without going through a Chernobyl-type burst, at a level given by the

balancing of the moderator and Doppler reactivities and the equilibration to natural convection conditions. Heat would be rejected directly to the condenser with the feedwater being operated manually as in Chernobyl-4. Eventually, even with the scram system bypassed, the reactor could be brought to a hot shutdown condition by adding boron to the core via the chemical volume control system charging pump flow.

C.2 BWR

A U.S. BWR performing a turbine trip test at low power would not be operated in the same manner as was the Soviet plant. Because of its negative moderator coefficient, a U.S. BWR would have control rods inserted rather than withdrawn to achieve a 7 percent power steady state (with recirculation flow of greater than 100 percent in the absence of xenon buildup.) If the Chernobyl-4 sequence of safety system bypass actions had been applied to a U.S. BWR, the same low power state had been obtained, and the test had been initiated with the scram system bypassed then the following scenario would have occurred. On turbine trip, the turbine stop valves would have shut, generating a pressure wave that would be transmitted down the steam line and attenuated by the steam dryer and separator in the dome region before entering the core. Simultaneously, the signal would be sent to open the turbine bypass valves to the condenser which would further dampen the pressurization. Ample bypass capacity is available at the low reactor power. No scram signal would be required nor sent as the transient pressurization at the low power condition would be insufficient to trigger either the high flux or the high pressure trip. A power burst would not occur. The simultaneous coastdown of the recirculation pumps would cause additional steam generation (voiding) in the core, and this would reduce the power further and effectively render the transient benign. Even without a scram, the negative moderator coefficient of the U.S. BWR would rule out the power burst which led to much of the disruption in the Chernobyl-4 accident.

Stability margins of the plant would also be enchanced at the high recirculation flow rate. Since reactor core stability applies for a wide range of power conditions on the natural circulation line, coastdown of the core flow at 7 percent power form the steady state condition should be within the stability range. This should also hold for the channel hydrodynamic performance with the feedwater being operated manually as in Chernobyl-4.

The power would stabilize, without going through a burst, at a level given by the balancing of the moderator and Doppler reactivities and the equilization of natural convection conditions; the steam production would be rejected directly to the condenser. Eventually utilization of the standby liquid

control system to inject boron into the primary system would be used to initiate a controlled cooldown to hot standby conditions.

5. U.S. Liquid Metal Reactors (LMRs)

A. EBR-II

The Experimental Breeder Reactor-II (EBR-II) is a liquid-metal-cooled reactor (LMR) power plant. It has a peak thermal power of 62.5 MWt and a corresponding electrical output of 20 MWe. It has been operated for 22 years. EBR-II is cooled with liquid sodium. The temperature of the sodium coolant leaving the reactor is 880 degrees F. The temperature at which sodium boils is 1650 degrees F, thus there is a large margin to boiling in the reactor.

While a loss-of-coolant flow with failure to scram is extremely unlikely, the response of EBR-II to this event has been examined in detail. In contrast to Chernobyl, EBR-II has a strongly negative coolant temperature coefficient of about 0.2¢/degree F. Thus if EBR-II experiences a flow reduction without action of the control system, the reactor shuts itself down rather than experiencing a power burst of the type that apparently happened at Chernobyl-4. This behavior has been experimentally verified at EBR-II. On April 3, 1986 two tests to demonstrate this behavior were carried out at EBR-II. The two tests were a loss of flow without scram from 100 percent power followed by a loss of heat sink without scram from 100 percent power. The tests showed that inherent reactivity feedback due to thermal expansion of reactor material shuts the reactor down, and thermal convention of the primary sodium coolant maintains cooling. No damage to the reactor occurred and the reactor was available immediately to be returned to service.

No boiling occurred in these tests but even if core voiding were somehow to occur, the negative coolant void coefficient would shut the reactor down.

B. Fast Flux Test Facility (FFTF)

The Fast Flux Test Facility (FFTF) is a 400 MWt sodium cooled fast reactor. It uses a uranium-plutonium oxide fuel. The temperature of the sodium leaving the reactor core is 900 degrees F. The temperature at which sodium boils is 1650 degrees F, thus there is a large margin to boiling in the reactor. While a loss-of-coolant flow with failure to scram is extremely unlikely, the response of FFTF to this event has been examined in detail. In contrast to Chernobyl-4, FFTF has a negative coolant temperature coefficient, thus if FFTF experiences a flow reduction without action of the control system, the reactor power goes down rather than experiencing a power burst of the type that apparently happened at Chernobyl-4.

The overall sodium void coefficient for the reactor is negative; that is, if sodium were removed from the core by some mechanism, a negative reactivity would result overall.

The sodium void coefficient for FFTF is spatially dependent and is strongly negative at the periphery of the core but positive for some regions of the center of the core. This situation was examined thoroughly for FFTF and extensive design features were incorporated and tested to ensure no voiding of this region could occur.

6. U.S. Military Production Reactors

United States military production reactors are located in Hanford and Savannah River.

The N-reactor (located at Hanford), is a graphite-moderated, pressure-tube, light-water-cooled reactor which, of all U.S. reactors, most nearly resembles Chernobyl-4. However, modifications from earlier production reactor designs have been incorporated in the more modern N-reactor to increase its stability and safety. Of primary importance, the reactor is undermoderated and thereby has negative moderator void and power/flow coefficients. The negative reactivity insertion resulting from total voiding is equivalent to full insertion of the entire system of control rods.

The N-reactor has a negative coolant coefficient, a negative power fuel (Doppler) coefficient, and the graphite moderator coefficient also becomes negative without the coolant. The necessary condition for avoiding a power burst upon loss of flow without scram is met by the undermoderated N-reactor design.

Savannah River reactors are heavy-water-cooled and moderated thermal reactors. Assembly charges for the Savannah River reactors are designed such that the net temperature coefficient of reactivity (Doppler, coolant, moderator, power coefficients) result in stable reactor are under moderated which leads to a negative void coefficient. Again, this assures avoidance of a power burst upon loss offlow without scram.

7. High Temperature Gas-Cooled Reactor (HTGR)

The High Temperature Gas-Cooled Reactor (HTGR) is significantly different from the RBMK. The HTGR uses ceramic-coated uranium-carbide fuel, inert helium gas as a coolant, and graphite as a moderator and core structural material. The fuel is in the form of microspheres clad with high temperature pyroloric carbon and silicon carbide. The reactor uses an indirect cycle which isolates the primary coolant from the turbine generator.

Of principal significance in relation to the accident at Chernobyl-4 are the following:

- The HTGR has a strong negative reactivity feedback effect due to temperature. Thus, any power increase is automatically terminated. In addition, there is no positive reactivity effect due to loss of helium coolant, and no coolant phase change is possible.

- In the HTGR, the helium coolant is inert and does not react with the graphite, fuel coatings, or other system components.

- Tests have shown that even in the highly unlikely event of air gaining access to the reactor core, it is difficult to induce a self-sustaining burning of the dense, massive graphite blocks in the HTGR. Since the HTGR is housed either in a thick, prestressed concrete pressure vessel or in a below ground silo, a large sustained air-graphite reaction is next to impossible.

References

1. GESSAR-251 BWR/6 Standard Safety Analysis Report, General Electric Company, San Jose, CA (February 1975).

2. E. D. Fuller, "Physics of Operating Boiling Water Reactors," Nuclear Applications and Technology, Vol. 9, November 1969.

3. P. G. Alpine et al., "The Physics of Non-Uniform BWR Lattice," BNES International Conference on the Physics Problems in Thermal Reactor Design, June 1967.

4. E. G. Fuller, "Physics of Operating Boiling Water Reactors," Nuclear Applications and Technology, Vol. 9, No. 5, November 1970.

5. CESSAR: System 80 CESSAR Final Safety Analysis Report, Combustion Engineering, Inc., Windsor, CT.

6. B. L. Darnell, T. D. Beu, and G. W. Perry, Methods for the Lattice Physics Analysis of LWRs, TVA-TR78-02A, 1978.

7. S. L. Forkner, G. H. Meriwether, and T. D. Beu, Three-Dimensional LWR Core Simulation Methods, TVA-TR78-03A, 1978.

8. TVA-TR79-01A, Verification of TVA Steady-State BWR Physics Methods, January 1979.

9. S. L. Forkner et al., BWR Transient Analysis Model Utilizing the RETRAN Program, TVA-TR81-01, December 1981.

10. The PDQ07 Discrete Model, July 1976, VEP-FRD-19.

11. D. J. Denver et al., Application of Yankee's Reactor Physics Methods to Maine Yankee, October 1978, YAEC-1115.

12. A. F. Ansari and J. T. Cronin, Methods for the Analysis of Boiling Water Reactors - A Systems Transient Analysis Model (RETRAN), YAEC-1233, April 1981.

13. Duke Power Company Oconee Nuclear Station Reload Design Methodology, NRS-1001, Revision 4, June 1981.

APPENDIX D

ASSESSMENT OF ACTION IDENTIFIED BY THE SOVIETS TO IMPROVE THE SAFETY OF RBMK REACTORS

ASSESSMENT OF ACTIONS IDENTIFIED BY THE SOVIETS TO IMPROVE THE SAFETY OF RBMK REACTORS

In the aftermath of the Chernobyl-4 accident, the Soviet Union identified several planned actions to improve the safety of RBMK type plants. An assessment was performed of safety related items that were actual or potentially significant contributors to the Chernobyl-4 accident. These are summarized in figure D-3. This assessment did not use detailed plant modeling or transient analyses. The assessment was based on review and evaluation of the analyses done by the Team, analyses of basic effects, and the reasoned judgement of these experts based on the information currently available.

The key safety related items are divided into two categories for examination:

1. Human Factors
2. Design

Human Factors Safety Items

The Soviet report of the accident placed considerable emphasis on the role of the operators. Numerous operator actions (described as "operator errors") that led to the accident were identified and have been described in section 3 of this report.

The human errors involved procedural and other management and operator errors. A single large contributor to the accident was the dedication to completing the safety-related test before the reactor was shut down. It is obvious that the people working on the Chernobyl-4 reactor for at least the three shifts that proceeded and included the accident were highly motivated to complete the test before the reactor shut down. This steadfastness of purpose was obviously a result of management action.

The Soviets have taken a number of actions to address the human factors aspects of the accident. These include institutional, management, and operational initiatives.

The Soviet report does not, however, provide sufficient information to allow an assessment of the impact of these actions on the safety of RBMK type reactors.

Design

The planned design changes are to the RBMK type reactors identified by the Soviets are associated with preventing a

Chernobyl-4 type accident. In addition to assessing the effectiveness of these changes in meeting this objective, the Team considered their impact on the overall safety of the RBMK.

The reduction or elimination of the positive void coefficient may improve the safety and the stability of the RBMK type reactors at all power levels. However, one consequence of increasing enrichment (to decrease the positive void coefficient) is to increase power and flux peaking over the entire power range of operation.

Increased power and flux peaking would exacerbate the effect of power and reactivity transients on the fuel temperature. The normal operating margins would be reduced and the potential for, and extent of, centerline fuel melting, and fuel failure mechanisms associated with excessive fuel temperatures could be increased. Due to the smaller margins that exist this will be a bigger problem in the RBMK-1500 than in RBMK-1000 reactors since the latter have a larger thermal margin. It would require extensive three-dimensional analyses to further assess this item and to qualitatively identify the impact of the item on the safety of the RBMK type plants.

Overall the design changes identified by the Soviets will increase the safety of the reactor in some respects, but reduce safety margins in other respects. The conditions where the safety improvements are most effective are below 700 MWt (where the plant is not normally operated). The conditions where the safety margins are reduced are those at which the plant is normally operated. Lacking information on the details of the analyses used by the Soviets to make this trade-off, and lacking the requisite three-dimensional analyses to independently assess this trade-off, the Team could reach no quantative conclusion on the overall effect of these changes on safety.

A number of additional items regarding actions to improve RBMK safety were identified.

- It is not clear as to the time scale on which the fuel enrichment will actually be increased. It may be years before existing fuel supplies are exhausted, and the plants are fueled on 2.4 percent enriched uranium.

- Increased enrichment may increase the likelihood of local criticality control problems. If the Soviets increase burn-up, the problem with the positive void coefficient may also recur.

- The Soviets place most of the blame for the accident on the operators and on the operator's failure to follow procedures. Yet many of the fixes appear to rely on

the operators following additional, perhaps more complex, procedures established as a result of the accident.

- It appears that it is extremely easy to bypass, to cutoff, or to otherwise render RBMK safety systems inoperative. It is not apparent how the actions identified will address this item.

- The reliability of these fixes depends heavily on the method used. For example, will the control rods be limited in how far they can come out of the core by adjustable limit switches or by physical barriers? The fix of inserting the control rods 1.2 meters in the core should be effective if assured by a mechanical stop or other form of physical barrier. The information provided by the Soviets does not provide a basis for confidence in relying upon procedures to implement this fix.

In addition to the above, the Soviets have provided no information regarding the potential role of the pressure tube transition joints in the accident, nor any actions to address this issue.

The pressure tubes in the core are made of zirconium (Zr) that contains 2.5 percent niobium. These pressure tubes are diffusion welded to the stainless steel coolant system piping by heating (to 600 degrees C) under a vacuum. Figure D-1 shows the design of these transition joints.

The joints are made separately and joined to the tube assembly before installation. Figure D-2 shows the RBMK fuel channel and the locations of the transition joint. These joints are located inside the reactor vault immediately above and below the graphite reflectors. A maximum permissible rate of heat-up and cooling of 15 degrees C per hour has been established based on thermal and strength tests conducted by the Soviets.

This operating limit was exceeded by the transients that occurred during th accident. It is apparent that the design capability of these transition joints was exceeded.

The fuel channel transition joint thermal transient capability does not appear to be consistent with the thermal transients that can occur under accident conditions.

Since it may not appear to be practicable to limit thermal transients to less than 15 degrees C per hour under all accident conditions, it would appear to be prudent to either use a transition joint with a greater capability to accommodate thermal

transients, or to provide some inherent physical protection to the transition joint to prevent its exposure to such transients. While it is not obvious that transition joint failures were a cause or contributor to the accident, they easily could have been. None of the planned actions address this item.

Since the thermal transient capacity of these fuel channel transition joints is limited, the thermal transients associated with accident and off normal conditions could provide a basis for a common-cause failure that could lead to the failure of more than one of these transition joints. (There is no apparent feature that precludes this from happening.) The impact of such a multiple of coolant channel Loss of Coolant Accident has both containment and control system implications:

- The reactor vault is designed to accommodate a single coolant channel failure. A multiple channel failure would fail the reactor's vault and could lead to other consequences that could exacerbate the consequences of the initial accident.

- The control system does not appear to have the negative reactivity insertion rate capability needed to accommodate the positive reactivity insertion that could be associated with a multiple coolant channel failure.

None of the planned actions appear to address these items.

In addition to analyzing the Chernobyl-4 accident, the Team performed some limited analyses in the related areas of similarities between RBMK-1500 and RBMK-1000 reactor systems.

The RBMK-1500 design is quite similar to the RBMK-1000 (figure D-4). In order to get 50 percent greater power, the new design uses "ribbons" on the fuel rods to improve the heat transfer and bigger pumps to overcome a larger two-phase flow pressure drop. Thus, the reactor is run at a higher power level, with a higher core design average void fraction.

When the RBMK-1500 void fraction is checked against the void coefficient curve used from the Chernobyl-4 analysis, a void coefficient of 10^{-4} Δ K/% void is consistent. Thus, the RBMK-1500 is normally operated in a "slightly" over-moderated condition. However, if the operators were to perform the same actions on the RBMK-1500 units that were performed at Chernobyl-4, the positive void coefficient problem would be comparable to that at Chernobyl-4.

While operating the RBMK-1500 at high void fractions is advantageous with respect to the void coefficient, there are

disadvantages to this mode of operation. First, even with the "ribbon" heat transfer enchancement, the cooling of the fuel rod surface is probably quite poor at the outlet of hot channels. This, a significant reduction in flow could result in more fuel failures in the RBMK-1500 relative to the RBMK-1000 due to undercooling.

Second, with significant voiding in the upper 75 percent of the core, the thermal-hydraulic and neutronic coupling could be much stronger in the RBMK-1500 than in the RBMK. Thus, although the RBMK-1500 has a small advantage in that the void coefficient under normal operations is not as positive as that for the RBMK-1000, problems appear to remain with respect to operational complexity and safety.

In conclusion, there exist reasonable grounds to be skeptical about the effectiveness of the planned activities to improve the overall safety of RBMK type reactors. Until a detailed systems analysis of the planned action is available it may be that certain of the actions, while reducing the potential for, or consequences of a Chernobyl-4 type accident, may increase the severity and probability of other accidents.

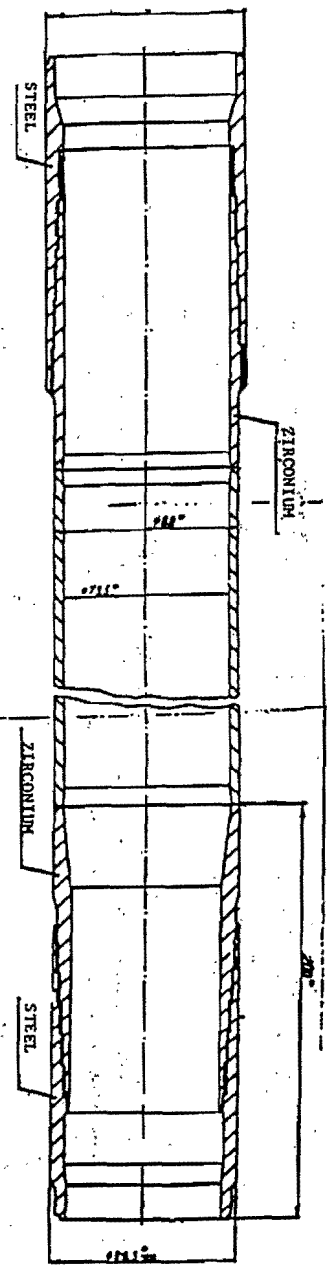

Zirconium-Stainless steel Transition Joint (Dollezhal' and Yemel'yanov 1980b)

Figure D-1.

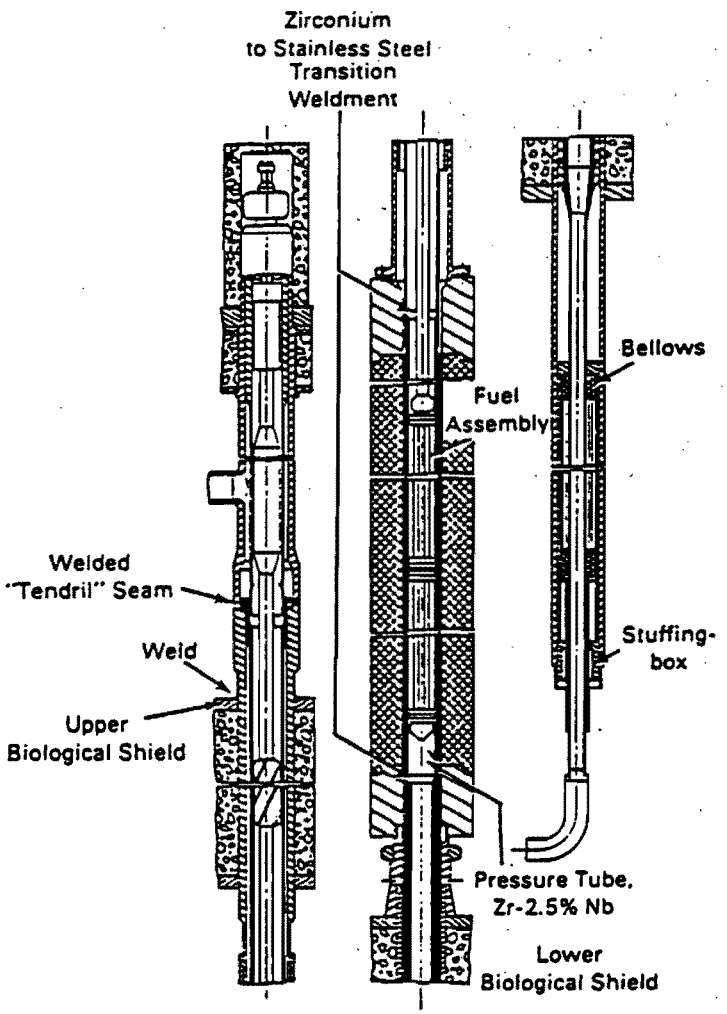

Fuel Channel (Dollezhal' and Yemel'yanov 1980b)

Figure D -2.

ONGOING OR PLANNED IMPROVEMENTS IN SOVIET SAFETY PROGRAMS
(As set forth in Soviet Report on Chernobyl, pp. 35. 64)

- Institutional Improvements
  - Formation of All-Union Ministry of Nuclear Power Engineering.
  - Intensified Government supervision of safety.
  - Enhanced international programs for safe development nuclear power.
  - Reorder priorities for R&D.
- Management and Operator Improvements
  - Organizational changes to improve plant discipline and quality of operations.
- Safety Analysis Improvements
  - Analyses of plant behavior in all modes, including beyond design bases.
  - Studies of passive safety systems for future application.
  - Probabilistic risk assessments and other "principles" for optimizing radiation.
- Design Features Improvements
  - Increase fuel enrichment to 2.4 percent U-235.
  - Additional pump sensors to increase protection against cavitation and loss of flow.
  - Automatic system for computing reactivity reserve and tie-in to scram system.
  - Creation of a rapid shut down system which can act within 1-2 seconds.
  - Reset control rod limit switches so that fully withdrawn rods are inserted 1.2 meters into the core.

Figure D -3.

Comparison of RBMK-1000 and RBMK-1500 Parameters

	RBMK-1000	RBMK-1500
Net Efficiency	29.9%	31,.3%
Coolant Flow Rate (t/hr)	37500-42000	29000-32000
Avg. Linear Power	315 w/g	485 w/g
Avg. Power Density	4.2 w/cc	6.3 w/cc
Max. Fuel Exposure	22.3 GWD/Mtu	21.6 GWD/Mtu
Power of Max. Channel	3.25 Mw	4.91 Mw
MCP Delta P	1.61 MPa	2.0 MPa
Steam Drum Prod. Rate	1450 t/h	2200 t/h
Drum Exit Steam Press.	6.86 MPa	7.0 MPa
Turbogenerator Power	2 @ 500 Mw	2 @ 750 Mw
Fuel Temp. Coeff. (Negative) (At Full Power and Average Fuel Exposure)	1.2×10^{-5}	1.02×10^{-5}
Void Coefficient (ΔK/% Void) (At Full Power and Average Fuel Exposure)	2×10^{-4}	10^{-4}
Approx. Core Average Void % (Assuming No Subcooled Boiling)	25.	40.
Core Outlet Quality %	14.5	29.

Figure D -4.

APPENDIX E

BACKGROUND INFORMATION ON CHERNOBYL-4, RBMK TYPE REACTORS, AND THE SOVIET NUCLEAR POWER PROGRAM

BACKGROUND
TABLE OF CONTENTS

1. A Description of Chernobyl-4
2. Soviet Description of the Chernobyl RBMK-1000 Reactors (Direct From Soviet Report)
3. Chernobyl-4 Design Parameters
4. Soviet Statement of Causes of Accident (From Soviet Report)
5. Relevance of Plant Characteristics to Accident
6. The Soviet Power Reactor Program

A DESCRIPTION OF CHERNOBYL-4

- Chernobyl-4 is a 1000 MWe reactor of unique design, constructed only in the Soviet Union.

- The design evolved from early demonstration and plutonium production reactors.

- There were 14 RBMK-1000 plants that provided about one half of the Soviet Union's nuclear electric generating capacity. The first RBMK-1000 began operation at Leningrad in 1973. Chernobyl-4 was the newest of these plants. Two more such plants were under construction at Chernobyl.

- An RBMK-1500 plant is in operation at Ignalina. This plant differs very little from the RBMK-1000, but has a 50 percent higher power level.

- General characteristics include the use of graphite as moderator, boiling light water as coolant, and online refueling. Pressure tubes, contained in vertical channels in the graphite. Specific design parameters are provided in the attached charts.

- The core is cylindrical graphite stack with a diameter of 38.7 feet and a height of 23 feet; penetrated by about 2000 channels that provide locations for fuel, control rods, and instrumentation.

- The fuel is 20 percent enriched uranium oxide clad with a zirconium-1 percent niobium alloy. The fuel elements are constructed in 18 element clusters connected to a central fueled pressure tube.

- This type of reactor has positive void reactivity coefficients under most operating conditions, a slow scram system, and makes extensive use of a relatively simple computerized control system.

- The plant uses a steam suppression bubbler pond/confinement system, as opposed to containment structures that can withstand internal pressure such as are used in LWR's in the U.S., the USSR, and other countries.

SOVIET DESCRIPTION OF THE CHERNOBYL RBMK-1000 REACTORS
(Direct From Soviet Report)

The basic design features of RBMK-1000 reactors are as follows:

(1) vertical channels with the fuel and the heat-transfer agent, which permit local reloading of fuel with a working reactor;

(2) fuel in the form of bundles of cylindric fuel elements of uranium dioxide in zirconium shell tubes;

(3) a graphite moderator between channels;

(4) a low-boiling heat-transfer medium in the forced circulaion recirculation mode (KMPTs) with direct feeding of steam to the turbine.

These design decisions, in combination, condition all the basic features of the reactor and the AES, both advantages and shortcomings. Advantages include:

- the absence of reactor vessels, which are awkward to produce on the poweplant maximum capacity and on the production base;

- the absence of a complex and expensive steam generator;

- the possibility of continuous reloading of fuel and a good neutron balance;

- a flexible fuel cycle, which is easily adapted to variations in the fuel market conditions;

- the possibility of nuclear superheating of the steam;

- high thermodynamic reliability of the thermal equipment and viability of the reactor due to the controlling of the flow rate for each channel separately, monitoring of the integrity of the channels, monitoring of the parameters and radio activity of heat-transfer medium of each channel and replacement of damaged channels while running.

Shortcomings include:

- the possibility of the development of a positive void coefficient of reactivity due to the phase change in the heat-transfer agent which determines the transient neutronic behavior;

- high sensitivity of the neutron field to reactivity

disturbances of different kinds, necessitating a complex control system for stabilizing the distribution of the release of energy in the active zone;

- complexity of the inlet-outlet piping system for the heat-transfer agent of each channel;

- a large amount of thermal energy accumulated in the metal structures, fuel elements and graphite block structure of the reactor;

- slightly radioactive steam in the turbine.

Chernobyl-4 Design Parameters

Chernobyl-4 Design Parameters	
Summary of General Design Characteristics	
Reactor type	Vertical pressure tube-boiling water-graphite moderated
Refueling	On-line
Design power generation	3140 MWt
Total reactor coolant flowrate	37,500 tonne/h (22,965 lbm/s)
Summary of Core Description	
Core dimensions (active zone):	
Height	7.0 m (23.0 ft)
Diameter	11.8 m (38.7 ft)
Volume	765.0 m^3 (2700 ft^3)
Total number of fuel channels	1661
Lattice spacing	25 cm x 25 cm (9.8 in x 9.8 in)
Moderator material	Graphite
Maximum allowable measured temperature	750°C (1382°F)
Material density	1.67 g/cm^3 (104.2 lbs/ft^3)
Reflector Dimensions:	
top and bottom	0.5 m (19.7 in)
sides	1.0 m (39.4 in)
Graphite weight	1700 tonne (3.74 x 10^6 lbs)
Summary of Fuel Description	
Design	Two 18 rod elements connected in series
Uranium form	UO_2
Cladding material	Zr-1% NB
Enrichment	2.0 wt% U^{235}

Chernobyl-4 Design Parameters	
Fuel assembly length	7.0 m (23.0 ft)
Maximum clad temperature	323°C (613°F)
Maximum fuel temperature	2,100°C (3812°F)
Total uranium weight	189 tonne (416,740 lbm)
Fuel exposure	22.3 Mwd/kg
Summary Description of Primary Water Recirculation System	
System material	Austenitic stainless steel
Independent flow loops	2
Steam drums (total/per loop)	4/2
Pumps (total/normally operating)	8/6
Pump dynamic head	2.0 MPa (290 psi)
Net positive suction head	0.6 MPa (87 psi)
Feed pump suction and discharge header diameters	90 cm (35.4 in)
Feed pump capacity	7000-9000 m^3/hr (31,000-40,000 gpm)
Dimensions of individual pressure tube inlet piping (OD x wall)	5.7 x 0.35 cm (2.2 x 0.14 in)
Dimensions of individual pressure tube outlet piping (OD x wall)	7.6 x 0.4 cm (3.0 x 0.16 in)
Summary Description of Fuel Channels	
Number	1661
Pressure tube diameter (OD)	8.8 cm (3.46 in.)
Pressure tube wall thickness	0.4 cm (0.158 in.)
Material	Zr-2.5% Nb
Connection	Diffusion welded Zr to SS joint in core zone

Chernobyl-4 Design Parameters	
Individual channel flow control	Manually adjusted regulating valve
Inlet temperature	270°C (518°F)
Outlet temperature (avg.)	284°C (543°F)
Operating pressure	6.8 MPa (986 psig)
Quality	14.5% (average steam) 20.1% (maximum)
Average tube power	1890 KWt
Axial peak/avg. power ratio	1.26-1.33
Radial peak/avg. power ratio	1.27-1.40
Summary Description of Steam Secondary System	
Steam collector	Primary system steam drum separators
Number of collectors	4/2 (total/per loop)
Collector (ID x Length)	2.6 x 30 m (8.5 x 98.4 ft)
Steam flowrate (total)	5500 MT/h (3368 lbm/s)
Power generation	1000 MWe (two 500 MWe turbogenerators)
Heat rejection w/o turbogenerators	Water reservoir (condenser)
Feedwater inlet temperature to steam separators	165°C (329°F)
Summary Description of Control-Shutdown and Safety Shutdown System	
Type	Boron carbide segments encased in aluminum, lowered and retrieved from above by a belt-cable and motorized drum.
Number of control-shutdown assemblies	211

Chernobyl-4 Design Parameters	
Neutron absorption material	B_4C
Control rod travel	6.25 m (20.5 ft.) except auto. control rod - 4.5 m (14.8 ft.) & axial control rod - 7.0 m (23 ft.)
Cooling method	Separate water cooling system with downward flow in individual channels of 4.3-5.4 M^3/hr (151-190 ft^3/hr)
Control rod full insertion time	20 seconds
90% reactivity insertion time	10 seconds
Summary Description of Over-pressure Control System	
Type	Partial steam suppression of releases from the reactor cavity, inlet piping and pumps
Enclosure	Reactor core inlet and piping system
Function	Condense steam from piping break or steam separator relief valves
Design pressure	Enclosure areas designed for either 0.4 MPa (58 psig) or 0.18 MPa (26 psig)
Operation	Steam - water from pipe break or steam separator relief valves directed to standing water in bubbler pond below reactor. Water spray above bubbler pond helps condensation process.

SOVIET STATEMENT OF CAUSES OF ACCIDENT
(From Soviet Report)

In the process of preparing for and conducting tests of a turbogenerator in a rundown mode with a load of system auxiliaries of the unit, the personnel disengaged a number of technical protection devices and violated important conditions of the operating regulations for safe performance.

The table presents a list of the most dangerous violations of operating conditions committed by personnel of the fourth unit at Chernobyl.

No.	Violation	Motivation	Results
1.	Decrease in the operting reactance reserve significantly below the acceptable value.	Attempt to get out of "iodine pit".	Emergency protection of reactor proved ineffective.
2.	Power dip below value envisaged by testing program.	Operator error in disengagement of control rods.	Reactor proved to be in hard-to-control state.
3.	Connection of all main circulation pumps to reactor with exceeding of flow rates established by regulations in regard to individual pumps.	Fullfillment of requirements of testing program.	Temperature of heat-transfer medium of forced circulation ducts came close to saturation temperature.
4.	Blocking of reactor protection on signal for shutdown of two Turbine Generators.	Intention to repeat experiment with disengagement of Turbine Generators if necessary.	Loss of possibility of automatic shutdown of reactor.

No.	Violation	Motivation	Results
5.	Blocking of protection in regard to water level and steam pressure in separator drum.	Attempt to conduct tests despite unstable operation of reactor.	Protection of reactor in regard to thermal parameters was disengaged.
6.	Disengagement of system for protection against maximum theoretical failure (disengagement of Emergency Cooling System).	Attempt to avoid false response of Emergency Cooling System during performance of testing.	Loss of possibility of reducing scale of accident.

RELEVANCE OF PLANT CHARACTERISTICS TO ACCIDENT

The RBMK-1000 type plants have stability problems and have been found to be difficult to control, p;articularly at low power levels. The reactor does not have sufficient excess of the core override xenon. The in-core fission detectors are slow and the ex-core detectors insensitive to fast transients.

The reactor is neutronically loosely coupled, acts like several reactors, and uses four different types of rods, six signals, and computer control to maintain control and flux distribution.

The moderator temperature and coolant void reactivity coefficients are positive over a wide range of conditions and vary with position, burnup, and power level. Upsets are not self correcting and must be controlled by active rod insertions. The scram rod speeds are slow. The shutdown reactivity margins are small.

The excursion could have been localized because of the decoupled nature of the core, and possibly because of the differences in chanel tube inlet valve positions. The core has 1,661 channels, each of which has an inlet valve that must be set to match the power in the channel. A localized excursion would be muh more damaging because the same power would be concentrated over a smaller volume.

The zirconium pressure tubes are joined by difussion welds to stainless steel tubes at the inlet and the outlet of the core. It is known that the temperature transietns allowed on these under startup and shutdown conditions are small (10 to 15 degree C/hr). The pressure tube strength would degrade as a result of a temperature excursion. The stress would increase as a result of the power excursion. Failure of the pressure tube due to an overstress condition and of the transition joint due to thermal shock could be repeated.

The reactor vault which has a design pressure of 26 psi, is designed to withstand the failure of one pressure tube. The upper biological shield supports the weight of the fuel channels, control rods and drives, and the upper reactor piping. Gross motion of this structure can lead to common mode multiple failures. Also, the graphite to the pressure tubes act like labyrinth seals. Alternate rings are joined to the surrounding graphite. This configuration would resist downward flow of steam released from pressure tube rupture to the suppression pool for failures near the top of the core (where they are more likely). The result is an upward disruptive force, with the upper vault diaphragm bearing most of the load.

The reactor contains large amounts of zirconium in the fuel cladding and the pressure tubes, that may react exothermally with water to gnerate large amounts of hydrogen and energy. The graphite could react with water vapor to form CO and hydrogen, both of which are explosive under a wide range of concentrations and temperature.

The Local Area Compartmentalization Approach used is designed to contain only limited parts of the primary system. If operative, suppression pools can be expected to retain significant fractions of fission product aerosols from the gas stream passing through them. The Chernobyl-4 suppression pool is designed to accommodate releases from only the lower portions of the reactor coolant system. There is no containment in the context of that provided on U.S. LWRs.

THE SOVIET POWER REACTOR PROGRAM

o Background

The Soviet nuclear power program was initiated in the 1950's. Although the Soviet Union has substantial non-nuclear energy resources, development of nuclear power was believed necessary because of the geographical mismatch between its energy resources and its population concentrations and because of the belief that nuclear power is less damaging to the environment than available alternative energy sources. The Soviets currently have a nuclear power generating capability of over 20 GWe. Over 10 percent of electricity generation within the Soviet Union is supplied by nuclear plants. Most of the plants are located in the European part of the Soviet Union.

The course of development of nuclear power for electricity production has followed two different paths resulting in the deployment of two substantially different types of thermal reactors: the VVER and the RBMK reactors. Additionally, the Soviets have an extensive research and development program for liquid-metal-cooled fast reactors and other special purpose reactors.

o VVERs Pressurized Water Reactors

The VVER reactors are pressurized water reactprs (PWRs) generically similar to many reactors developed elsewhere in the world including the United States. VVERs have been deployed domestically and have been exported to Eastern European countries and to Finland, and Cuba. The first two VVERs were sized at 210 MWe (Novo Voronezh, 1964) and 365 MWe (Novo Voronezh, 1970). They are currently constructed in two sizes : 440 MWe and 1000 MWe. Although, these reactors are similar in some ways to Western-designed PWRs there are substantial design differences which, to a large extent, reflect differences in approach to safety. These differences are most evident in the design of containment systems. It is evident that Soviet philosophy concerning reactor safety is continuing to evolve. Later VVERs have more robust safety and containment systems than earlier models. Success in exporting the VVER can be at least partially attributed to a willingness to adapt the designs to meet the need of the purchaser (e.g., containment system design on the Finnish VVER), and a willingness to involve the purchaser in both design and construction efforts.

- RBMKs, Graphite-Moderated, Water-Cooled Reactors

  The Soviet RBMK reactor is a graphite-moderated, boiling water-cooled reactor (GWR) and represents a unique design used only in the Soviet Union. The design is an outgrowth of experience with their first demonstration powe reactor (Obninsk, 5 MWe, 1954), dual-purpose (plutonium production as well as electricity generation) reactors (Siberian Atomic Power Station, 100 MWe, 1958), and early graphite moderated reactors (GMRs) (Beloyarsk, 100 - 200 MWe, 1964). RBMKs have been deployed in sizes of 1000 MWe (14 operating) prior to the Chernobyl accident) and 1500 MWe (1 operating) and plans exist for sizes as large as 2400 MWe. The RBMK design also reflects evolving changes in Soviet philosophy concerning reactor safety. Containment/confinement systems in later models have a number of improvements including the use of a suppression pool (bubbler pond). RBMKs have not been available for export.

- BNs, Liquid-Metal Cooled, Fast Breeder Reactors

  The BN reactors are liquid sodium cooled, fast breeder reactors (LMFBRs). The Soviets have built a number of small research LMFBRs and there are currently two plants producing electricity. The BN-350 plant on the Caspian Sea produces electricity and process heat for desalinating water. The BN-600 plant at Beloyarsk is a 600 MWe plant. Plans exist for deploying a half-dozen or more 800 MWe LMFBRs before the end of the century.

- Specialized Reactors

  The Soviets use a number of their existing power reactors to produce a relatively small amount of heat for district heating as well as for producing electricity. Construction is now underway on specialized plants that will be used exclusively for district heating. These plants are boiling water reactors utilizing a three-loop thermal exchange system. Additionally, several combined district heating/electricity production plants are under construction that are based on a modified VVER-1000 design that sacrifices a significant portion of the electrical production capability for district heating capability.

- Fuel Cycle

  The Soviets are actively involved in all parts of the fuel cycle including uranium mining, uranium enrichment, fuel fabrication, fuel reprocessing, and waste disposal. Reprocessing of VVER fuel commenced in the mid-1970's. Reprocessing of RBMK fuel is being indefinitely deferred. Export agreements associated with reactor sales includes a stipulation that the Soviets will supply the fuel and that fuel will be returned to the Soviet Union for reprocessing.

APPENDIX F

CHERNOBYL-4 VOID COEFFICIENTS AND NEUTRON KINETICS PARAMETERS

CHERNOBYL-4 VOID COEFFICIENT

Much effort has been expended by various U.S. groups to duplicate the Soviet mathematical analysis of the Chernobyl accident. The Soviets provided much information in the form of calculated results (the famous figure 4), but little information on the input parameters used in their study. The purpose of this report is to provide information on the void coefficient used by the Soviets in their model.

Determination of the void coefficient for an RBMK is not an easy task. The coefficient is a complex function of fuel enrichment, fuel exposure, control rod positions, supplemental absorber loading and coolant void faction. All these parameters vary considerably over the reactor volume. In the Soviet literature, the void coefficient is usually given as a single value "at the operating point". The operating point defines a single void fraction (approximately 30%), typical inserted rod worth (30 rods equivalent) and average exposure (approximately 10 GwD/MtU).

In Vienna the Soviets were asked to give the value used in their analysis. The Soviet reply was that a void coefficient of 0.0002/% void was used in the physics calculations based on 30 rods excess reactivity. With all rods out, as during the accident a value of 0.0003/% void was quoted. No further details were provided. It is not clear from this response if they used 0.0002 or 0.0003.

The void coefficient used by the Soviets can be determined from studying the results presented in their figure 4. Since this figure shows a curve of total reactivity (curve B) along with reactor average void fraction (curve P), the void coefficient can be deduced from the relationship between the two curves during a time when no other factors are affecting the total reactivity. There are two such time intervals. From 1:23:40 until 1:23:43 there is a significant change in the void fraction and little change in any other parameter (there is some control rod motion but it is not believed to affect the total reactivity). Also, in the fraction of a second near the end of 1:23:44 there is again a large change in void coefficient and little or no change in any other parameter affecting reactivity.

Of this two intervals, the fraction of a second near 1:23:45 provides the best choice for use in calculating the void coefficient. The time interval is very short thus limiting any other effects on the total reactivity. The attached figure F-1 shows a blow-up of Soviet figure 4 in the region near 1:23:45. Only the void fraction and total reactivity curves are shown. Using the scales provided, 5 mk/division and 0.1 void fraction/division, the change in reactivity is approximately

15.6mk and the change in void fraction is approximately 0.57. Dividing .0156 (15.6 mk) by 57% (0.57 void fraction) gives a void coefficient of 0.000274/% void. This is very nearly equal to the Soviet stated value of 0.0003 for the conditions at the time of the accident. The small difference is attributed to difficulty in reading precise values from the curves.

The reason for not choosing the time interval from 1:23:40 to 1:23:43 is our belief that at 1:23:40 an external reactivity insertion simulating the positive reactivity from the scram rods is included in the model. This insertion is estimated to be 1.0 to 1.5 mk/sec. During this time interval the void fraction changes from 0.25 to 0.34 and the reactivity changes from 1.4 mk to 8.0 mk. For all this reactivity increase to be caused by voiding alone, the void coefficient would have to be 0.00073. This is far in excess of any calculated or quoted value. Clearly something else is going on that affects the reactivity.

If a void coefficient of 0.0003 is applied to this time interval the reactivity increase resulting from voiding alone can be calculated. Subtracting the calculated void reactivity from the total reactivity curve gives the external reactivity ramp that begins at the time of the scram. This is shown in the attached figure F-2. The difference between the total reactivity and the calculated void reactivity is seen to be a ramp starting at 0.25 seconds after the scram and having a slope of 1.5 mk/second. This result is consistent with our assertion that a positive reactivity ramp of 1.0 to 1.5 mk/second occurs as a result of the control rod followers displacing the water in the rod channels.

Based on the above arguments we believe the Soviets used a constant void coefficient of 0.0003/% void in their analysis. They did not use a void coefficient that varies with void fraction. Also, they inserted an external positive reactivity ramp with a slope of 1.5 mk/second starting 0.25 seconds after the scram to simulate some form of external positive reactivity insertion (the effect of scramming the rods from their fully withdrawn position).

NEUTRON KINETIC PARAMETERS FOR CHERNOBYL

Accurate values of delayed neutron fraction (Beta) and prompt neutron lifetime (1*) are required to perform analyses of the Chernobyl-4 accident. There exists little information in the Soviet literature about these parameters for the conditions at the time of the accident (2 percent enriched fuel, 10.3 GwD/MtU exposure). Values for Beta given in Dollezhal's book on channel tube reactors are for 1.8 percent enriched fuel and the Soviet's experimentally determined value for 1* (0.89 milliseconds) is for 2 percent enriched fuel at beginning of life and cold conditions.

There are two methods for obtaining more relevant values for Beta and 1*. Values can be obtained from RBMK lattice calculations or they can be deduced from the results of the Soviet mathematical model of the Chernobyl-4 accident. The purpose of this report is to compare the values of Beta and 1* obtained by these two methods.

Calculated Neutron Kinetics Parameters

Values for Beta and 1* can be calculated from the results of an RBMK unit cell lattice analysis. Beta can be determined from a detailed fission reaction rate edit of the fissionable nuclides and 1* can be calculated from the multigroup, cell averaged macroscopic cross sections and corresponding group neutron velocities.

Using the results from a WIMS calculation, the values for Beta and 1* are found to be 0.0048 and 0.77 milliseconds respectively. These values are for a fuel exposure of 10 GwD/MtU, average temperatures and void fraction, and equilibrium fission product concentrations. Table F-1 gives calculated values of Beta for a range of fuel exposures and enrichments of 1.8, 2.0, and 2.4 weight % U-235.

Comparison of the Beta values in table F-1 against the Soviet published values for 1.8 percent fuel (table F-2) shows good agreement. No published data is available for the 2.0 and 2.4 percent fuel.

Validation of the method of using WIMS calculated multigroup cross sections to derive the neutron lifetime can be made by comparing the calculated lifetime for a cold, green unit cell with the Soviet experimental value of 1* based on the millisecond for these same conditions. For this case the value of 1* based on the WIMS cell averaged cross sections is 0.83 milliseconds (this value is the sum of the thermal neutron lifetime and an assumed value of 0.15 millisecond slowing down time). A second data point for validation is to use N-reactor as a model. Its experimentally determined lifetime is 0.54 milliseconds. Based on the WIMS calculated cross sections for an N-reactor unit cell the calculated 1* is 0.58 milliseconds. In both cases the values based on WIMS calculations agree with the experimentally reported values with 10 percent.

Therefore, based on the above calculated results the expected values for Beta and 1* used in the analysis of the Chernobyl-4 accident are 0.0048 and 0.77 milliseconds.

Parameters Deduced From Figure 4

Beta and 1* used by the Soviets can be deduced from their results presented in figure 4 of the Chernobyl-4 accident report. The

value of Beta can be simply read from the total reactivity curve at the times when the power curve has zero slope. Using this value of Beta, the prompt neutron lifetime can be determined by finding the value that allows reproduction of their power and temperature versus time curve. The calculation requires only a simple point kinetics model using the Soviet total reactivity as input and no thermal hydraulic feedback (the Soviet analysis was performed using a point kinetics model).

The determination of Beta is based on the fact that for a prompt critical system in which the delayed neutron precursors cannot keep up with the power increase, the time rate of change in the power is given by:

dn/dt=(Reactivity-Beta)/Prompt Neutron Lifetime.

Therefore, when the time rate of change of the power is zero reactivity must be equal to Beta.

The attached figure F-1 is an enlargement of the Soviet figure 4 showing the last four seconds of the transient. There are two times at which the power curve (curve D) has zero slope with the reactor prompt critical; just before 1:23:43 and at 1:23:45:5. At the first of these two times the reactivity cure (curve B) is approximately 0.0045 which agrees with the expected value of 0.0048. However, at the second time the corresponding value of reactivity is 0.0. This is not reasonable.

A possible explanation is that the power curves on figure 4 were hand drawn without adequate attention to the exact shapes of the peaks. In the calculations we have performed the power peaks are Gaussian-shaped. The Soviet peaks are not. There are discontinuities in the slope, particularly just after the peaks begin to turn over. Small errors in drawing in the peak shapes can lead to large errors in determining the corresponding values of reactivity. This is particularly true at the second peak where the reactivity curve has a very large slope. Based on these finding, figure 4 cannot be used to provide a reliable estimate of the value of Beta used in their analysis.

The value of 1* used in the Soviet analysis can be determined by finding the value that allows duplication of the Soviet calculated powers, fuel temperatures and accident timing. Using a six delayed group point kinetics code with a Beta of 0.0045 and an 1* of 1.75 milliseconds we were able to match the fuel temperatures and time sequence of the power transients, but we were not able to match the power peak magnitudes. The Soviet values are four times higher than our calculated values.

One possible explanation for the differences is the number of delayed neutron groups used in the point kinetics model. Our

model used six delayed groups. Brookhaven National Laboratory (BNL) has made a similar calculation using only one delayed groups. BNL's results for 1*=1.8 millisecond and Beta=0.0045 show a peak power in the first excursion that is approximately 40 percent larger than the Soviet calculation (much better agreement than our six group calculation).

Based on this evidence, it appears reasonable to assume the Soviets used a single delayed group and a neutron lifetime of slightly less than 1.8 milliseconds. <u>However</u>, there is still a problem--fuel temperature. Our calculated fuel temperature agrees with the Soviet value even though our powers are lower by a factor of four. If we change the neutron lifetime to get the peak power to agree with the Soviet's, our calculated fuel temperatures become unrealistically large. This is shown in the attached figures F-2 and F-3 which show the effects of using different lifetimes on peak power and fuel temperature. (BNL did not calculate fuel temperatures in their one group model). Thus, there appears to be an error in either the Soviet temperature or power scale.

If we assume the temperature scale is in error, and use lifetime much shorter than 1.75 milliseconds to get the six group calculated power magnitude to agree with the Soviet value than the time sequence of power versus reactivity does not agree with the Soviet figure 4. The attached figures F-4 and F-5 show the effect of using 1*=1.0 millisecond and 1*=1.75 milliseconds on the timing of the power peaks. To preserve the time of the accident events, the neutron lifetime must be on the order of 1.75 milliseconds. Therefore, ignoring the Soviet temperature scale and using a lifetime that produces agreement with the power peak magnitudes is not reasonable.

The other choice is to assume the Soviet power scale is wrong. Rescaling the Soviet calculated power by a factor of four (0-12000 percent instead of 0-48000 percent) allows the six group calculated power peak magnitudes, fuel temperatures and timing to all agree with the Soviet figure 4. Rescaling the power curve on Soviet figure 4 appears to be more reasonable than assuming the temperature scale is wrong. Perhaps the Soviets rescaled the power curve to show the effect of power peaking. That is, the power shown is not the total reactor power but in some way represents the power increase in the lower portion of the core.

<u>Conclusions</u>

Calculated values of Beta and 1* obtained from WIMS modeling of experimental lattices (both RBMK and in the U.S.) have shown good agreement with the measured results. The calculated values for Beta and 1* for the conditions at the time of the accident are 0.0048 and 0.77 milliseconds.

Attempts to arrive at these same values by deducing the values from Soviet figure 4 were not successful. At the two times on the curve where the power curve has zero slope with the reactor prompt critical, the corresponding values of Beta are 0.0045 and 0.0. A possible explanation is that the power curves were hand drawn without careful attention to maintaining the relationship between power and reactivity. Using a Beta of 0.0045 the value of 1* that reproduces the fuel temperature and power peak timing is 1.75 milliseconds (more than twice as large as expected). Although the fuel temperature and timing are reproduced using these values, the peak power is not. The calculated power is four times lower than the Soviet value. Perhaps the Soviets included a power peaking factor in the power scale.

The study of figure 4 raises more questions than it answers. Why don't the power and reactivity curves agree with the mathematics/ Why was such a large value of neutron lifetime used? Why don't the fuel temperature and power agree?

Table F-1. Calculated Delayed Neutron Fraction for Various Fuel Enrichments

	Fuel Enrichment		
Exposure(GwD/MtU)	1.8	2.0	2.4
0.0	0.0065	0.0065	0.0065
5.0	0.0052	0.0055	0.0056
10.0	0.0046	0.0048	0.0050
15.0	0.0040	0.0043	0.0046
20.0	0.0036	0.0038	0.0042

Table F-2. Soviet Reported Delayed Neutron Fraction for 1.8% Fuel

Exposure(GwD/MtU)	Beta
0.0	0.0065
2.1	0.0056
5.2	0.0050
9.0	0.0044
9.9	0.0043
10.8	0.0042
14.0	0.0039
14.8	0.0038
15.5	0.0037
16.9	0.0036
17.6	0.0036

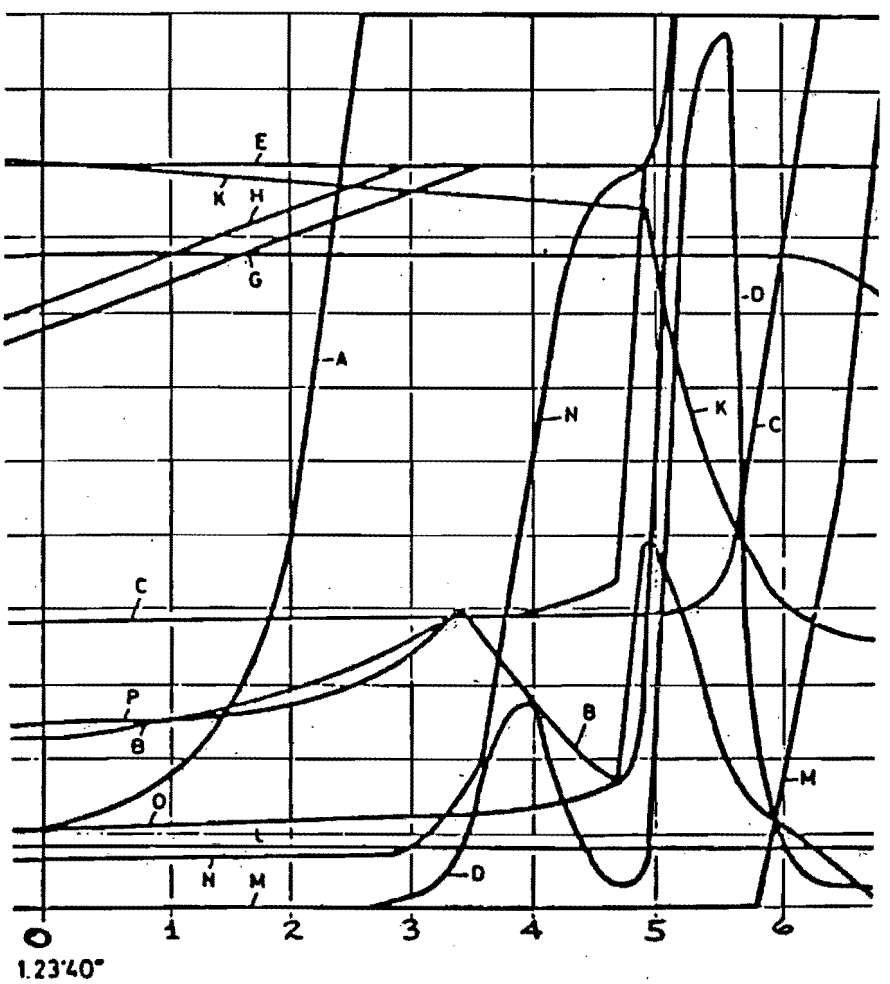

Figure F-1. Enlargement of Soviet Figure 4.

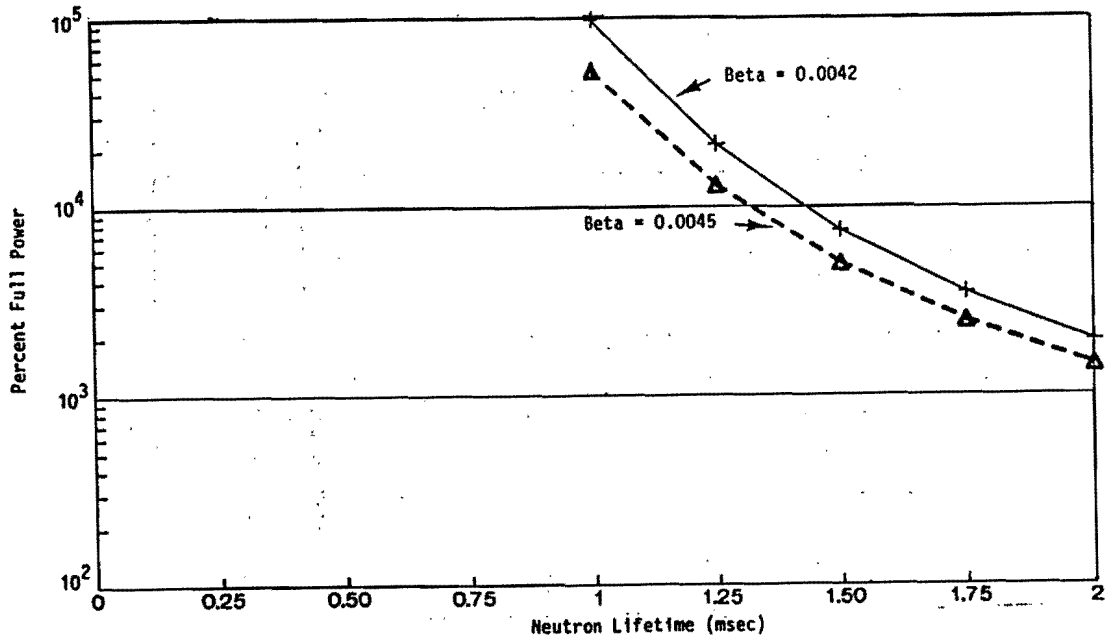

Figure F-2. Effect of Neutron Lifetime on Calculated Peak Power (First Peak).

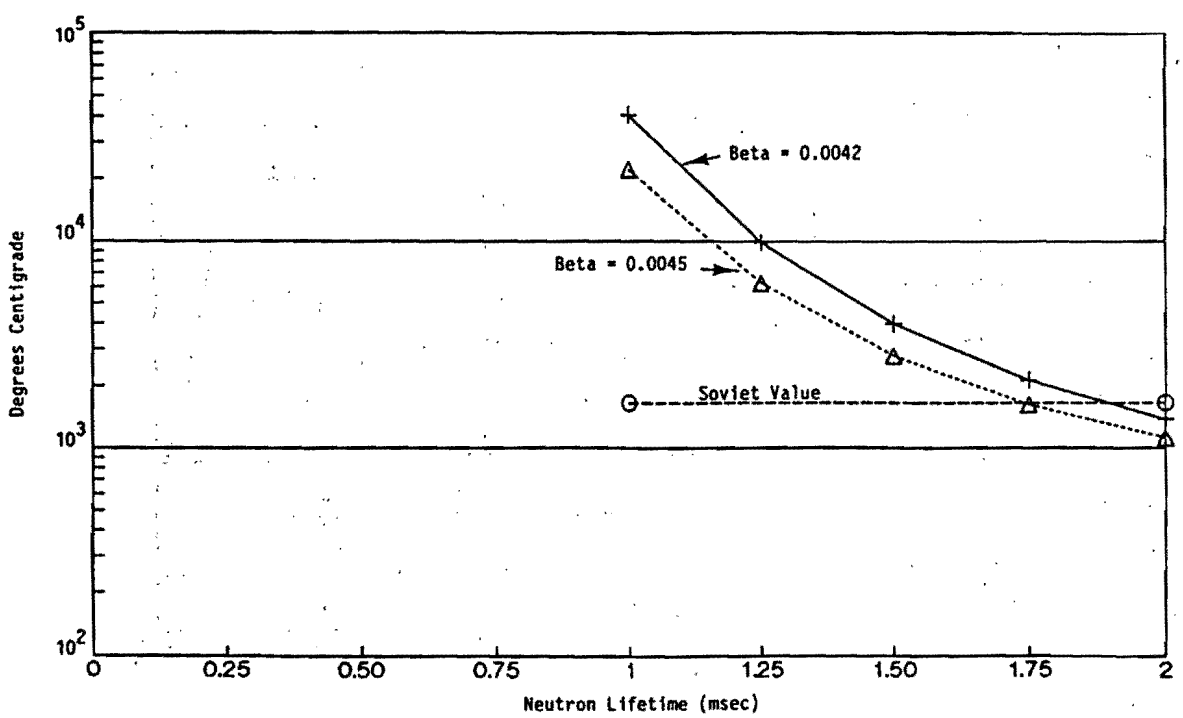

Figure F-3. Effect of Neutron Lifetime on Calculated Fuel Temperature at 1:23:44.7.

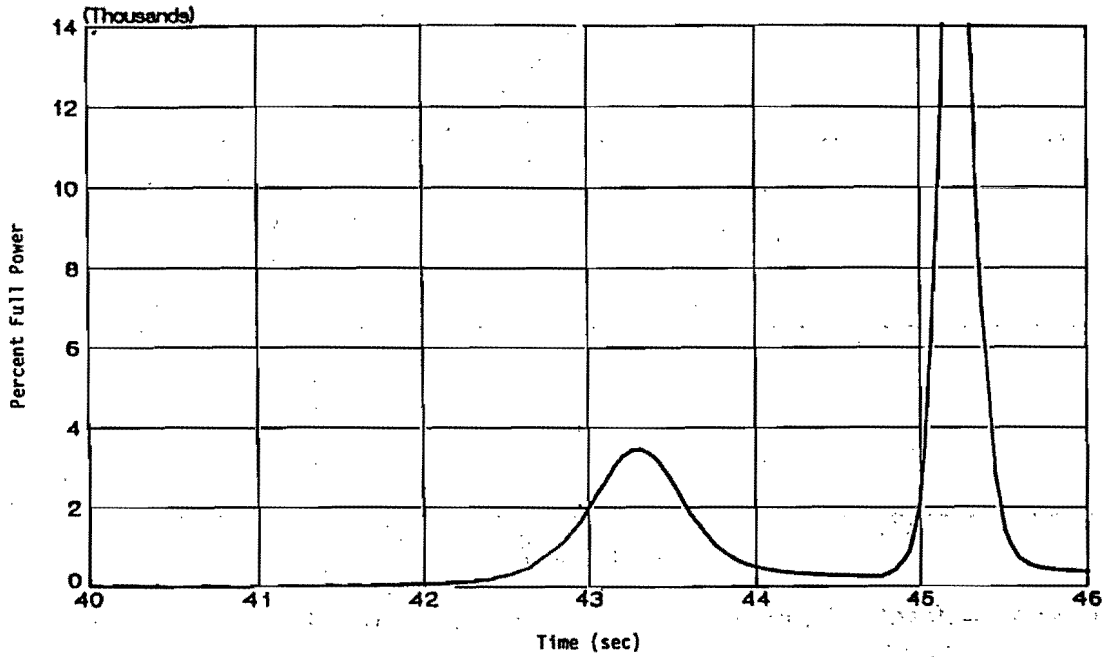

Figure F-4. Calculated Power Using a Neutron Lifetime of 1.0 msec.

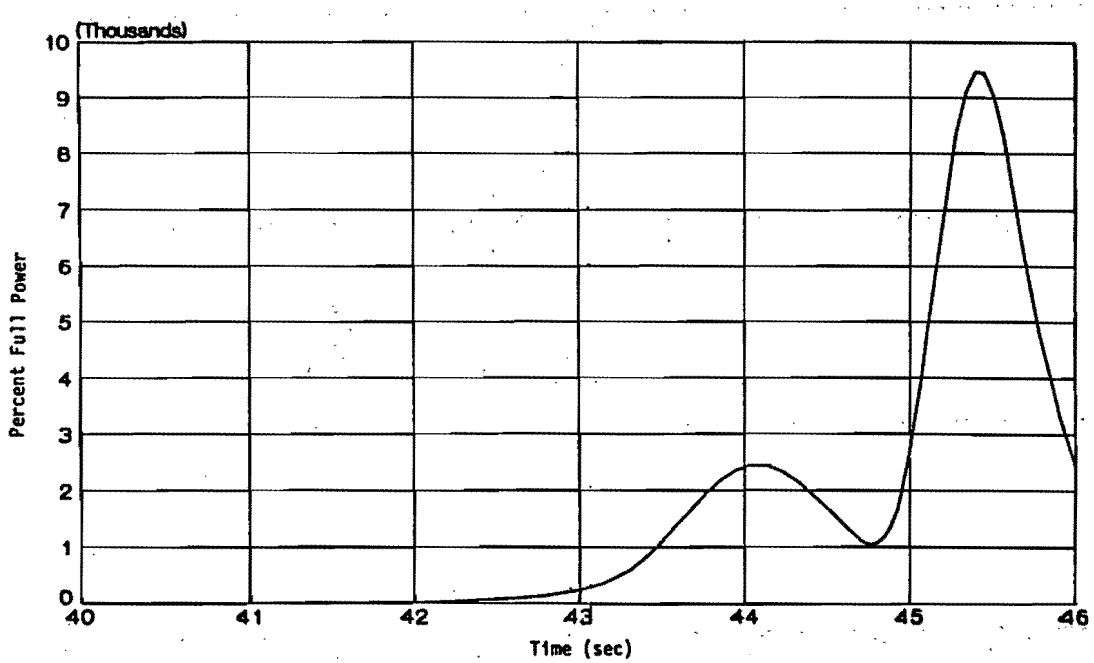

Figure F-5. Calculated Power Using a Neutron Lifetime of 1.75 msec.

APPENDIX G

RBMK CONTROL ROD SYSTEM DESCRIPTION

RBMK CONTROL ROD SYSTEM

The control rod system consists of 211 movable rods. The rods are functionally divided into manual control rods (RR), two sets of automatic control rods (AR and LAR), emergency power reduction or scram rods (AZ), and shortened absorbing rods (USP). The number and function of these various types of rods are listed in Table G-1.

Description of Control Rod Design

The absorbing material of the rods is boron carbide fabricated in a sleeve design (see figure G-1). The boron carbide is enclosed in a sealed annular element formed from an aluminum alloy. The RR, AR, LAR, and AZ rods are assembled from five absorbing sections for a total length of 5.12 meters. The USP rods are assembled from three absorbing sections and have a total length of 3.05 meters. All rods are lowered into the core from the top, except the USP rods, which are raised from the bottom.

With the exception of the AR and LAR rods, all the rods have sections to displace water as the absorber sections are withdrawn from the core. This enhances the effectiveness of the rods by preventing the rod channel from being filled with water coolant which is a strong neutron absorber. The displacer is made up of five, one meter long cylindrical sections formed of aluminum alloy with sealed end caps. Each section is filled with graphite sleeves and cylindrical graphite blocks. When a control rod is fully withdrawn, the five meter long displacer is located symmetrically with respect to the core such that the one meter rod channel sections on either end are filled with water (see figure G-2).

Specifications for selected control rods are given in table G-2.

Description of Rod Drive Mechanism

The rod drive mechanism is used to raise, lower, and monitor the position of the control rods (see figure G-3). The mechanism has a direct current motor with a built-in electromagnetic brake that stops rotation of the shaft when voltage is applied. The motor transmits rotation through a geared transmission link to a drum. A belt-cable wound around the drum supports the control rod. Rotation is monitored by a selsyn sensor. Cams driven by a screw move when the rod moves. Limit switches activated by the cams indicate when the control rod has reached its extreme upper or lower position.

In the absence of motion commands, the circuits of the armature and the excitation winding of the electric motor are deenergized;

voltage is applied to the electromagnetic brake; and the drum, which holds the belt-cable and rod, remains motionless. When a command to extract the rod is transmitted, voltage is removed from the brake, the drum is released, and the electric motor raises the rod. Motion continues until either a stop signal is given or the upper limit switch is activated.

Rods are inserted into the core in one of three ways.

1. When a signal to lower the rod is received, the electromagnetic coupling is deenergized and, due to the weight of the rod, the drive initiates a lowering movement, working in a self-exciting dynamic braking mode.

2. The drives can also initiate a lowering movement mode when voltage is applied to the excitation winding. The brake is deenergized and, due to the weight of the rod, the drive initiates a lowering movement in dynamic braking mode with a weak current.

3. It is also possible to use the motor to initiate the lowering of the rod, thus reducing the transition time. In this case, full voltage is applied to the armature circuit and to the excitation winding, and power is cut-off from the electromagnetic brake. The drive initiates a lowering movement in the motor mode. Then the power is cut off from the armature winding but not from the excitation winding. The rod continues to fall, but its motion is slowed by the presence of electrical current in the excitation winding of the motor.

Table G-1. Types of Control Rods

Name	Symbol	Number	Function
Manual Control	RR	139	Operator controlled for power shaping.
Local Automatic Regulation	LAR	12	Maintains radial power shape. Twelve rods moved independently.
Automatic Power Regulation	AR	12	Maintains total reactor power. Three sets of four ganged rods.
Scram	AZ	24	Scram rods. Normally withdrawn from core.
Short Absorbing	USP	24	Used to control axial power shape. Manually controlled and moved upward into the core from the bottom.

Operation of the Control Rod System

Manual control is provided by manual control (RR) rods. These rods are divided into four groups as a function of their location in the reactor. One group is located in the periphery of the core, and the remaining three are located centrally in the core. The central rods are divided into three regular, intermixed lattices. Control of excess reactivity is accomplished by the RR rods of one of these central groups and by the peripheral rods, which are moved up or down to equalize the current in the peripheral ionization chambers. The rods of each central group are moved sequentially to maintain the position within ± 0.5 m (20 in.) of each other. The rods of the two other central groups are at the extreme upper or lower positions depending upon the reactivity reserve.

The average power control system consists of three identical sets of automatic regulators. Each set consists of four ionization chambers placed around the reactor and provides information on the basis of which four automatic regulating rods are moved synchronously. The use of ionization chambers of different sensitivity enables these sets to work in different ranges: the low-power range from 0.5 to 10% of full power and the working-power range from 5 to 100% of full power. In the low-power range there is one automatic regulator (3AR); in the working-power range there are two (1AR and 2AR). One of the working regulators is switched on, while the second is in "hot" standby. The second regulator is automatically switched on if the first regulator is switched off automatically as a result of a malfunction.

An emergency signal is generated if the set limit of a chamber is exceeded and the signal is recorded on at least two measuring channels of different groups. If an emergency signal is generated, the emergency control rods are lowered. This action protects the reactor as a whole from power excursions, and it also protects the reactor from peripheral local power excursions.

Stabilization of the power density distribution in the reactor is achieved by the local automatic regulating and local emergency protection systems. The former is designed on the principle of independent power regulation in 12 local zones of the reactor by means of 12 regulating rods. The local automatic regulating system rods are controlled on the basis of information from two detectors positioned in the core around the local automatic regulating rods at a distance of 0.63 mm from the rods.

The local automatic regulating system is switched into the automatic mode in the power range after the required power density distribution has been achieved. In transitional regimes, the local automatic regulating system has considerable

advantages, since it not only provides measurement and regulation of the overall power, but also smoothes out power distortions due to local perturbations in the equipment.

The local automatic regulating system is the main system for automatic average power regulating in the power range from 10 to 100% of full power. The average-power automatic regulating system is used for standby and is automatically switched on when the local automatic regulating system is switched off as a result of malfunction.

The speed of movement of the automatic control rods is limited to 0.3 meters/sec so as not to exceed the limits established by the Nuclear Safety Regulations for the rate of insertion of positive reactivity when 12 rods of the local system are moved at the same time. There is a built-in limitation on the continuous withdrawal of the automatic regulator rods for over 8 seconds.

When a power overshoot alarm signal appears in one of the channels of the local emergency protection zone, the withdrawal of the local automatic regulating rods is automatically blocked. When emergency power overshoot signals appear in both channels of the local emergency protection zone, two local emergency protection rods are lowered into this zone of the core until at least one of the emergency signals disappears. In this case the average power of the reactor is reduced by automatic lowering of the power transducer settings at their operational rate change.

The withdrawal of more than 8 to 10 of the manual regulating and emergency protection system or shortened absorber rods upon any malfunction is prevented by a "power blocking" circuit. This circuit automatically determines the number of rods in whose servo drive armature circuit a voltage for rod withdrawal is given. If this number is greater than 8 to 10, the circuit is automatically disconnected from the servo drive power supply source and no additional rods can be withdrawn from the core. There are three power blocking channels that process the signals by a two-out-of-three logic.

Table G-2. Control Rod Specifications

Control Section	
Absorber Material	Boron Carbide
Absorber Density	1.65 gm/cc
Clad Material	Aluminum Alloy
Absorber Length/Section	98.4 cm
Total Length/Section	102.4 cm
Outer B_4C Diameter	6.5 cm
Inner B_4C Diameter	5.75 cm
Outer Clad Diameter	7.0 cm
Outer Clad Thickness	0.2 cm
Inner Clad Diameter	5.0 cm
Inner Clad Thickness	0.2 cm

Displacer Section	
Displacer Length/Section	100 cm
Displacer Material	Graphite
Cladding Material	Aluminum Alloy
Clad Diameter	7.4 cm
Clad Thickness	0.25 cm

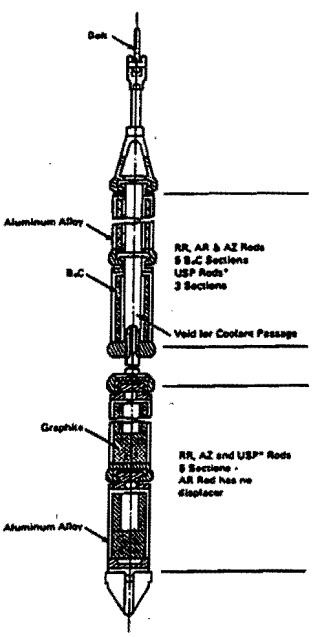

*USP rods have their displacers on the top and the B_4C absorber on the bottom.

Figure G-1. Control Rod Design

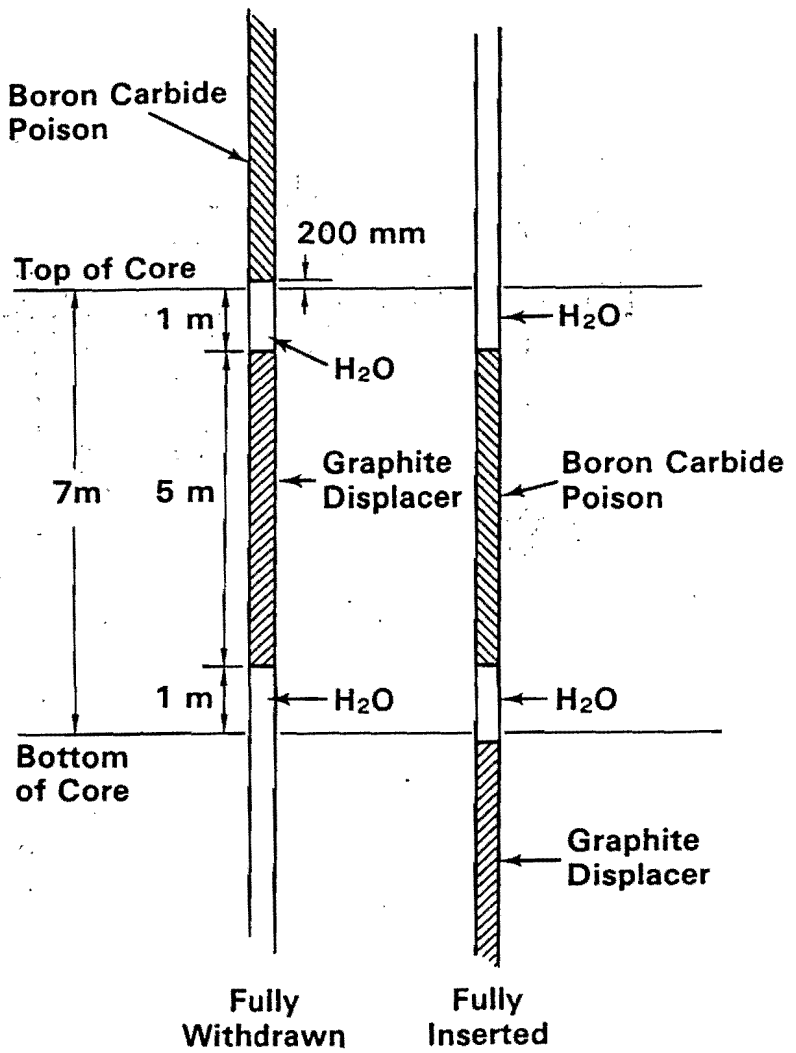

Figure G-2. Control Rod Displacer Positioning

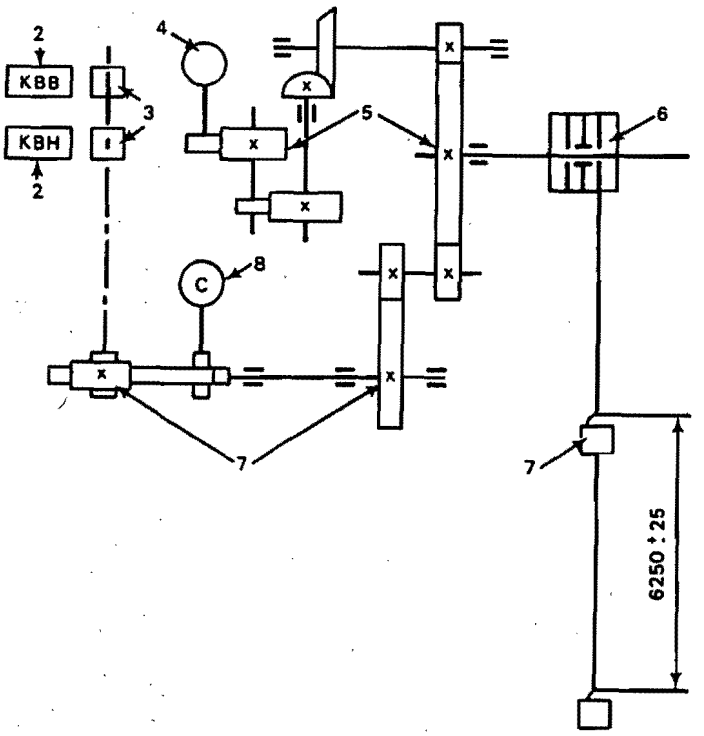

Figure G-3. Functional Diagram of a Control Rod Drive
1 - Kinematic Drive; 2- Limit Switches, Upper and Lower; 3- Cams; 4 - Motor D. C.; 5 - Gears; 6 - Drum; 7 - Absorber Rod; 8 - Selsyn Transmitter

APPENDIX H

THREE-DIMENSIONAL TRANSIENT CALCULATIONS

THREE-DIMENSIONAL TRANSIENT CALCULATIONS

In order to evaluate the impact of spatial effects on the transient dynamics and fuel failure energetics, three-dimensional RAMONA-3B [1] calculations were performed in parallel with the point kinetics MINET analysis. The RAMONA-3B calculations have focused on two questions: (1) the role of three-dimensional effects on the course of the Chernobyl-4 transient and (2) the possibility of a positive reactivity insertion as a result of a reactor scram.

Due to the lack of detailed information concerning the reactor state at the time of the transient, certain assumptions were made concerning the fuel loading and exposure distribution, channel flow distribution and initial conditions. In addition, there are known differences between the RAMONA-3B and Point Kinetics input data, and detailed comparisons between the three-dimensional and point kinetics results should not be made.

The RAMONA-3B model for the Chernobyl-4 reactor consists of a quadrant symmetric reactor core represented by 118 neutronic and 30 hydraulic channels totalling to 1,416 neutronic and 360 hydraulic computational cells corresponding to 12 axial nodes. Each neutronic channel in the RAMONA-3B model represents either four Chernobyl-4 fuel channels or three fuel channels and one control rod channel embedded in four blocks of graphite moderator.

The model cross sections were developed using the WIMS [2] multi-group collision probability code. The cross sections were adjusted in order to match the void reactivity coefficient ($\alpha_\emptyset = 3 \times 10^{-2}$ $\Delta k/k/\Delta\alpha$ at a void fraction of $\alpha = 0.4$) published in the Soviet report [3].

The Chernobyl-4 reactor thermal-hydraulics model included the downcomer piping, core, riser piping, a steam separator which represents four plant steam separator drums, and a steam line equipped with Main Steam Isolation Valve (MSIV), bypass valve, and safety/relief valves. Distributed channel inlet orificing was introduced in order to maintain approximately the same power-to-flow ratio in all hydraulic channels at steady state.

Initial conditions in the RAMONA-3B calculation corresponded to the reactor state as of 1:23:00 on April 26. The reactor parameters were as follows: thermal power - 200 MWt, core flow - 120 percent of nominal, and initial steam separator pressure - 63 MPa. The transient was initiated by a linear core flow reduction to 85 percent of the initial value in 45 seconds (as indicated in figure 4 of the Soviet report).

Results and Analysis

Three RAMONA-3B calculations were performed. In each calculation the MSIV was opened[1] and the time of reactor scram was varied. The cases included: Case A - no scram, Case B - scram at a power level of 539 MWt (corresponding to the power level at which the scram was activated, and a time of 39 seconds in the present calculations), and Case C - scram at 41 seconds accounting for the expected initial delay in rod motion.

The RAMONA-3B calculation for Case B (scram on power at 39 seconds) indicates that a scram initiated sufficiently early in the transient shuts the reactor down before any significant power excursion takes place. The results of the Case C calculation which approximates the Chernobyl-4 accident are presented in figures H-1 - H-10.

The global system parameters and the corresponding reactivity components are presented in Figures 1 and 2, respectively. The peak thermal power attained is about 160,000 MWt at 43 seconds and is still increasing. The scram reactivity in the first 3 seconds is small (<50 cents) and is not sufficient to appreciably offset the large ($3.3) positive void reactivity (figure H-3). The core axial void distribution is shown in Figure 3 with a peak exit void fraction of ~.6 at 43 seconds. As a consequence, significant changes in the axial power and fuel temperature distributions occur at the time of the power excursion. These effects are shown in figures 4 and 5 for a hot channel located radially about 4 meters from the core center.[2]

The RAMONA-3B predictions also show a substantial radial power redistribution during the course of the accident. The initial radial power shape is shown in figure 6 and indicates a center peaked distribution with a slight octant asymmetry due to the control rod pattern. The radial power distribution is shown in

---

[1]An open MSIV in this context refers to a steam flow proportional to pressure boundary conditions in the steam line calculations. It is noteworthy that a preliminary calculation with a constant steam flow boundary condition resulted in only a mild transient due to the core void collapse under increasing system pressure.

[2]In these calculations the axial power shape was a typical cosine, however, RAMONA-3B calculations were also performed for a double-peaked axial power shape (as described in the Soviet report) and the axial power was observed to shift slightly towards the top of the core during the power excursion.

figure H-7 and indicates the presence of two well defined diametrically opposed high-powered regions at the time of the power excursion (43 seconds). The rapid growth of this flux shape (and associated power peaking) at the time of the excursion is a result of the inherent radial-azimuthal flux instability of the RBMK design. (It is noteworthy that the growth of the first harmonic is expected to be faster and result in even stronger local peaking than observed in these calculations. However, due to the symmetry implicit in the quarter-core representation used in the present calculations, these modes are not excited). In figure H-8, the resulting radial power shift from the center of the core to the core periphery is presented; the peak power location shifts to the group of channels located approximately 4 meters from the center of the core. As shown in figure H-9, this spatial power redistribution results in local "hot spots" consisting of up to one hundred fuel assemblies in which the fuel centrline temperature exceeds the core average centerline temperature by ~ 200°C. These lead assemblies would be expected to undergo early fuel failure during the accident and, in the case in which the initial power excursion is terminated by doppler and/or scram reactivity before significant fuel damage occurs, may have provided the thermal-hydraulic and mechanical mechanism (see description of fuel energetics in section 4) which initiated a second power excursion (as indicated in figure 4 of the Soviet report) resulting in the ultimate core damage.

As discussed in section 4, certain features of the Chernobyl-4 design have the potential for contributing a positive component to the scram reactivity. In order to determine the magnitude of this effect RAMONA-3B three-dimensional scram reactivity calculations were performed. The calculational model included an explicit representation of the control rod, graphite displacer rod and water regions above and below the displacer rod (figure 12) for all the scram rods. The scram reactivity was determined as a function of rod insertion for selected reactor state points ranging from 7 percent to 100 percent of rated power. In figure H-10 the scram reactivity curve is presented for a case at 20 percent of rated power, and indicates a very slight increase (on the order of a few cents) during the initial meter of rod insertion followed by a strong negative reactivity insertion.[3] All calculations were generally consistent indicating that the initial positive reactivity insertion due to reactor scram is < 10 cents.

---

[3] It should be noted that the scram reactivity curve represents the overall core reactivity, which determines the temporal dependence of the total core power, and does not represent the local reactivity distribution which determines the time dependence of the core power distribution.

Conclusions

Based on the RAMONA-3B three-dimensional calculations and the various assumptions implicit in the Chernobyl-4 modeling the following conclusions can be made.

- The steam flow, to a large extent, determines the core pressure and void generation, and the severity of the transient.

- For the assumed initial conditions and flow coastdown, the core undergoes a prompt critical power excursion as a result of positive void reactivity insertion.

- If the scram had occurred earlier, the negative reactivity insertion would have been sufficient to suppress the transient.

- During the transient, the core power distribution undergoes a strong radial-azimuthal shift from the center of the core towards the periphery, in which the hot channel fuel temperature leads the central core fuel temperature by ~2000 C. This power redistribution will lead to early fuel failure in these lead fuel assemblies.

- The positive reactivity insertion associated with a reactor scram is negligible (< 10 cents).

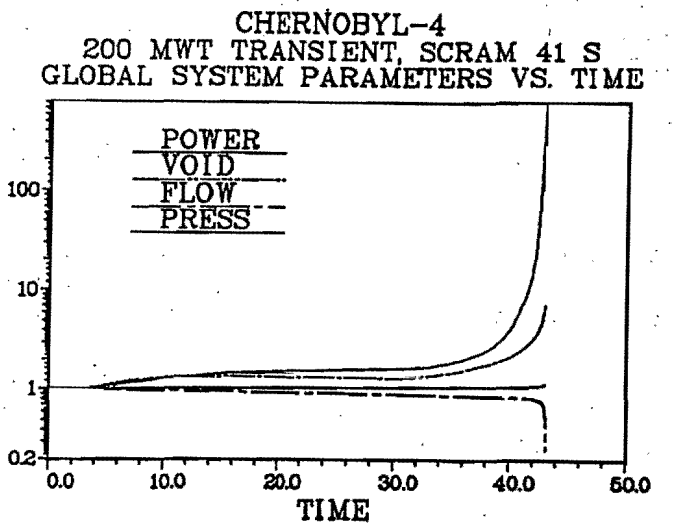

Figure H-1. Global System Parameters vs. Time

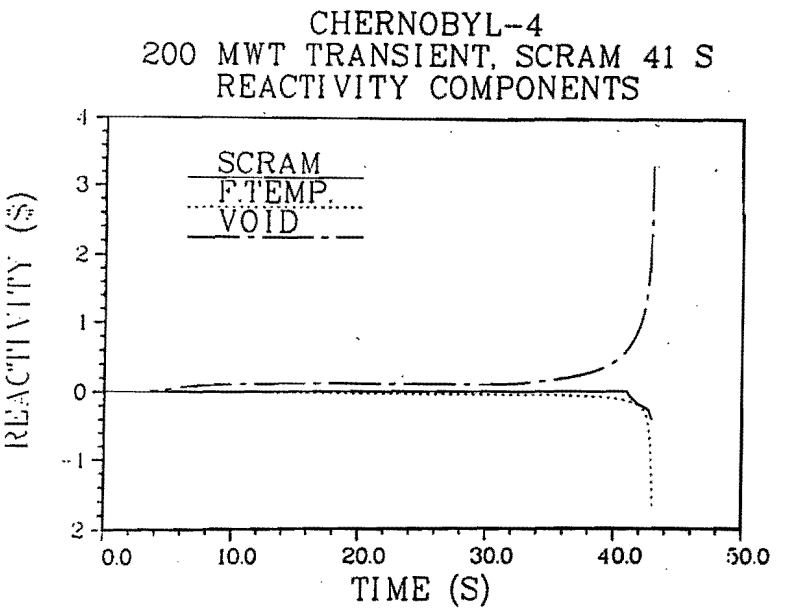

Figure H-2. Reactivity Components vs. Time

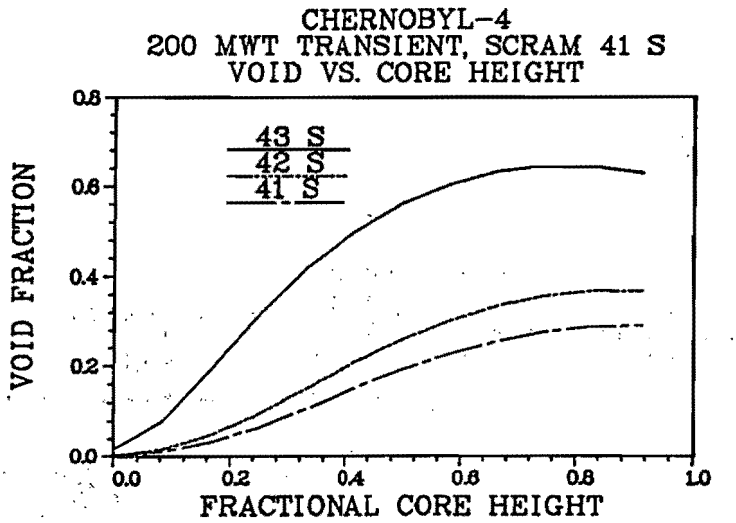

Figure H-3. Core Axial Void Distribution

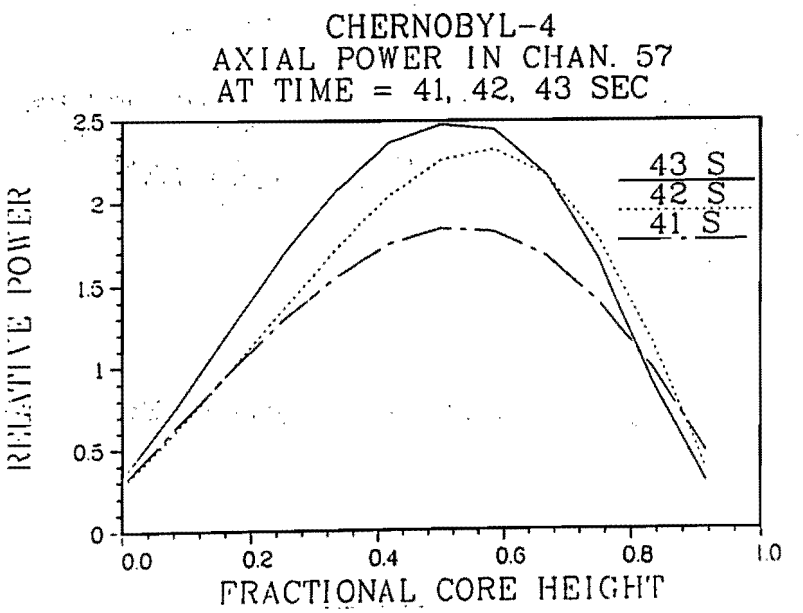

Figure H-4. Axial Pellet Average Power Distribution in Channel 57

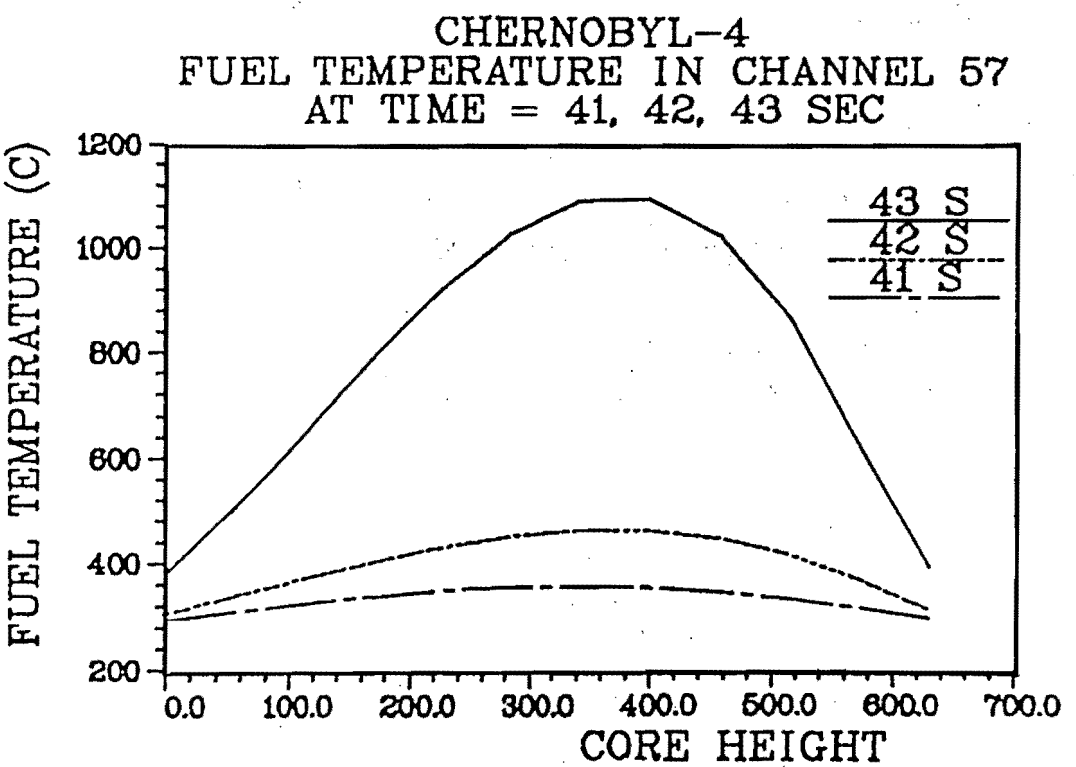

Figure H-5. Axial Pellet Average Temperature Distribution in Channel 57

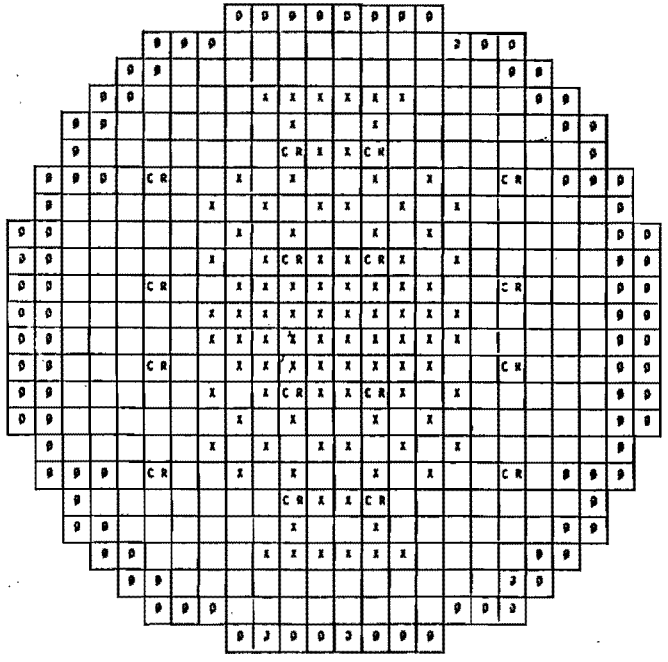

Figure H-6. Initial Radial Power Distribution

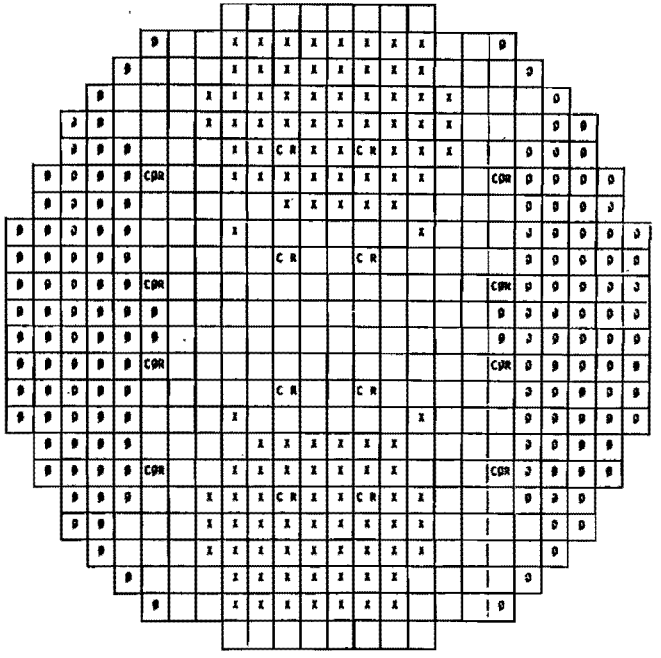

Figure H-7. Radial Power Distribution at the Time of the Power Excursion.

x - P > 1.3 P_{avg}

ϕ - P < 0.7 P_{avg}

CR-Control Rod

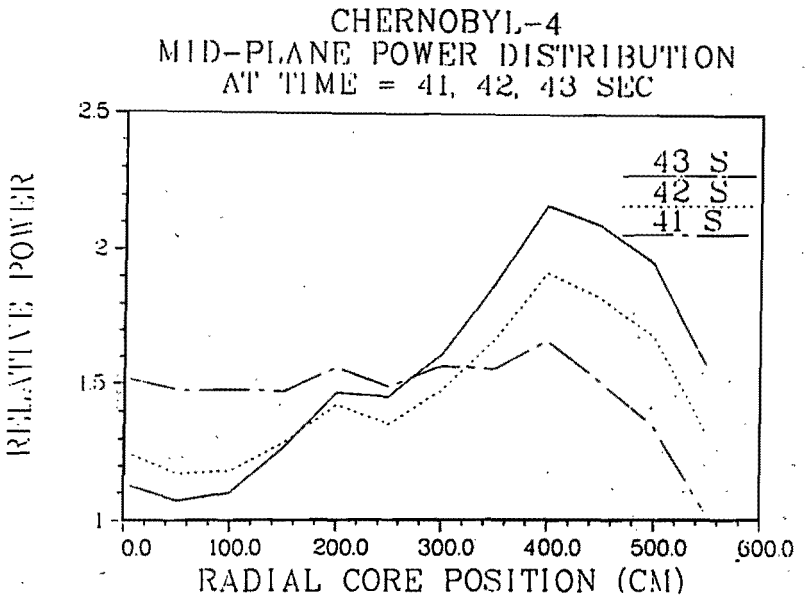

Figure H-8. Radial Power Distribution at the Core Mid-Plane

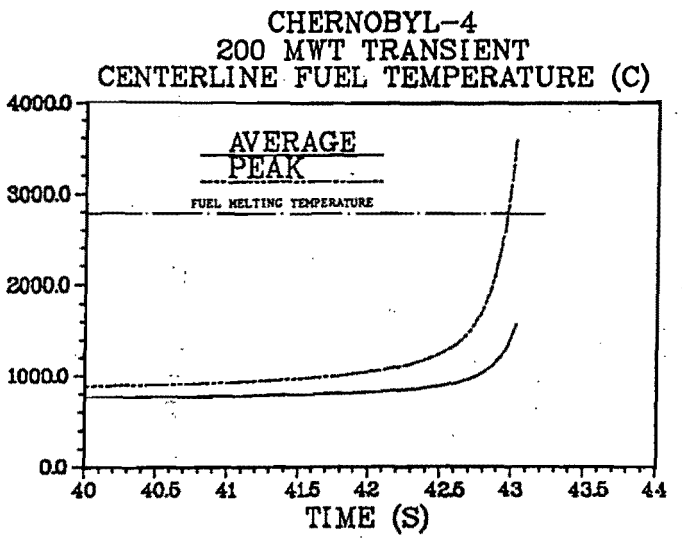

Figure H-9. Core Maximum and Average Fuel Temperatures vs. Time

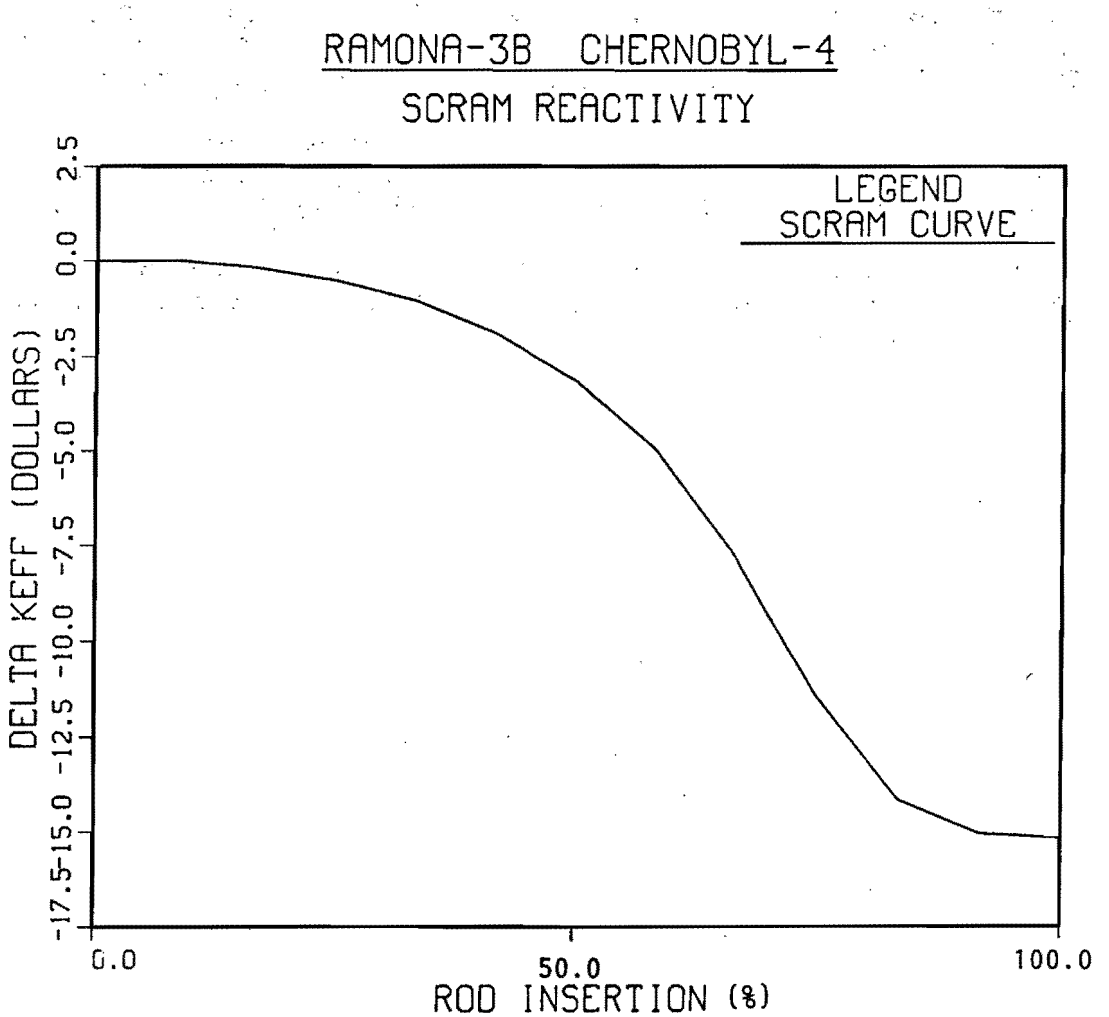

Figure H-10. Chernobyl-4 Scram Curve

References

1. W.W. Wulff, et al., "A Description and Assessment of RAMONA-3B MODO Cycle 4: A Computer Code with Three-Dimensional Neutron Kinetics for BWR System Transients," BNL-NUREG-51746, NUREG/CR-3664, January 1984.

2. F.J. Fayer, et al., "LWR-WIMS, A Modular Computer Code for the Evaluation of Light Water Reactor Lattices," AEEW-R785 Atomic Energy Establishment, Winfrith, 1972.

3. "Working Document for Chernobyl Post Accident Review Meeting," State Committee for Using the Atomic Energy of USSR, August 1986.

*U.S. GOVERNMENT PRINTING OFFICE:1986-181-179:50090

UNITED STATES
DEPARTMENT OF ENERGY
WASHINGTON, D.C. 20545

OFFICIAL BUSINESS
PENALTY FOR PRIVATE USE, $300

POSTAGE AND FEES PAID
U.S. DEPARTMENT OF ENERGY
DOE 350

U.S. MAIL

THIRD CLASS MAIL